



GROUNDWATER FLOW THROUGH A
CONSTRUCTED TREATMENT WETLAND

THESIS

Andrew C. Entingh, Major, USMC

AFIT/GEE/ENV/02M-03

**DEPARTMENT OF THE AIR FORCE
AIR UNIVERSITY
AIR FORCE INSTITUTE OF TECHNOLOGY**

Wright-Patterson Air Force Base, Ohio

APPROVED FOR PUBLIC RELEASE; DISTRIBUTION UNLIMITED

The views expressed in this thesis are those of the author and do not reflect the official policy or position of the United States Air Force, Department of Defense, or the U.S. Government.

AFIT/GEE/ENV/02M-03

GROUNDWATER FLOW THROUGH A CONSTRUCTED TREATMENT WETLAND

THESIS

Presented to the Faculty

Department of Systems and Engineering Management

Graduate School of Engineering and Management

Air Force Institute of Technology

Air University

Air Education and Training Command

In Partial Fulfillment of the Requirements for the

Degree of Master of Science in Engineering and
Environmental Management

Andrew C. Entingh, B.S.

Major, USMC

March 2002

APPROVED FOR PUBLIC RELEASE; DISTRIBUTION UNLIMITED.

Acknowledgements

I would like to thank my thesis advisor and committee chairman, Dr. Michael L. Shelley, for the opportunity to work on such an interesting project. The patience, support and confidence you extended my way during the course of the effort were very much appreciated.

I would also like to thank my other committee members: Lieutenant Colonel Al Thal, for acting as a sounding board on groundwater matters amidst a busy schedule, and Dr. Junqi Huang, for the many patient hours of instruction and support with the numerical modeling portion of this thesis; without your help, my product would be deficient.

Last, I thank God for the aptitude to tackle graduate level studies and the opportunity to study a very small but intricate piece of His awesome creation. The whole earth proclaims your glory!

Andrew C. Entingh

Table of Contents

	page
Acknowledgements	iv
Table of Contents	v
List of Figures	vii
List of Tables	ix
Abstract	x
I. Introduction	1-1
Problem Statement	1-7
Research Questions	1-8
Scope and Limitations	1-8
II. Literature Review	2-1
Wetlands	2-1
Contaminant Fate in Wetlands	2-5
Organic Contaminants	2-10
PCE Degradation	2-11
Groundwater Flow	2-16
Groundwater Flow Determination	2-28
Groundwater Flow Analysis	2-35
III. Methodology	3-1
Overview	3-1
Sampling Grid	3-2
Piezometer Installation	3-4
Piezometric Measurements	3-9
Parameter Estimation	3-11
Numerical Model	3-32
IV. Results	4-1
Sampling Grid	4-1
Piezometer Installation	4-1
Piezometric Surface	4-7
Parameter Analysis	4-11
Numerical Model	4-15

	page
V. Conclusions and Recommendations for Further Study ..	5-1
Study Strengths	5-3
Study Weaknesses	5-3
Recommendations for Further Study	5-5
Appendix A: Piezometer Grid and Construction Data	A-1
Appendix B: Contours of Hydraulic Head (11-01-2001)	B-1
Appendix C: Contours of Hydraulic Head (02-19-2002)	C-1
Appendix D: Water Level Measurements	D-1
Appendix E: Bouwer and Rice Slug Test Results	E-1
Appendix F: Mathcad® Template for Slug Tests	F-1
Appendix G: Mathcad® Template for Pump Tests	G-1
Appendix H: Calibration Plots	H-1
Bibliography	BIB-1
Vita	VITA-1

List of Figures

	page
Figure 1-1. Concept Design of the Wright-Patterson Air Force Base Wetland Treatment Cells	1-5
Figure 2-1. Proposed PCE Dechlorination Pathway by PCE/TCE De-chlorinating Granules.	2-13
Figure 2-2. Layered Heterogeneity.	2-22
Figure 2-3. Hydraulic Gradient.	2-25
Figure 2-4. Hydraulic Head, Pressure Head, and Elevation Head for a Field Piezometer.	2-27
Figure 2-5. Simple Flow Net	2-30
Figure 2-6. Refraction of a Flow Line Crossing a Hydraulic Conductivity Boundary.	2-32
Figure 2-7. Method to Determine Direction of Flow in Anisotropic Media.	2-33
Figure 2-8. Three-dimensional Flow Through a Representative Control Volume.	2-36
Figure 3-1. Piezometer Placement	3-3
Figure 3-2. Profile View of Piezometer Placement.	3-5
Figure 3-3. Geometry for Bouwer and Rice Slug Test.	3-14
Figure 3-4. Piezometer Geometry	3-15

	page
Figure 3-5. Arithmetic and Semi-log Plots of Change in Head Versus Time for the Bouwer and Rice Slug Test.	3-17
Figure 3-6. Overhead View of the Wetland Model in Visual MODFLOW®	3-33
Figure 4-1. General Effect of Developing the Piezometers.	4-4
Figure 4-2. Regions of Particularly Poor Trafficability in the Wetland.	4-10
Figure 4-3. Cross Section Views of the Wetland	4-16
Figure 4-4. Calibrated Model.	4-18
Figure 4-5. Model Validation.	4-19

List of Tables

	page
Table 1-1. Composition of the Soil Layers	1-6
Table 4-1. Comparison of Hydraulic Head Distribution for November 1, 2001 and February 19, 2002. .	4-8
Table 4-2. Mean Standard Deviation in Hydraulic Head Distribution for All Dates Measured. ..	4-11
Table 4-3. Hydraulic Conductivity Estimates from In-situ Tests (ft/sec)	4-12
Table 4-4. Geometric Means of Hydraulic Conductivity (ft/sec)	4-12

Abstract

This study examines the flow of groundwater through a constructed treatment wetland. The wetland was built to explore the viability of constructed wetlands as a treatment technology for groundwater contaminated with perchloroethylene, and it employs an upward vertical flow design. A major goal of the study is to determine whether the system design facilitates uniform vertical flows through the subsurface soil sediments or if preferential flows occur. Conceptually, uniform flows will achieve the most efficient degree of contaminant removal possible by evenly dispersing the groundwater contaminants throughout the full volume of the subsurface media.

A three-dimensional grid of piezometers is used to generate potentiometric contour maps, and in-situ tests of hydraulic conductivity facilitate construction of a numerical computer model. The contours of hydraulic head, measured conductivities, and numerical model simulations imply preferential flows and a wetland operating at less than an optimal level of efficiency. Hydraulic residence times for representative water particles released in the model range from 16.5 hours to 15 days with a mean residence time of three days. The divergence from the

uniform flow ideal suggests an alternative construction approach may be appropriate.

GROUNDWATER FLOW THROUGH A CONSTRUCTED TREATMENT WETLAND

I. Introduction

The purpose of this research is to characterize the flow of groundwater through a constructed treatment wetland. The location, purpose and description of the wetland are covered below. Hydraulic head measurements from a three-dimensional grid of piezometers will be used to construct potentiometric contour maps, conduct simulation modeling, and calculate hydraulic residence times. An understanding of the flow through the wetland will: (1) provide insight into where important wetland and contaminant interactions may be occurring; (2) indicate the amount of time that the interactions have to occur; and (3) substantiate or dispel concerns over the possibility of water preferentially flowing through the wetland media.

Two wetland cells were constructed at Wright Patterson Air Force Base in Dayton, Ohio, during the summer of 2000. The cells were constructed by the Air Force Institute of Technology (AFIT) to study the ability of constructed wetlands to naturally degrade perchloroethylene (PCE). The

study represents a joint effort between students and faculty of AFIT, the Air Force Research Laboratory, and Wright State University.

Both wetland cells are situated over an aquifer that is contaminated with a plume of PCE. The site has been identified and documented with the Ohio Environmental Protection Agency with no current requirement for remediation. The origin of the plume is unknown, but dry cleaning operations are known to have existed in the area (Shelley, 2001). The concentration of PCE in the aquifer in the aqueous phase is approximately .05 mg/L.

PCE - or tetrachloroethylene as it is also known - is a volatile organic compound (VOC) and a prevalent groundwater contaminant; it is among the three most frequently detected groundwater contaminants nationwide (National Research Council, 1994). PCE is used as a solvent in applications such as metal degreasing and commercial dry cleaning. PCE is a potential carcinogen and regulated drinking water contaminant; it has an assigned maximum contaminant level of .005 mg/L (Masters, 1998).

A common approach to treating groundwater contaminated with VOCs is to employ energy intensive technologies such as pump and treat systems. This is because VOCs - by their

nature - will volatilize at room temperature. Although costly, technologies that aerate contaminated groundwater to encourage vaporization allow for a high degree of control during the remediation process (Masters, 1998).

Another remediation strategy lies at the other end of the energy-use and technology spectrum. It is called natural attenuation, and it is essentially letting nature run its course. Natural attenuation relies on natural processes and energies to degrade contaminants into less harmful substances. Research indicates that, under the right conditions, PCE will degrade as a result of microbial activity into less chlorinated degradation products and possibly even all the way down into innocuous substances (Lee et al, 1998). Natural attenuation may require some degree of human intervention, however, to create the right conditions for the contaminant degradation to occur. For example, a contaminated aquifer could be seeded with microorganisms that are known to decontaminate PCE as well as a substrate to serve as a source of carbon and energy for the microbes (Fogel et al, 1995; Wu et al, 1995). One disadvantage with such a method is that it may be difficult to *control* the attenuation process and achieve the desired remediation outcome in the natural setting.

The wetland cells at Wright Patterson Air Force Base represent a low cost, low energy, pump and treat system that relies on natural processes to attenuate PCE. The concept is supported by findings at a U.S. Department of Defense site in Aberdeen, Maryland, where a natural, groundwater-fed wetland appears to demonstrate the complete destruction of trichloroethylene - a related VOC and also a degradation product of PCE (Lorah and Olsen, 1999). Because the wetland cells are constructed above ground, their design accommodates a greater degree of process control than that available with natural attenuation.

The design of the wetland cells is unique to wetlands constructed for the purpose of treating contaminants. Both wetland cells are approximately 120' long and 60' wide, and they function in the following manner. Contaminated water from the aquifer is pumped into the bottom of each wetland cell and distributed through three parallel 3" diameter PVC pipes. The pipes are perforated along the sides and run lengthwise through a 9" gravel layer along the bottom of the wetland cells. (An impermeable liner isolates the water in the cells from the surrounding environment.) The water forced through these pipes gradually works its way up to the surface of the wetland

cells through approximately 54" of wetland sediment. The water then flows across the wetland surface to exit weirs located at one end of each wetland cell. Plots of different emergent wetland plant species grow in both wetland cells. Figure 1-1 is a sketch of the wetland cell construction.

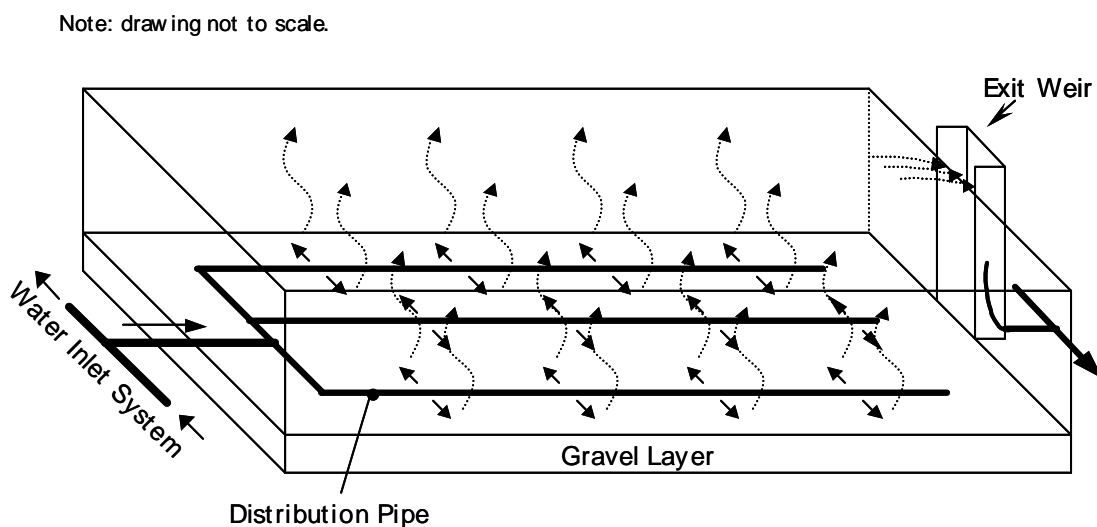


Figure 1-1. Concept Design of the Wright-Patterson Air Force Base Wetland Treatment Cells

The soil composition of the subsurface media differs slightly between cells. In one cell, 18" of historically saturated or *hydric* soil (i.e., soil characterized by anaerobic or reducing conditions when saturated) with 10% woodchip amendment sits over the bottom gravel layer followed by two 18" layers of hydric soil without any added

woodchips. The woodchips in the bottom layer were added to provide a more concentrated source of carbon for the anaerobic microbes. In the second cell, an 18" layer of locally obtained, iron-rich fill is sandwiched between two 18" layers of hydric soil (without any woodchips added). The iron-rich layer of indigenous soil was added to observe the effects of Fe^{+3} on the reduction of vinyl chloride - a degradation product of PCE and potent human carcinogen. Vinyl chloride is known to readily degrade under iron reducing conditions (Bradley and Chapelle, 1997). The differences in cell design will allow researchers to compare the efficiency of the different types of media and recommend an optimal design approach. Both cells are planted with various plots of emergent wetland vegetation. Table 1-1 provides a summary of the subsurface sediment composition.

Table 1-1. Composition of the Soil Layers

<u>Layer</u>	<u>Cell 1</u>	<u>Cell 2</u>
Top	Hydric Soil (likely root zone)	Hydric Soil (likely root zone)
Middle	Hydric Soil	Local, Iron-rich Fill
Bottom	Hydric Soil (organic matter added)	Hydric Soil

Since their construction, researchers active in the study have voiced concerns that water may be preferentially

flowing through certain portions of the wetland media. Of equal concern is whether this particular design approach (i.e., water distributed through pipes in a gravel layer with uniform sediment layers above and an outfall at one end of the cell) facilitates uniform vertical flows and whether soil heterogeneities - or pockets of low hydraulic conductivity - disrupt that flow. This research seeks to characterize the behavior of water within the wetland cells and address such concerns. An understanding of how water moves through the wetland media, and how long it resides in the wetland media, is critical to understanding what processes may be at work to degrade the PCE. The results of this study will add to efforts that seek to explore the potential of wetlands to de-chlorinate PCE and other related substances. The ultimate goal of this and related research is to develop design guidelines should such a remediation approach prove relevant and successful.

Problem Statement

Early indications are that the Wright-Patterson Air Force Base wetland cells are effectively de-chlorinating PCE from the contaminated groundwater. Little is known, however, about the specific processes that are affecting

the contaminant's removal, where such processes are occurring, and at what rate they occur. A better understanding of how water flows through the wetland media will facilitate efforts that seek to answer such questions.

Research Questions

(1) Is the flow of water uniform through the wetland sediments or has the water found preferential flow paths?

(2) Does the behavior of groundwater flow change with varying loading rates or environmental conditions?

(3) What is the approximate residence time for groundwater particles moving through the subsurface media?

Scope and Limitations

This research will characterize the flow of groundwater through the wetland media and give subsequent researchers an idea of where to focus their investigative efforts. Observations of hydraulic head will provide an indication of flow behavior in the wetland. Analysis of various wetland soil parameters will allow simulation modeling and provide a visual representation of the water dynamics within the media. Subsequent runs of the model will aim to fit the observed hydraulic head observations

with the numerical model's calculations. The fit data will enable calculations of hydraulic residence times and may contribute to the development of design parameters that apply to like systems.

II. Literature Review

Wetlands

"Wetlands are defined as land where the water table is at (or above) the ground surface long enough each year to maintain saturated soil conditions and the growth of related vegetation" (Reed et al., 1995). Wetlands can exist as transitional areas between terrestrial and aquatic ecosystems, and they can also occur as isolated ecosystems wherever ground waters intersect the earth's surface. Wetlands can derive their water from surface sources - such as precipitation, runoff from rainfall events, and flooding or overflows from adjacent bodies of water - or they can be groundwater fed.

Wetlands are complex ecosystems that perform a variety of beneficial functions in nature. As depressions in the ground, wetlands can buffer downstream locations from the effects of heavy rainfall events and reduce the potential for flooding (Wetlands Research Program, 1993). When situated next to other bodies of water, they provide erosion control from rainfall and tidal flooding. The damping motion caused by wetland vegetation also reduces the velocity of waters passing through the wetland; this

discourages the re-suspension of sediments, which in turn improves water clarity and quality (Wetlands Research Program, 1993). As highly productive ecosystems, wetlands can support life at several ecological levels and provide a suitable habitat for migratory water fowl and many other kinds of species. Their service as nature's "kidneys of the landscape" (Mitsch and Gooselink, 1993) makes them particularly beneficial in areas where they recharge surface and ground waters. An appreciation of this capability has made wetlands a popular alternative to remedy some of the more concentrated streams of pollution generated by man.

There are essentially two broad classifications of wetlands: natural and manmade. While the different sub-classifications of natural wetlands may be of interest in ecological studies, a discussion on natural wetlands here is relevant only where the mechanisms of pollutant removal apply to manmade wetlands as well. Because natural wetlands are considered *waters of the United States*, they are subject to regulatory control under the Clean Water Act. The Clean Water Act requires a permit for the addition or discharge of any pollutant from a point source into waters of the United States, and such permits normally require

pre-treatment to specified effluent standards (Gallagher, 1999). This regulatory status generally limits their use in pollutant remediation. Furthermore, because uniform hydraulic flows seldom occur in natural wetlands, only a small portion of the wetland may actually come into contact with the waterborne pollutants that enter the system. It is often not possible to correct such *treatment inefficiencies* barring a significant engineering effort, and this - along with the addition of any contaminants - would undoubtedly alter the ecology of these naturally developed systems (Reed et al., 1995).

Manmade wetlands constructed to treat pollutants, on the other hand, are largely free from the regulatory oversight and ecological concerns inherent with natural aquatic ecosystems (Reed et al., 1995). Furthermore, the construction of wetlands to treat pollutants allows for an optimum design consistent with known parameters. While there are always difficulties in engineering efforts, constructed wetlands can often be designed to accommodate flows that achieve a desired level of contaminant treatment.

There are two main types of manmade wetlands: free water surface and subsurface flow wetlands. The free water surface variety is characterized by a water surface that is

exposed to the atmosphere. Free water surface wetlands may contain floating, submerged, and emergent vegetation. The concept behind free water surface wetlands is that pollutants in the water flow across the surface of the wetland and degrade through various natural processes active in the largely aerobic (i.e. plant) portion of the wetland. The subsurface flow wetland, in contrast, is characterized by a water table that is below the surface of the wetland. Water flows through a subsurface flow wetland in a similar fashion as groundwater flows through an aquifer. The concept is that the pollutants in the water flow uniformly through the wetland media (rather than over the surface of it) and degrade through processes that occur in this largely anaerobic region. A sufficiently porous media is a pre-requisite for this type of wetland to function properly. Wetland plants, if present, may provide for a slightly aerobic region in the root zone strata of subsurface flow wetlands.

The subsurface flow wetland is generally considered the more efficient of the two types of constructed wetlands (Reed et al, 1995). This may be somewhat counterintuitive to persons familiar with wastewater treatment processes as rates of aerobic degradation generally far exceed those of

anaerobic processes. In manmade wetlands, however, the degradation processes believed to be at work occur largely as the result of attached growth organisms, and the larger reactor volume of subsurface flow wetlands make up for the (generally slower) anaerobic processes at work in them.

The wetland cells at Wright-Patterson Air Force Base represent a hybrid design where water moves vertically up through the wetland media until it pools and drains off the surface of the wetland. While the water is moving up through the wetland media, the cells function as subsurface flow wetlands. As the water moves across the surface of the wetland, the cells function as free water surface wetlands.

Contaminant Fate in Wetlands

Microorganisms, plants and wetland sediments may all play an active role in the pollutant degradation processes at work in both natural and manmade wetlands. The temperature, pH, dissolved oxygen concentration, and water depth of the wetland influence these components and affect the overall system performance (Reed et al, 1995).

Microorganisms. Bacteria are the unchallenged champions of pollutant degradation in wetland ecosystems as

they are in most wastewater treatment systems. Bacteria manufacture enzymes that enable them to consume or modify pollutants in the environment. In most cases, the presence of the right kind of bacteria will result in some degree of pollutant degradation, while their absence may mean that the wetland is only capable of facilitating transport to destinations unknown. Conceptually, aerobic bacteria are the predominant consumers of nutrients in free water surface wetlands, while anaerobic bacteria inhabit the sediments of subsurface flow wetlands.

Bacteria are not the only microorganisms that take up their residence in wetlands. The presence of wastes, bacteria and decaying matter will attract other consumers (primary, secondary and tertiary) of the animal world. For a contaminant such as PCE however, the right kind of bacteria are believed to be the sole consumers or modifiers of the chlorinated solvent. The presence of higher animals - sometimes waterfowl, fish and even small mammals - signals a vibrant ecosystem with several trophic levels present above that occupied by the active microorganisms.

Plants. Plants play a beneficial role in wetland ecosystems, although there is disagreement over the extent to which they contribute to pollutant removal. Some

possible contributions may include plant uptake, support of microorganisms, and modification of soil properties.

During transpiration, plants draw in water through the roots to support various plant processes. Plants internally transport this water to the leaves to support photosynthesis, and they *transpire* the excess water (actually most of what they take in through the roots) to the atmosphere through openings in the leaves called stoma. Research indicates that plants may also be able to expel volatile waterborne contaminants along with the water they transpire (Newman et al., 1997; Nietch et al., 1999). Another possible fate for waterborne contaminants is storage in the internal plant tissues by diffusion. Contaminants warehoused in this manner may or may not exceed the plant's tolerance and unleash a toxic effect on the plant. Additionally, stored contaminants are often released back into the wetland when the plants die and decompose.

During transpiration, plants also take in carbon dioxide and oxygen through their stoma in the leaves to support photosynthesis and respiration. Plants transport some of the oxygen generated from these processes to the roots along with the products of photosynthesis to maintain

cell functions. Various studies indicate that some of the oxygen transported to the roots diffuses into the surrounding soil creating aerobic *microzones* in the root zone area of the wetland sediments (Brix, 1994 and referenced sources). While the amount of oxygen delivered in this manner may be minimal, it could provide attached aerobic microorganisms with enough oxygen to transform contaminants into substances more readily taken up by the plant, assimilated into its tissues, or volatilized into the air from stoma in the leaf. The submerged portions of wetland plants also provide a surface for microorganisms in free water surface wetlands to attach themselves to (Reed et al., 1995). In addition to these potential contributions, plants may also alter the physical properties of the wetland soil as will be discussed later in the chapter.

Soil. In their saturated condition, wetland soils are a mixture of mineral sediments, organic matter and water. The water occupies - and in the case of subsurface flow wetlands moves through - the voids or pore spaces that exist between the individual soil particles. Various physical properties influence the manner and rate at which water moves through these voids, and these will be

introduced later in the chapter. For now it is sufficient to note that water will move through different soils at different rates, and, generally, the longer the water remains in the soil, the longer contaminants have to react in the wetland sediment.

Soils also differ in chemical composition, and this can affect the fate of some contaminants in the water. For example, soils that are high in organic content (such as many clays and silts) can react readily with various waterborne pollutants, while soils that are low in organic content (such as gravels and sands) are often relatively inert. Metals and many organic contaminants often exhibit a strong affinity for soils that are high in organic content and may actually *sorb* - or attach - to the individual soil particles. Sorption is not necessarily a permanent phenomenon, and often contaminants that have sorbed to soil particles will de-sorb back into the water due to a change in environmental conditions. A shift in the water's pH, for example, can generate such a change in affinity.

Like the surfaces and roots of wetland plants, the soil particles in a wetland also provide a surface for the microorganisms active in pollutant degradation to attach

themselves to. Finally, wetland soils filter suspended solids out of passing waters, and they contain and store the nutrients that are generated from decomposing plant and animal matter in the wetland; such nutrients are essential to support new plant and animal growth.

Organic Contaminants

While there are a number of processes that can affect contaminant fate in the environment, organic contaminants are particularly susceptible to the transformation, volatilization, and sorption pathways (Sawyer et al., 1994).

Transformation reactions can occur through biotic and abiotic mechanisms. Bacteria can transform contaminants through microbial processes, and this is frequently the more rapid of the transformation mechanisms.

Transformation reactions relevant to organic contaminants in the environment include oxidation, reduction, hydrolysis and photolysis. Of these, oxidation, reduction, hydrolysis reactions may occur through biotic and abiotic mechanisms (Sawyer et al., 1994).

Volatilization is the process that occurs when a contaminant vaporizes upon being exposed to the atmosphere. PCE, as well as all of its chlorinated degradation products,

is highly volatile, although like other organic compounds it is generally less volatile at lower temperatures (Sawyer et al., 1994).

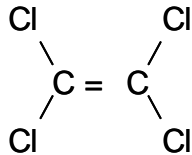
Sorption was discussed earlier in the chapter. It is a process by which a contaminant sorbs or attaches to a solid particle's surface. Sorption is a general term that is often used to describe natural processes (rather than engineered processes where the terms adsorption and absorption carry more precise meanings). Hydrophobic organics like PCE can be particularly susceptible to such a fate in wetlands due to the high organic content of many hydric soils (Sawyer et al., 1994; Charbeneau, 2000). As indicated earlier, sorption is not necessarily a permanent phenomenon: contaminants can sorb to soil particles and desorb back into the water as a result of changing environmental conditions. A contaminant sorbed to a soil particle's surface, however, may be more available to the microorganisms that are also resident there.

PCE Degradation

The transformation of PCE to un-chlorinated substances is believed to occur through different biologically mediated mechanisms, each requiring the right environmental

conditions at the right stage in the process. A basic understanding of how PCE is believed to degrade in the environment will set the stage for why it is important to understand the flow of water through a wetland designed for its remediation.

PCE is a chlorinated ethene that is represented as follows:



As seen in this representation, PCE is a fully chlorinated ethene. If a molecule of PCE loses a chlorine molecule and gains a hydrogen molecule, it becomes trichloroethylene (TCE). If PCE exchanges two chlorine molecules for two hydrogen molecules, it becomes dichloroethylene (DCE). The chlorinated ethene with only one chlorine molecule and three hydrogen molecules is known as chloroethylene or vinyl chloride. The de-chlorination of PCE is known to occur sequentially, and a conceptual pathway for PCE de-chlorination is demonstrated in figure 2-1.

Although similar in their basic structure, these related chlorinated ethenes degrade through different processes and under different environmental conditions.

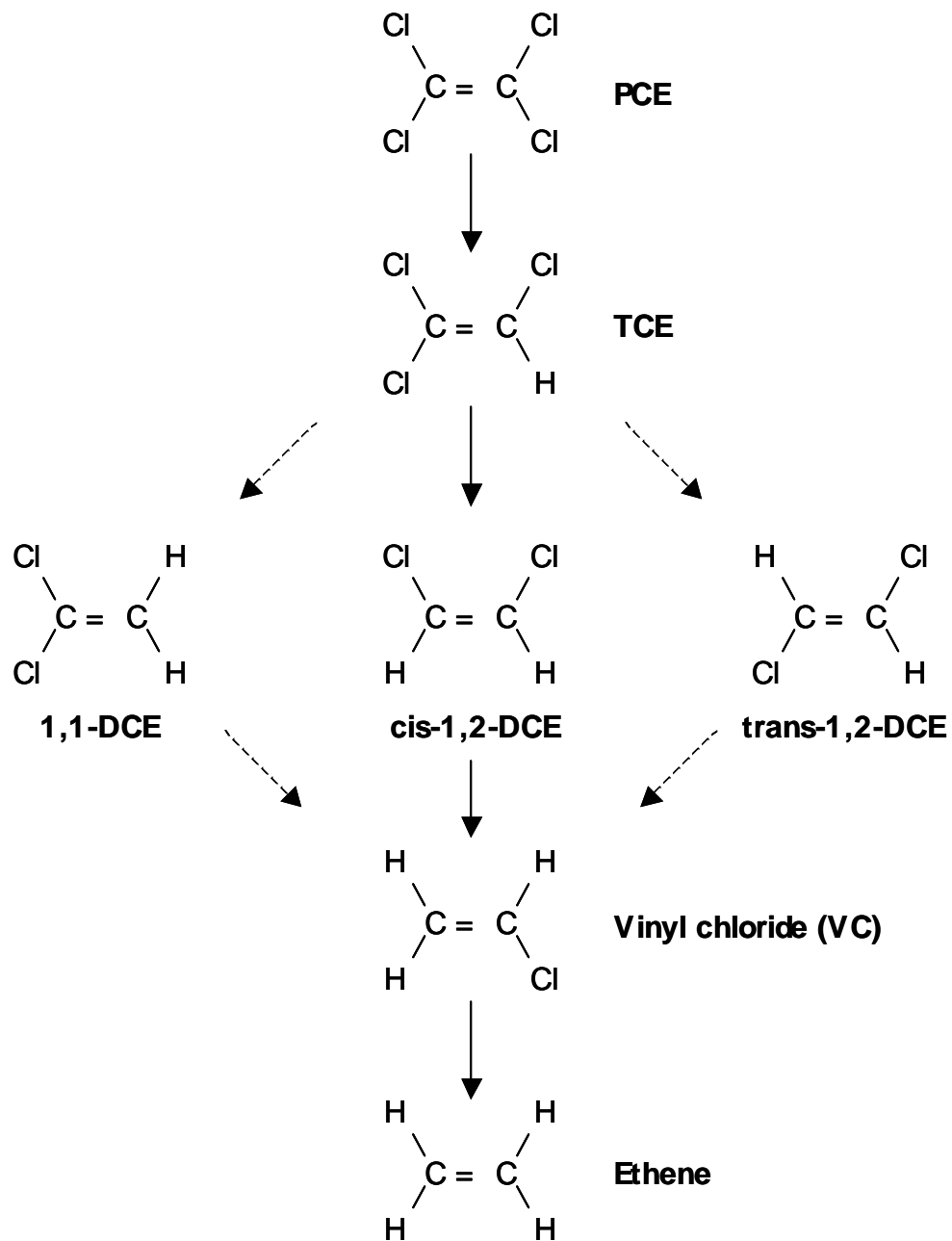


Figure 2-1. Proposed PCE Dechlorination Pathway by PCE/TCE Dechlorinating Granules. (Source: Fogel et al. "PCE Treatment in Saturated Soil Columns with Methanogens" in *Bioremediation of Chlorinated Solvents*. Eds. R.E. Hinchee, A. Leeson, and L. Semprini. Columbus, OH: Battelle Press, 1995.)

Hoefer (1999) summarizes the likely *oxidation* and *reduction* reactions that occur as the result of microbial activity. Such reactions may produce energy for the microbes as the intended result of the their enzymatic activity, or they may be *co-metabolic* and occur as the result of enzymatic activity intended for other purposes.

Of the chlorinated ethenes, vinyl chloride can readily degrade under aerobic conditions as an energy-yielding oxidation reaction. TCE, cis-DCE and vinyl chloride can degrade as a result of co-metabolic oxidations, while all of the chlorinated ethene variants can degrade under the reducing conditions present in anaerobic environments. The initial dechlorination of PCE is strictly limited to anaerobic conditions, however, and can only occur as a co-metabolic reductive reaction (Lee et al., 1998).

In addition to these biotic transformation pathways, the chlorinated ethenes may also be able to exit the wetland system as a result of volatilization. This may be true especially for vinyl chloride which has a particularly high *Henry's constant* value relative to the other chlorinated ethenes. (The Henry's constant reflects the degree to which a substance will partition between an aqueous and gaseous state (Sawyer et al., 1994); the higher

the Henry's constant, the greater the tendency to volatilize or partition to a gaseous state.) Also, the tendency for these organic contaminants to sorb to soil particles is high given their hydrophobic nature. While, as indicated, sorption is not necessarily a permanent condition, contaminants sorbed to soil particles in the wetland sediments may be more available to microorganisms that are resident and active there.

Exactly what processes are taking place in the Wright-Patterson Air Force Base wetland treatment cells, as well as where they are taking place, is a matter of ongoing research. The volatilization, sorption and transformation reaction pathways may all be relevant. Transformation processes do require time, however, and the amount of time that water remains in or transits through the wetland system could determine the effectiveness of the processes responsible for PCE degradation. It is reasonable to assume that if the flow of groundwater through the wetland cells occurs too fast, the PCE will have less of an opportunity to react with the anaerobic bacteria responsible for cleaving off the first chlorine molecule. Likewise, if the flow of groundwater occurs predominately through preferential flow paths, only a small portion of

the wetland may be active in de-chlorinating the PCE and related degradation products. Any non-uniform flow of water in the treatment cells will reduce their efficiency as will any short-circuiting of the wetland media.

Groundwater Flow

Various physical properties influence the flow of water through soil. In wetlands, the type of soil, the strength of hydraulic gradients and pressures, and other factors such as the roots of plants will impact the manner and rate at which water moves through the wetland sediments.

Soil Composition and Porosity. Soils are a porous media. The observation of ocean waters seeping into sand on a beach illustrates this fact. A representative volume of soil consists of both solid particles and void spaces. Both liquids (normally water) and gasses (normally air) can occupy the spaces that are empty or *void* of the solid soil particles. If the voids in a soil are 100% full of water, the soil is called *saturated*. Soils that are not fully saturated are labeled *unsaturated*. While this distinction may be obvious, it distinguishes between applicable groundwater equations.

The property of soil that characterizes the amount of void space relative to total soil volume is *porosity*.

Porosity, n , equals

$$n = \frac{V_v}{V_T} \quad (1)$$

where V_v is volume of the void spaces and V_T is the total soil volume. The intrinsic properties of a soil define its *primary porosity*, while various other influences, such as the roots of plants or fractures in rocks, contribute to its *secondary porosity*. Collectively these factors define the percentage of water a fully saturated volume of soil can hold.

Another aspect of porosity is also important to note. When water moves through the ground, it moves through some but not all of the soil pores. Some of the pores may be isolated and not facilitate water movement. The *effective porosity*, n_e , of a soil represents the volume of interconnected voids in a given volume of soil through which the water is actually able to flow. A soil's effective porosity will be less than the overall porosity for the soil, especially for fine-grained sediments (Kresic, 1997).

Darcy's Law. Darcy's law can be used to analyze the flow of water through wetland sediments. Darcy's Law determines the amount of water that moves through a representative volume of soil under saturated conditions. Darcy's law is defined as

$$Q = -K \frac{dh}{dl} A \quad (2)$$

where Q is the flow rate or discharge (in units of cubic length per unit time [L^3/T]), K is hydraulic conductivity [L/T], dh/dl is hydraulic gradient [dimensionless], and A is area [L^2]. (The negative convention recognizes that water flows from a position of higher to lower hydraulic head.) Another usage of Darcy's law defines the specific discharge or *Darcy velocity* as $q = Q/A$ in units of [L/T]. Whereas Q reflects the *amount* of water that can move through a representative volume of soil per unit of time, q reflects the *rate* at which the water moves across a given cross-sectional area.

The Darcy velocity is a measure of velocity on a macro or superficial scale. In reality, groundwater doesn't move through the entire cross section of a representative soil volume. The Darcy velocity neglects the existence of the microscopic pores within a representative volume of soil through which water actually flows. Because the pores

represent only a fraction of the total soil volume, water will move through the pores at a rate faster than that reflected by the Darcy velocity. Freeze and Cherry (1979) define this rate as

$$v_L = \frac{q}{n} \quad (3)$$

where v_L is *average linear velocity* [L/T], q is Darcy velocity [L/T], and n is porosity [unitless]. Kresic (1997) presents a similar variable but substitutes effective porosity (n_e) for overall porosity.

Although it can be derived analytically, groundwater flow calculations based on Darcy's law are generally only accurate to within an order of magnitude precision. This is due to the inherent variability that exists in nature. For example, even very similar soils can be observed to move water at different rates. For groundwater flow, such variability manifests itself in the hydraulic conductivity parameter in Darcy's law.

Hydraulic conductivity. Hydraulic conductivity represents the ease at which water can move through a representative volume of soil (U.S. EPA, 1992). Hydraulic conductivity depends on both the properties of the liquid moving through the soil pores and on the properties of the soil that yield a unique configuration of pore spaces. A

fluid such as motor oil, for example, will move through a porous media at a slower rate than a less viscous fluid such as water. In a similar manner, a soil comprised of rough, angular particles will exhibit more drag on passing water molecules than a soil comprised primarily of smooth, spherical particles. The contribution of the liquid and soil particles can be seen in

$$K = \left(\frac{\rho g}{\mu} \right) k \quad (4)$$

where

K = hydraulic conductivity [L/T]

ρ = fluid density [M/L³]

μ = viscosity [M/(L*T)]

g = gravity [L/T²]

k = intrinsic permeability [L²]

In equation (4), the grouping of variables inside the parentheses ($\rho g/\mu$) represents the properties of the fluid that contribute to hydraulic conductivity, while a soil's *intrinsic permeability, k*, reflects the influence of the soil particles on the ease at which a fluid moves through a porous media.

Hydraulic conductivity can vary with respect to location and direction. If a soil's hydraulic conductivity

is constant with respect to location, the soil is said to be *homogeneous* (otherwise it is *heterogeneous*). If the horizontal and vertical components of a soil's hydraulic conductivity are constant with respect to direction, a soil is labeled *isotropic* (otherwise it is *anisotropic*).

Homogenous and isotropic soil conditions permit relatively easy calculations of groundwater flow. Soils that diverge from the homogenous, isotropic ideal are commonplace however. When layers of different homogenous and isotropic soils overlay each other in the same area of interest, the condition is termed *layered heterogeneity*. To account for the differing hydraulic conductivity values between soil layers, the formation can be treated as a single composite layer with notional horizontal and vertical components of hydraulic conductivity. (Figure 2-2 illustrates this concept.) The horizontal and vertical components of hydraulic conductivity for this composite layer are determined by

$$K_h = \sum_{i=1}^n \frac{K_i b_i}{B} \quad (5a)$$

$$K_v = \frac{B}{\sum_{i=1}^n b_i / K_i} \quad (5b)$$

where n is the number of layers.

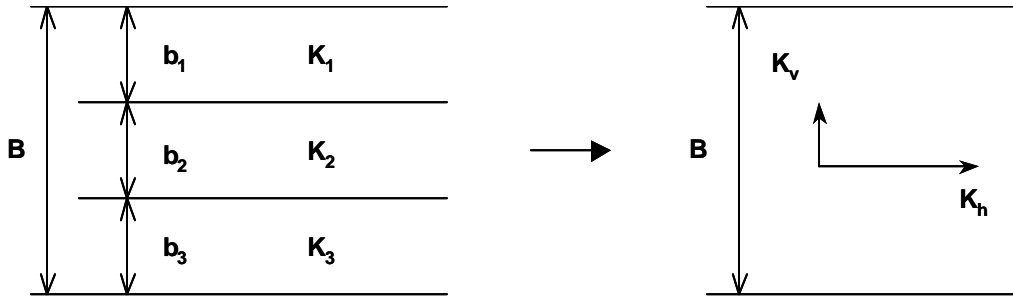


Figure 2-2. Layered Heterogeneity. (Adapted from Freeze and Cherry, 1979)

Anisotropic soil conditions also complicate analysis of groundwater flow. For anisotropic conditions, the one-dimensional form of Darcy's law (equation 2) may be written in three dimensions as

$$v_x = -K_x \frac{\partial h}{\partial x} \quad (6a)$$

$$v_y = -K_y \frac{\partial h}{\partial y} \quad (6b)$$

$$v_z = -K_z \frac{\partial h}{\partial z} \quad (6c)$$

where v_x , v_y and v_z represent directional components of an overall velocity vector v_s ; K_x , K_y and K_z represent the hydraulic conductivity values in these directions; and $\partial h/\partial x$, $\partial h/\partial y$, $\partial h/\partial z$ represent the partial derivatives of the hydraulic head h in the x , y and z directions. This *simplification* for anisotropic conditions applies as long as the x , y and z coordinate axes coincide with the

principal directions of hydraulic conductivity (Freeze and Cherry, 1979).

Various factors can influence the conductivity of wetland sediments. The intrinsic properties of the soil have a major influence; the presence of clay particles, for instance, will generally reduce hydraulic conductivity. The temperature of the environment will affect the water's viscosity, with higher temperatures resulting in lower viscosities and a faster moving liquid. Compaction of the wetland sediments could degrade hydraulic conductivity by reducing the pore volume available for fluid flow. The presence of waterborne sediments and decomposing plant and animal matter will add fines to the wetland media and reduce the hydraulic conductivity of the soil through sedimentation. The roots of plants appear to degrade hydraulic conductivity by forming a very dense mass around which the water prefers to flow (Bowmer, 1987; Fisher, 1990; McIntyre and Riha, 1991; Hilton, 1993; Brix, 1994; Kadlec and Knight, 1996; and Marsteiner, 1997). Most of these studies concern the effects of roots in sand or gravel based constructed treatment wetlands, however, and Kadlec and Knight (1996) suggest that reductions in fine-grained sediments may not be significant due to the already

low hydraulic conductivities of these soils compared to the more permeable medias. The main concern over potential soil clogging from sedimentation and root zone development is that, eventually, hydraulic conductivity could degrade to such an extent where the water in the wetland will seek the path of least resistance and short-circuit portions of the subsurface media.

Hydraulic conductivity can be measured in the field and in the laboratory. Fetter (1994) discusses relevant tests but cautions that the results of laboratory tests may differ from those obtained under field conditions. Ward and Dorsey (1995) indicate that the results of laboratory tests yield lower hydraulic conductivity estimates than in-situ tests, while Herzog and Morse (1990) report that laboratory and field tests on fine grained sediments can vary by more than two orders of magnitude. In any case, the results obtained from any hydraulic conductivity test are merely order of magnitude estimates of a soil property that is highly variable in nature. Methods used to measure hydraulic conductivity in this study are presented in the following chapter.

Hydraulic Head and Gradient. A fundamental concept of groundwater flow is that water moves from a position of

higher hydraulic head (or energy) to a position of lower hydraulic head. This principle reveals itself by the hydraulic gradient variable (dh/dl) in equation (2).

Hydraulic gradient is defined as the change in the potentiometric surface divided by the horizontal distance over which that change is observed. The potentiometric surface is the elevation to which water would rise in an observation well or piezometer that penetrates an aquifer. The hydraulic gradient, therefore, is merely the slope of hydraulic head plotted against horizontal distance. Figure 2-3 illustrates this concept.

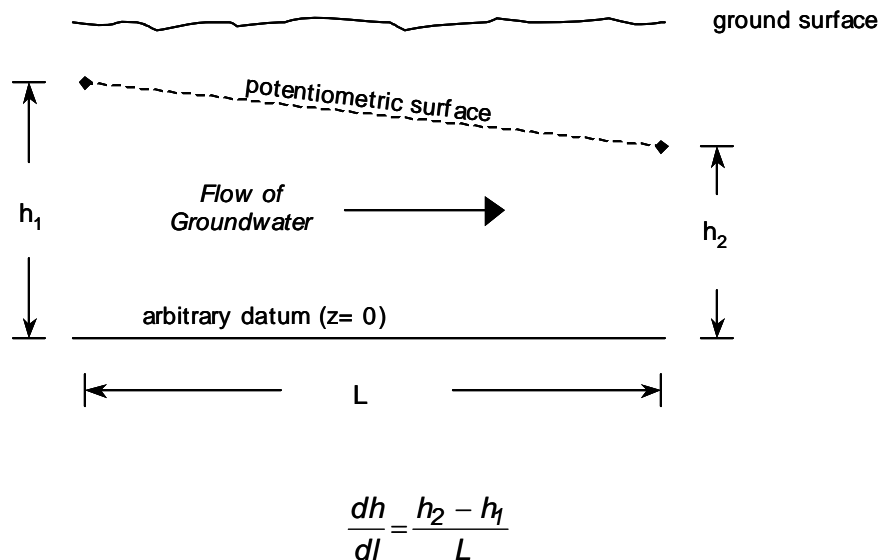


Figure 2-3. Hydraulic Gradient.

Hydraulic head consists of three components: pressure head, elevation head, and velocity head. *Pressure head* is the energy available to a particle of water due to external forces being exerted upon it. Pressure head is positive at depths lower than the water table and negative above it. (The water table is assigned an atmospheric pressure value of 0.) *Elevation head* is the potential energy available to a particle of water due to its height above some arbitrary datum point. *Velocity head* is the energy inherent in a water particle due to the particle's velocity. Total hydraulic head is represented as

$$h_T = h_z + h_p + h_v \quad (7)$$

where h_T is total hydraulic head, h_z is elevation head, h_p is pressure head, and h_v is velocity head. Additionally,

$$h_z = z \quad (8)$$

$$h_p = \psi \quad (9)$$

$$h_v = \frac{v^2}{2g} \quad (10)$$

where z is the elevation above the datum point [L], ψ is the distance of fluid surface over the point of measurement [L], v is velocity [L/T], and g is gravity [M/T²]. Due to the characteristically slow velocity of groundwater flows, the velocity head element of the total hydraulic head

equation is negligible relative to the other two components. Figure 2-4 depicts the contribution of the pressure and potential head components to total hydraulic head.

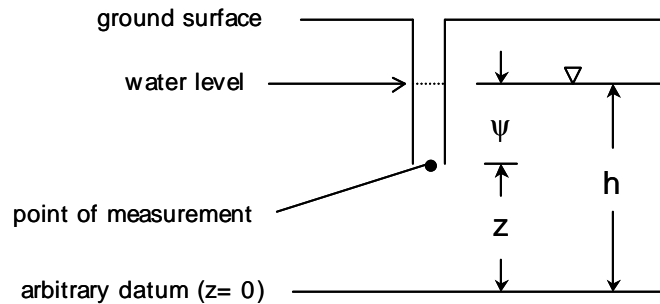


Figure 2-4. Hydraulic Head, Pressure Head, and Elevation Head for a Field Piezometer. (Source: Freeze and Cherry, 1979). Note: the contribution of velocity head ($v^2/2g$) to total hydraulic head (h) is negligible compared to the pressure head (ψ) and elevation head (z) and, therefore, is not depicted.

Limits of Darcy's Law. Darcy's law does not apply for extremely slow flows - or "flows through low-permeability sediments under very low gradients" - and it does not apply to flows that approach turbulent conditions (Freeze and Cherry, 1979). The low-end limit is difficult to quantify, but the high-end limit begins with *Reynolds numbers* of 10 and higher. For the purposes of this discussion, the Reynolds number, R_e , for groundwater flow is defined as

$$R_e = \frac{\rho v d}{\mu} \quad (11)$$

where ρ is the fluid density [M/L³], μ is the fluid viscosity [M/(L*T)], v is the specific discharge [L/T], and d is the mean grain diameter [L].

Groundwater Flow Determination

Hydraulic head measurements can be used to determine the flow patterns of water in the ground. Because water flows from a position of higher to lower hydraulic head, piezometric measurements can indicate the direction of groundwater flow and permit the construction of flow nets.

Flow Direction. Most groundwater literature assumes horizontal flow (i.e. the horizontal component of flow greatly exceeds that in the vertical direction as depicted in Figure 2-3.) The assumption of horizontal flow is generally true in aquifers - or highly permeable sediments - relative to confining layers. Highly permeable layers act as conduits and facilitate horizontal flows while layers of low permeability impede flow and encourage water to move vertically along the most direct route out of the media. Areas of *recharge* - where waters recharge the ground below - or *discharge* - where water discharges into the area - can also have substantial vertical gradients.

Natural springs are another phenomena where the vertical component of flow can be significant.

Observation wells and piezometers sited at the same elevation will exhibit head loss in the direction of flow provided the movement of water is predominately horizontal. If a significant vertical component to flow is suspected, the use of *nested piezometers* can reveal such a phenomenon. A nest of piezometers is a collection of piezometers that penetrate a groundwater formation in very close proximity to each other but at different depths. The existence of an upward vertical gradient will manifest itself in hydraulic head readings that increase with piezometer depth (Sprecher, 2000). In other words, the static water level in deep piezometers will exceed that in shallow piezometers of the same nest. (The opposite situation would characterize a recharge zone.) For a wetland with a water table above ground, the existence of an upward vertical gradient will manifest itself in piezometer water levels that are above the surface of the water (Haynos, 1991).

Flow Nets. A flow net is a graphical representation of water particle trajectories. A flow net consists of representative particle flow paths (or flow lines) that traverse equipotential lines in the direction of decreasing

hydraulic head. Equipotential lines represent the locus of all points of equal hydraulic head. The combination of equipotential and particle flow lines results in a flow net. Figure 2-5 is an example of a simple flow net.

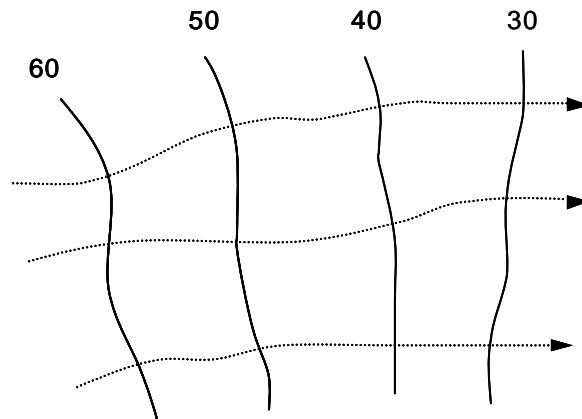


Figure 2-5. Simple Flow Net

Various useful references present techniques for flow net construction (Freeze and Cherry, 1979; Cedergren, 1989; Fetter, 1994; Kresic, 1997). All of these authors remark that the construction of flow nets is somewhat of an art. For homogeneous and isotropic conditions, the procedures for flow net construction are as follows:

(1) Flow lines intersect equipotential lines at right angles to form a mesh of curvilinear squares.

(2) Equal gradients of hydraulic head separate consecutive equipotential lines as indicated in Figure 2-5.

(3) Equipotential lines form right angles with impermeable boundaries while flow lines run parallel to them (there can be no flow across an impermeable boundary).

(4) Equipotential lines run parallel to constant head boundaries while flow lines form right angles with them.

(5) Flow lines form oblique angles with water table boundaries where discharge or recharge conditions exist but remain parallel to it in the absence of discharge/recharge.

In heterogeneous and isotropic systems, flow lines intersect equipotential lines at right angles within formations of constant conductivities, but they refract at boundaries of dissimilar conductivities. When crossing a conductivity boundary, groundwater obeys the tangent law where

$$\frac{K_1}{K_2} = \frac{\tan(\theta_1)}{\tan(\theta_2)} \quad (12)$$

as demonstrated in Figure 2-6. In Figure 2-6, the water is moving from a media of lower to higher hydraulic conductivity.

Because of the refraction of flow lines, curvilinear squares cannot exist throughout the entire region of interest in heterogeneous systems. If a flow net is drawn with curvilinear squares in the region of K_1 , for instance,

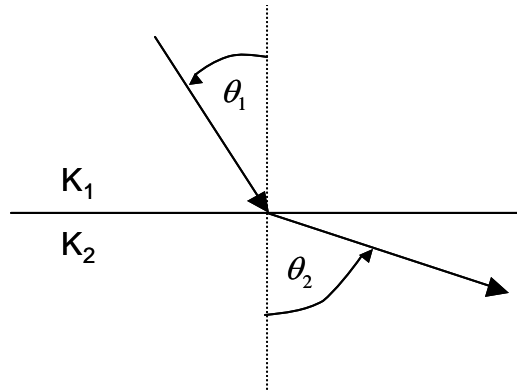


Figure 2-6. Refraction of a Flow Line Crossing a Hydraulic Conductivity Boundary (Adapted from Fetter, 1994).

rectangles will result in areas where $K \neq K_1$ (Freeze and Cherry, 1979).

Anisotropic conditions further complicate flow net construction. In anisotropic conditions, flow lines do not traverse equipotential lines at right angles. In anisotropic systems, the angle of intersection can be determined graphically by using the *inverse hydraulic conductivity ellipse* (Freeze and Cherry, 1979). With reference to Figure 2-7, the technique presented by Fetter (1994) is as follows:

- (1) Draw an inverse hydraulic conductivity ellipse with semi-axes oriented along the major axes of anisotropy.
- (2) Draw an equipotential line (dashed line) through the origin of the ellipse.

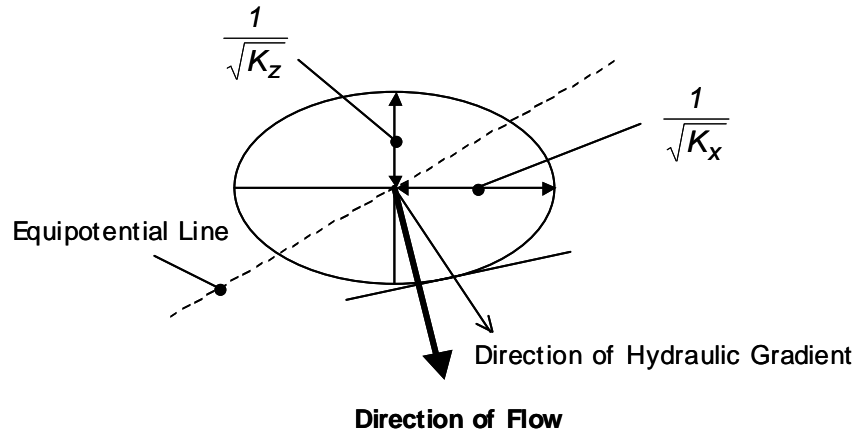


Figure 2-7. Method to Determine Direction of Flow in Anisotropic Media (Source: Fetter, 1994).

(3) Draw an arrow (thin arrow) in the direction of the hydraulic gradient that emanates from the origin of the ellipse and is perpendicular to the equipotential line.

(4) Draw a tangent through the point on the ellipse where the hydraulic gradient arrow intersects the ellipse.

(5) Draw an arrow (bold arrow) from the origin of the ellipse that intersects the tangent line at a right angle.

When properly constructed, flow nets can facilitate calculation of flow rates and hydraulic residence times provided the hydraulic conductivity of the media is known. This is possible by applying Darcy's law for flow between flow lines realizing that the quantity of water moving between flow lines remains constant throughout the system.

The sum of the individual flow segments, then, equals the flow through the entire system. This graphical method of flow calculation is possible for relatively simple systems that diverge little from the homogeneous and isotropic ideal. For highly complex systems where heterogeneous and anisotropic conditions prevail, such a method is seldom practical however. Where quantitative analysis is not possible, flow nets can still provide valuable qualitative insight into groundwater flow and behavior. For example, equipotential lines closely spaced can indicate regions of low conductivity where the aquifer thickness remains constant (Kresic, 1997). Likewise, converging flow lines can indicate discharge areas while flow lines that diverge can signal recharging conditions (Fetter, 1994).

Vertical gradients complicate the interpretation of potentiometric contour maps. If a significant vertical element to groundwater flow is suspected, vertical contour profiles are necessary to characterize flow throughout the three-dimensional region.

Various computer programs facilitate potentiometric contouring of hydraulic head. Surfer® by Golden Software is a popular contouring program that permits quick display of groundwater contours. Surfer is capable of numerous

interpolation options (e.g. triangulation with linear interpolation and geostatistical methods such as kriging) to fill in *missing* data and produce contours of equal hydraulic head. The potentiometric contour maps included in this study are generated using Surfer.

Groundwater Flow Analysis

A development of Darcy's law in three dimensions provides the basic equations for analytical solution and numerical modeling of groundwater flow systems.

Development of Darcy's Law in Three Dimensions. The one-dimensional form of Darcy's law can be applied to three-dimensions by considering the flow through a representative control volume (Freeze and Cherry, 1979). By applying a conservation of mass approach, the flow through a representative control volume is illustrated in Figure 2-8 where ρ is the fluid density; v_x , v_y and v_z are the velocity vectors of the fluid in the x, y, and z directions, respectively; and the operators $\partial/\partial x$, $\partial/\partial y$, and $\partial/\partial z$ represent the change in the product of fluid density and velocity in the x, y, and z directions, respectively.

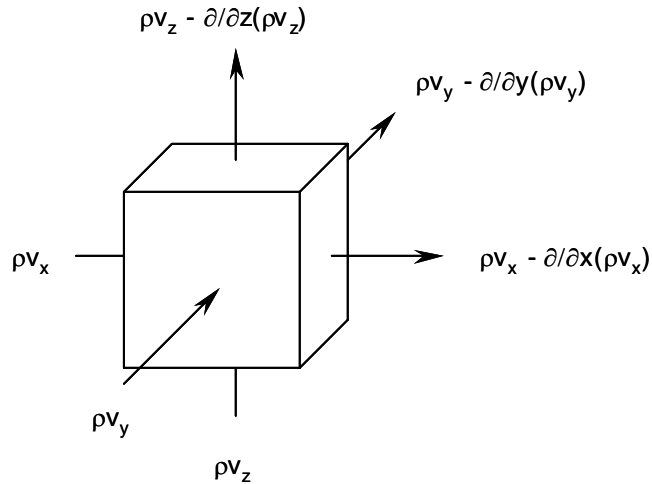


Figure 2-8. Three-dimensional Flow Through a Representative Control Volume.

A mass balance for steady-state flow (i.e. where hydraulic head does not change with time) yields

$$-\frac{\partial}{\partial x}(\rho v_x) - \frac{\partial}{\partial y}(\rho v_y) - \frac{\partial}{\partial z}(\rho v_z) = 0 \quad (13)$$

By assuming an incompressible fluid - Freeze and Cherry (1979) demonstrate this is a valid assumption for groundwater flow - and by substituting the directional equivalent of Darcy's law for v_x , v_y and v_z vectors (equations 6a, 6b, and 6c, respectively), Equation (13) becomes

$$\frac{\partial}{\partial x} \left(K_x \frac{\partial h}{\partial x} \right) + \frac{\partial}{\partial y} \left(K_y \frac{\partial h}{\partial y} \right) + \frac{\partial}{\partial z} \left(K_z \frac{\partial h}{\partial z} \right) = 0 \quad (14)$$

for an anisotropic media. For homogenous and isotropic conditions, $K_x = K_y = K_z$ and Equation (14) reduces to

$$\frac{\partial^2 h}{\partial x^2} + \frac{\partial^2 h}{\partial y^2} + \frac{\partial^2 h}{\partial z^2} = 0 \quad (15)$$

Equation (15) is a well-known partial differential equation known as the Laplace Equation.

Freeze and Cherry (1979) present a similar, but slightly more rigorous, derivation for transient flow in anisotropic conditions to obtain

$$\frac{\partial}{\partial x} \left(K_x \frac{\partial h}{\partial x} \right) + \frac{\partial}{\partial y} \left(K_y \frac{\partial h}{\partial y} \right) + \frac{\partial}{\partial z} \left(K_z \frac{\partial h}{\partial z} \right) = \frac{S}{b} \frac{\partial h}{\partial t} \quad (16)$$

where S is the *storage coefficient*, b is the average aquifer thickness for confined systems or average saturated thickness for unconfined systems, and $\partial h/\partial t$ represents the change in hydraulic head per change in time. The storage coefficient is a dimensionless measure of the volume of water per unit surface area stored or expelled from storage for a unit change in head (Fetter, 1994). In confined aquifers, water is stored or expelled from storage due to compression or expansion of the mineral skeleton and liquid and

$$S = b S_s \quad (17)$$

where S_s is specific storage [L^{-1}]. Specific storage, therefore, is a measure of the amount of water stored or expelled from storage due to compression or expansion of

the mineral skeleton per volume of media for a unit change in head (Fetter, 1994). Fetter (1994) demonstrates that specific storage is represented by

$$S_S = \rho_w g (\alpha + n\beta) \quad (18)$$

where

ρ_w = density of water [M/L³]

g = gravity [L/T²]

α = compressibility of the aquifer skeleton [1/(M/LT²)]

n = porosity [L³/L³]

β = compressibility of water [1/M/LT²]

Values of specific storage are generally very small - on the order of 10⁻⁴ ft⁻¹ or less. For homogenous and isotropic conditions, Equation (16) reduces to

$$\frac{\partial^2 h}{\partial x^2} + \frac{\partial^2 h}{\partial y^2} + \frac{\partial^2 h}{\partial z^2} = \frac{S_S}{K} \left(\frac{\partial h}{\partial t} \right) \quad (19)$$

for transient flow in confined systems.

In unconfined aquifers, water is produced from gravity drainage of the pore spaces as the water table declines in addition to the water being expelled by the compressing mineral skeleton and expanding fluid. For unconfined systems,

$$S = b S_S + S_y \quad (20)$$

where S_y is specific yield [dimensionless]. Specific yield - or drainable porosity - is a ratio of the volume of water that will drain under the force of gravity from a saturated volume of soil. Because the specific yield is generally orders of magnitude larger than the product of bS_s , equation (20) is often approximated as

$$S = S_y \quad (21)$$

for unconfined aquifers. (Fetter (1994) cautions, however, that values for specific yield may approach the same order of magnitude as the product of bS_s in fine-grained sediments.) Although the saturated thickness of unconfined systems can change with time, if the change is small compared to the average aquifer thickness then the general flow equation for unconfined, transient conditions can be approximated by

$$\frac{\partial}{\partial x} \left(K_x \frac{\partial h}{\partial x} \right) + \frac{\partial}{\partial y} \left(K_y \frac{\partial h}{\partial y} \right) + \frac{\partial}{\partial z} \left(K_z \frac{\partial h}{\partial z} \right) = \frac{S_y}{b} \frac{\partial h}{\partial t} \quad (22)$$

in anisotropic systems and

$$\frac{\partial^2 h}{\partial x^2} + \frac{\partial^2 h}{\partial y^2} + \frac{\partial^2 h}{\partial z^2} = \frac{S_y}{bK} \left(\frac{\partial h}{\partial t} \right) \quad (23)$$

in homogeneous and isotropic systems (Fetter, 1994).

Homogenous and isotropic soil conditions permit relatively easy calculations of groundwater flow. Under

such conditions, analytical solutions - which combine the foregoing differential equations with relevant boundary conditions - are fairly straightforward and normally the method of choice for quantitative analysis. Soils that diverge from the homogenous, isotropic ideal are commonplace however, and aquifers characterized by complex heterogeneities and anisotropic conditions require the use of numerical methods for solution.

Numerical Models. Numerical models recast relevant differential equations (i.e. Equations 14, 16 or 22) in algebraic form and apply numerical approximations to achieve approximate solutions (Fetter, 1994). A numerical model solves one approximation for each cell in a subdivided area of interest, essentially solving a series of x equations and x unknowns (where x is the number of cells in the model). The inherent complexity of numerical models requires the use of computers for solution. The two most common types of numerical modeling approaches are the finite difference method and the finite element method. Both methods partition the area of interest into a grid that attempts to characterize the actual formation with relevant hydrological parameters and boundary conditions. The finite difference method is simpler to conceptualize

and use; it divides the aquifer into a grid of rectangular cells and is best suited to simple aquifer geometries. The finite element method solves over a grid of irregularly shaped triangles or quadrilaterals; although it is more difficult in practice, it can accommodate complex hydrological settings such as multiple principle directions of anisotropy (Freeze and Cherry, 1979; U.S. EPA, 1992).

To build a numerical model, the modeler assigns known parameter values (such as hydraulic conductivity and porosity) and boundaries (such as no flow or constant head) at relevant points or cell *nodes* in the model. Once built, the modeler attempts to simulate the hydraulic head distribution of an observed reference condition through various runs of the model; the modeler *calibrates* the model by adjusting the input parameter values or boundary conditions to *correct* deviations from the observed conditions. Once calibrated, the modeler must then *verify* the model through simulations under a different set of observed conditions (such as a flood event or drought for instance). A verified model is one that can *accurately* mimic many observed conditions. (The *root mean square error* between the calculated and observed values of hydraulic head provides a quantitative assessment of model

accuracy.) The strength of a verified model is that it can be used to explore the effect of inputs or events yet to be observed.

MODFLOW. MODFLOW is a finite difference model that was developed by McDonald and Harbaugh (1988) for the U.S Geological Survey. MODFLOW is one of the more popular numerical modeling computer models, and its accuracy has been verified against numerous applications (Pohll, 1993; Fetter, 1994; Kresic, 1997). MODFLOW is a highly flexible numerical modeling application: it contains a couple of basic modules to run the numerical simulations and a number of independent packages or sub-routines to handle features such as constant sources of head, evapotranspiration and recharge, wells, and drains. Kresic (1997) provides a brief overview with application and the authors (McDonald and Harbaugh, 1988) provide a more comprehensive review.

III. Methodology

Overview

A three-dimensional grid of piezometers was installed in wetland cell number one to facilitate the objectives of this study and the research of students investigating PCE degradation in the wetland. Measurements of hydraulic head taken from water levels in the piezometer grid were used to determine the direction and gradients of groundwater flow. Contours of hydraulic head were produced from this data using an automated computer software application to portray the predominate behavior (uniform or otherwise) of flow. Slug and pump test methodologies were employed on numerous piezometers in the grid to obtain in-situ estimates of hydraulic conductivity. Laboratory tests of soil samples collected from various locations in the wetland were used to estimate porosity and effective porosity. The measured hydrological parameters were incorporated into a numerical computer model of the wetland to further explore the behavior and estimate the rate of groundwater flow. The observed values of hydraulic head on a representative day facilitated model calibration, and an alternate set of boundary conditions was used to validate the model.

Sampling Grid

A three-dimensional grid of piezometers was installed in wetland cell number one during the late summer and early fall months of 2001. The grid was designed to accommodate the aims of this study and the efforts of researchers investigating PCE degradation in the wetland. A systematic sampling grid was selected to adequately characterize the flow of groundwater and facilitate numerical modeling; although a systematic grid can introduce bias, it is often preferred in environmental studies for estimating patterns of contamination (Gilbert, 1987) or in this case trends in groundwater flow. Additionally, Millard and Neerchal (2001) point out that the magnitude of such bias varies inversely with grid resolution: the finer the grid, the less the bias. The fine resolution of the sampling grid in this wetland (relative to many groundwater investigations) alleviates some of the concern over introduced bias. Nests of piezometers were employed to verify the existence and magnitude of vertical flow gradients. The nests were spaced to ensure at least three nests per plot of wetland plant species to allow for statistical analysis of contaminant degradation. A total of 66 nests, with three piezometers per nest, were installed as shown in Figure 3-1.

Wetland Cell #1

- (B) A: Top Layer
- B: Middle Layer
- (C) (A) C: Bottom Layer

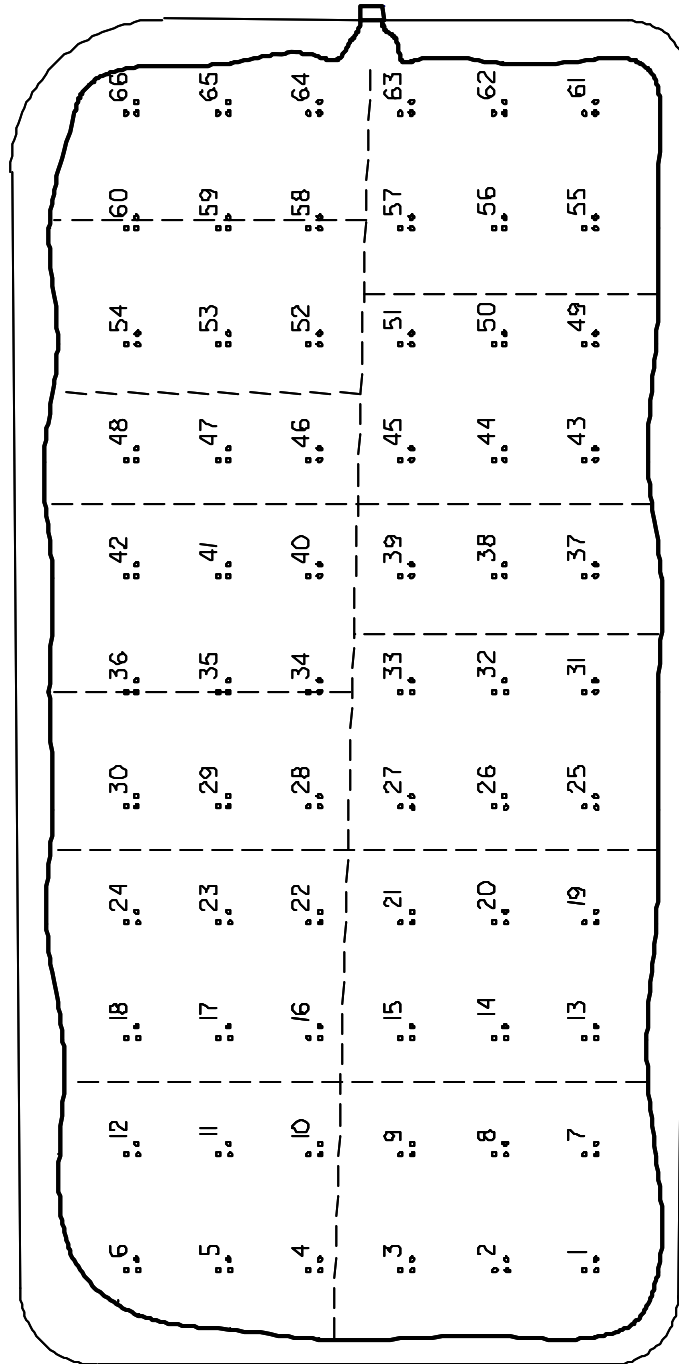
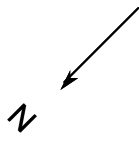


Figure 3-1. Piezometer Placement

Piezometer Installation

A total of 198 Solinst® Model 615S Shielded Drive-Point Piezometers were assembled, measured, and driven into place to construct the sampling grid. The stainless steel piezometers were chosen to minimize the potential of reactions between the organic contaminants under study and the sampling equipment (Neislen and Schalla, 1991); an interior ½" diameter Teflon-lined tube also facilitates a high degree of chemical sampling integrity. Most of the piezometer tips were affixed to ¾" stainless steel riser pipes; galvanized steel risers, which may be more susceptible to corrosion, were used on 13 piezometers in the top layer near the weir end of the wetland when the supply of the more expensive stainless steel pipes ran short. A grid of surveyed-in stakes and string lines ensured the proper placement of the piezometer nests. The measured piezometers were driven down to a predetermined depth below the surface of the wetland and then retracted six inches to separate the shield from the screened portion of the piezometer tip. (The shield feature of this model piezometer reduced the potential for sediment smearing and clogging of the screens during installation.) Figure 3-2

is a profile representation of piezometer placement in the wetland.

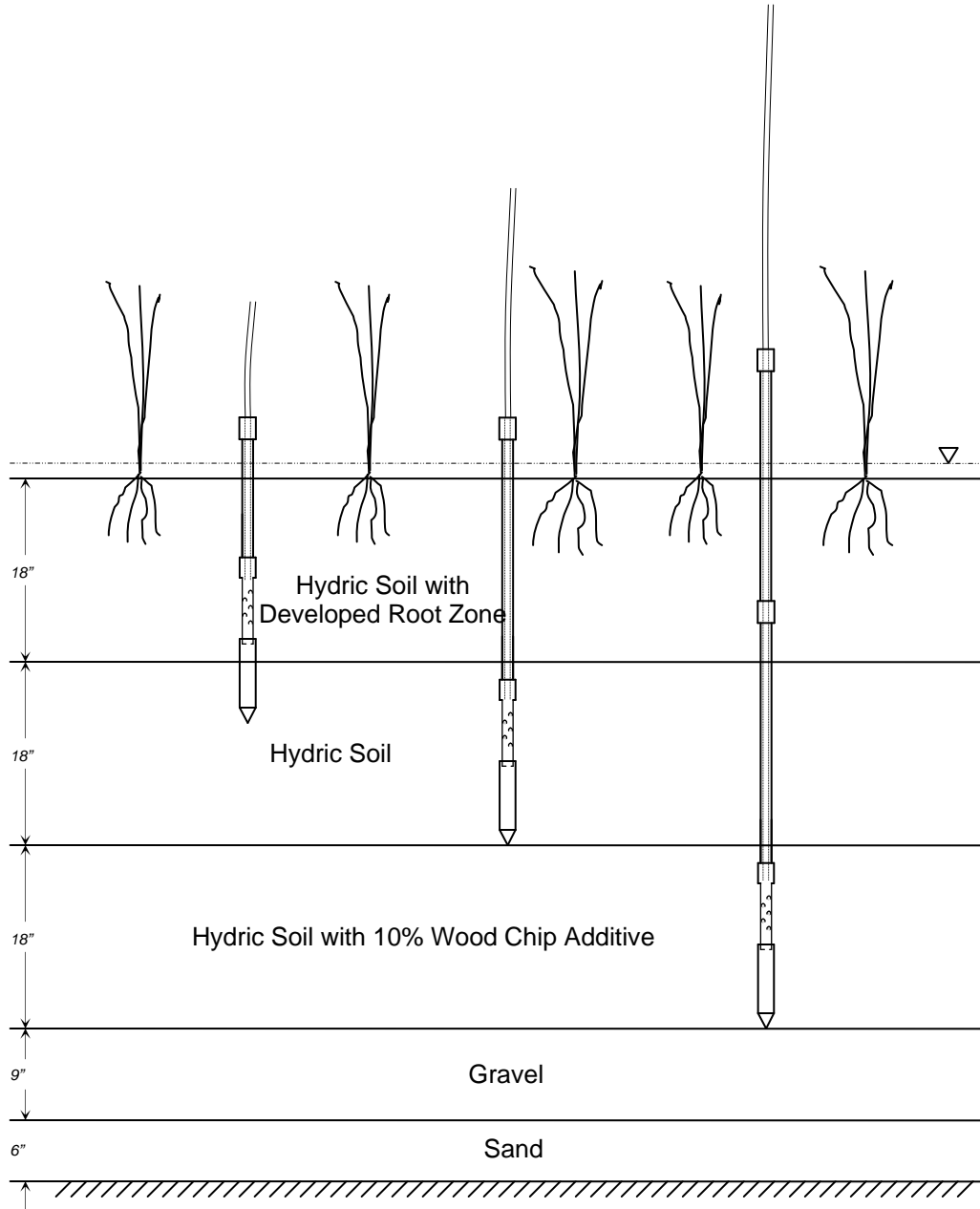


Figure 3-2. Profile View of Piezometer Placement.

Bentonite pellets were placed around the steel riser pipes to form an effective seal between the pipes and the wetland sediments following piezometer installation. This is recommended by various sources to inhibit the vertical migration of water and contaminants along the surface of the pipes (Sprecher, 2000; Nielsen and Schalla, 1991), although the use of bentonite is not without issue. As a clay material, bentonite has a high cation exchange capability, and it generally sets up with a high pH; Nielsen and Schalla (1991) caution that these two factors could interfere with chemical monitoring investigations. Additionally, the presence of a high chloride concentration, as well as some organic solvents, may "interfere with the ability of the bentonite to form an effective seal" (Nielsen and Schalla, 1991). Despite these concerns, the use of a bentonite seal was warranted to provide stability and to keep many of the piezometers from sinking down into the wetland. There was an initial concern over an apparent migration of bentonite from around the riser pipes shortly after flooding of the wetland. Approximately 1½" of quick setting cement was, subsequently, poured around the risers over the bentonite in an effort to impede the suspected migration. In hindsight, a cap of indigenous wetland soil

as recommended by Sprecher (2000) may have worked better than the Quickcrete®, as many of the cement caps cracked shortly after hydration. (Soil caps would not crack upon hydration and, conceptually, they could contain the bentonite in the annular space if thick enough.)

Fortunately, a subsequent eruption of bentonite from under the cracked caps did not ensue, and additional migration has not been an issue.

The piezometers were *developed* approximately one month after installation of the sampling grid. Well development is a common practice used to maximize the efficiency and yield from production wells in aquifers; it often involves the extraction or surging of large amounts of water to clear away fine sediments from the well intake area. Its practice in wetland studies is not as well documented, although Sprecher (2000) comments on its use if clogging has occurred. The requirement to develop the piezometers was initially ignored as the researchers involved with constructing the grid assumed the piezometer shields would prevent clogging during installation.

The decision to develop *some* of the piezometers was based on the requirement of the researchers investigating PCE degradation to be able to purge and extract enough

water for chemical sampling; many of the piezometers in the top and middle layer recovered too slowly and were not yielding enough water to obtain representative samples for analysis. Twenty-six piezometers in the top layer and 10 piezometers in the middle layer were initially developed with this aim in mind. The piezometers were developed by using a Solinst Model 410 Peristaltic Pump in the following manner: the piezometers were pumped dry and then water from the wetland was pumped back in, often until bubbles were observed coming up through the wetland sediments; this process was repeated once again. A decision to develop the remaining piezometers was based on the results of slug tests conducted before and after the initial round of development that differed by more than an order of magnitude. The goal of the second round of development was to homogenize the sampling grid, and the remaining piezometers in the top and middle layers were subsequently developed.

A complete survey of the sampling grid was performed approximately two months after piezometer emplacement using Sokkia Set 2100 total station survey equipment. The survey was conducted by civil engineering personnel of the 88th Airbase Wing, Wright-Patterson Air Force Base and is based

on a second order survey of the base. The longitude and latitude coordinates were converted to local coordinates for use in the numerical computer model.

Piezometric Measurements

Water level measurements were taken on eight separate occasions to observe trends in the contours of hydraulic head. The measurements were taken using a Solinst Model 101M Water Level Meter and sometimes a ruler. Comparison of measurements taken with the Solinst water level meter and ruler provided instrument familiarization and an accurate interpretation of the sound of the meter.

Each round of water level measurements (i.e., 198 piezometers) took about three hours. Although not a true snapshot in time, the duration of each sweep was assumed short enough to ignore slight changes in barometric pressures, at least during periods of clear, steady weather. (Water levels in small diameter piezometers will adjust rapidly to changing barometric pressures and at a much faster rate than that which the pressures are transmitted through the wetland media (Bouwer, 1978.))

The water levels in the piezometers were recorded by measuring down from the top of the Teflon-lined tube. The

distance from the top of the tube to the top of the surveyed, above ground riser coupling permitted calculation of water levels in the piezometers above the reference datum (in this case the approximate elevation of the impervious liner underlying the wetland). The water levels in the piezometers relative to this datum provide the magnitude of hydraulic head at the midpoint elevations of the piezometer screens in the wetland.

Displays of potentiometric contour maps for the three soil layers were generated using the Surfer® groundwater contouring program by Golden Software. In order to compensate for slight vertical deviations in piezometer screen intake elevations, the measured heads were adjusted prior to contouring to generate maps of hydraulic head at the mean midpoint elevation of piezometer screens for each layer of the wetland. Least squares regression was used to establish a linear relationship of hydraulic head versus elevation for each piezometer nest, and the values of hydraulic head were adjusted based on the deviation of the recorded measurements above or below the regression line. The adjusted values were contoured using the default settings of the kriging interpolation option available in

Surfer® (ordinary kriging, linear variogram, nugget effect equal to zero) to interpret the data and generate the maps.

Parameter Estimation

A substantial amount of time and effort was spent conducting hydraulic conductivity tests on the installed grid of piezometers. Sufficient characterization of the wetland was necessary to facilitate construction of the numerical model. Analysis using slug test methodology (description to follow) was generally possible for the top and middle layer piezometers due to the relatively low hydraulic conductivities in this portion of the wetland. Slug tests were not a practical means to measure the conductivity of the bottom layer sediments, however, due to the nearly instantaneous rate of water recovery in these piezometers. As a result, pump tests were attempted on a few piezometers to characterize this portion of the wetland. Tests for porosity were also conducted and are discussed herein.

Slug Tests. The literature is open to interpretation when selecting a relevant slug test for a hydrological setting similar to that of the Wright-Patterson Air Force Base wetland treatment cells. Dawson and Istok (1991)

instruct that the Hvorslev method applies only to confined aquifers while the Bouwer and Rice method is appropriate for unconfined or leaky confined settings. Although the Wright-Patterson wetland cells, conceptually, represent an unconfined hydrological setting, the presence of a piezometric surface above the surface of the water table mimics the behavior of a confined aquifer system. Similarly, while the Bouwer and Rice method measures the rate of recovery in wells relative to the initial water table elevation, the Hvorslev test measures the rate of recovery relative to the initial potentiometric surface. Finally, the Bouwer and Rice test was intended to test hydraulic conductivity from wells, while the Hvorslev test is normally associated with hydraulic conductivity tests using piezometers. In spite of these concerns, the Bouwer and Rice method was selected for use in this study because the geometry of the piezometer intakes conceptually mimicked that of the Bouwer and Rice test, and an appropriate "shape factor" for use with the Hvorslev method (1951) was not found in the literature until late in study. The observed rate of recovery in this study, therefore, measures the hydraulic head differential from the initial piezometric surface rather than the initial water table

elevation. Thompson (1993) also used the Bouwer and Rice test with piezometers to evaluate hydraulic conductivity in a natural wetland.

The Bouwer and Rice slug test - like the Hvorslev test - involves the displacement of a known volume of water in an observation well or piezometer to create a sudden change in hydraulic head; the observed rate of water-level recovery following displacement is related to Darcy's law and can be used to determine the hydraulic conductivity of the media immediately surrounding the intake area of the monitoring device. Like the Hvorslev test, the Bouwer and Rice test can be used on partially penetrating and partially screened wells and piezometers (i.e., wells or piezometers that do not penetrate and are not perforated along the entire saturated thickness of the aquifer). The water for the test can be physically added to or extracted from the piezometer; alternatively, the water can also be displaced by introducing or extracting a solid metal object to produce the necessary instantaneous change in head.

The well geometry for the Bouwer and Rice test is illustrated in Figure 3-3

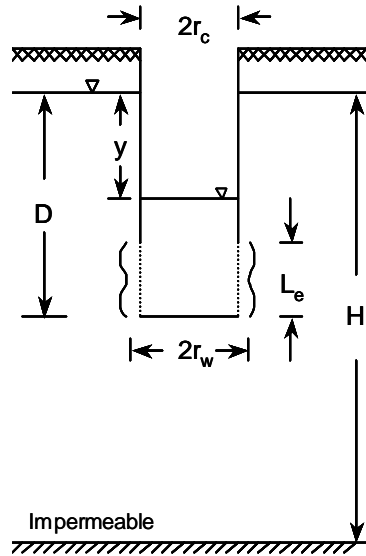


Figure 3-3. Geometry for Bouwer and Rice Slug Test (Source: Charbeneau, 2000).

where

L_e = effective height of the screened area or perforated zone

r_w = radius of the piezometer point or developed zone

r_c = radius of the standpipe through which the water level rises/falls

D = distance between the equilibrium water level and bottom of the piezometer screen

H = height of equilibrium water level above the impermeable strata

y = water level following displacement from the equilibrium position

The geometry for the piezometers used in this study is depicted in Figure 3-4, and the same notation applies.

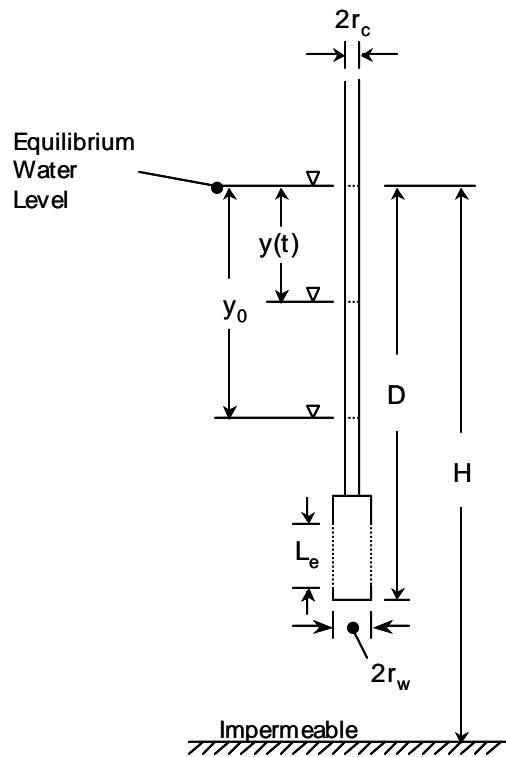


Figure 3-4. Piezometer Geometry

The basic equation to determine hydraulic conductivity using the Bower and Rice test is

$$K = \frac{r_c^2 \ln(R_e/r_w)}{2L_e} \frac{1}{t} \ln\left(\frac{y_0}{y_t}\right) \quad (24)$$

where R_e is the effective radial distance over which the head change is dissipated in the media (Bower, 1978).

Bower and Rice (1976) present the following equations to compute the value of $\ln(R_e/r_w)$:

$$\ln(R_e/r_w) = \left(\frac{1.1}{\ln(D/r_w)} + \frac{A + B \ln\left(\frac{H-D}{r_w}\right)}{L_e/r_w} \right)^{-1} \quad (25)$$

and, if $H=D$,

$$\ln(R_e/r_w) = \left(\frac{1.1}{\ln(D/r_w)} + \frac{C}{L_e/r_w} \right)^{-1} \quad (26)$$

Bouwer and Rice (1976) developed a graph that relates the constants A , B , and C to the known ratio of L_e/r_w . This graph is widely available in many groundwater texts that discuss the test (e.g. Bouwer, 1978; Fetter, 1994; Kresic, 1997). Bouwer and Rice (1976) indicate that the variable $\ln((H-D)/r_w)$ in Equation (25) has an upper bound of 6 based on the results of analog simulations, so a value of 6 should be used for $\ln((H-D)/r_w)$ if the calculated value exceeds 6. Because water flows into or out of the piezometer intake in a predominately radial - rather than vertical - manner, the test primarily yields values of K_H (Bouwer, 1978).

Ideally, plots of the change in hydraulic head versus time should appear as indicated in Figure 3-5. Although the variable y_0 is hard to measure in a practical sense without the aid of automated measuring equipment, its value can be closely computed using the method of least squares

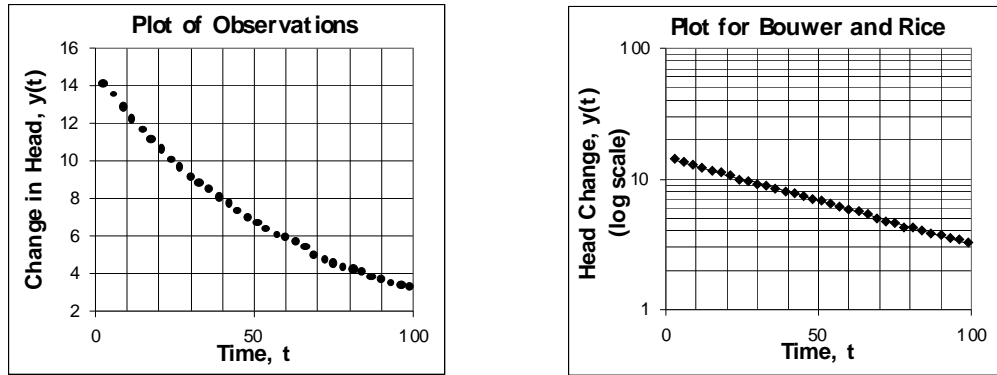


Figure 3-5. Arithmetic and Semi-log Plots of Change in Head Versus Time for the Bouwer and Rice Slug Test.

regression. Alternatively, Fetter (1994) points out that any two points along the straight line portion of the semi-log plot can be used in Equation (24) provided the variable t reflects the time interval between the two points. Sometimes, the semi-log plot of change in head versus time will yield a curve with two straight-line portions, the first having a steeper slope than the second. Kresic (1997) indicates this may be due to the more permeable sand or gravel packs that surround many well screens relative to the undisturbed surrounding aquifer soil. Values of y and t from the second straight-line segment should be used in Equation (24) to calculate hydraulic conductivity if this situation occurs. Also, Bouwer (1989) reports that the data points will characteristically taper off and away from

the straight-line portion of the semi-log plot during the later portion of the test.

Most texts recommend taking measurements until the water has recovered to 90% of the pre-test, equilibrium levels to obtain a representative amount of data points. Kraemer et al. (1990) suggest that a goal of 50% recovery may suffice in low conductivity sediments whose slow recovery rates do not make a recovery of 90% practical, although they do not provide a supportive basis for this.

Slug Test Methodology. The tests were conducted by adding or extracting water through the interior $\frac{1}{2}$ " Teflon-lined tube. To measure the rate of water level recovery, masking tape was affixed to the outside of the plastic piezometer tube, and the rate of recovery was marked at regular intervals on the tape; the ability to see the water level through the transparent tube greatly enhanced the degree of measuring precision. Hydraulic conductivity values were computed using Equations (24) and (25). Values for y_0 , y_t and t were extracted from the straight-line fit of data points on the semi-log plot of y versus t . Where the data deviated significantly from the theoretical straight line fit (generally for an R^2 of less than 98%), points forming a straight line during the middle portion of

the test were used to compute hydraulic conductivity. A total of 64 and 61 slug tests were conducted on the top and middle layer piezometers, respectively; some of these were repeat tests to assess the impact of piezometer development.

Pump Tests. Pump tests were performed on select piezometers in the bottom layer of the wetland to obtain estimates of hydraulic conductivity. (As already noted, the rapid recovery rate of water in the bottom layer piezometers precluded the use of slug tests to characterize hydraulic conductivity in this portion of the wetland.) Where feasible, pump tests are often preferred over slug tests to obtain in-situ estimates of hydraulic conductivity because they evaluate a much larger region of soil. Additionally, other hydrologic parameters - such as specific storage and specific yield - can also be estimated depending on the particular method used to evaluate data from the test.

The majority of the pump tests presented in the literature involve observations of water level (or potentiometric surface) decline in wells or piezometers as another well is pumped, normally at a constant rate. When water is pumped out of a well, a cone of depression forms in the water table (or potentiometric surface) and expands

outward from the well until a recharge boundary is reached. Analytical equations that compute hydraulic conductivity from the drawdown once this *steady-state* condition is reached are straightforward but require wells that fully penetrate the aquifer. An analysis of *transient* time-drawdown data is necessary for wells that only partially penetrate an aquifer as well as for tests that do not reach steady state conditions.

Various methods for analyzing transient time-drawdown data from aquifer pump tests exist in the literature. Many employ a *curve-fitting* technique that compares the transient time-drawdown data obtained from the test with the plot of a theoretical *type-curve*. In addition to the extent of well penetration, the type of aquifer (confined, leaky, or unconfined) also influences the choice of an appropriate test for transient conditions. Dawson and Istok (1991) provide a useful summary of aquifer tests that are applicable over a wide range of geological settings.

The piezometers installed in wetland cell number one only partially penetrate the soil layer of interest, and by design the hydrogeologic setting is conceptually that of an unconfined aquifer. The appearance of transient time-drawdown data collected during the pump tests, however,

mimicked that of a confined, leaky aquifer with influence from a source bed (i.e., an aquifer with an overlying *confining* layer that is permeable enough to transmit water down into the aquifer from a constant source of recharge) as illustrated by Dawson and Istok (1991). Fetter (1994) cautions that the effects of partial penetration can produce a time-drawdown curve that appears similar to that for a confined, leaky setting, but he also considers an aquifer *confined* when it is overlain by strata with a conductivity that is two orders of magnitude less than that of the aquifer of interest. The evidence supporting confined and leaky conditions (rather than unconfined) for the bottom soil layer of the wetland was two-fold. First, the water level recovery observed for slug tests attempted in the bottom layer was considerably faster (virtually instantaneous) compared to that for tests conducted in the top two layers of soil indicating a hydraulic conductivity much higher than that above. Second, the pump tests measured the decline of the potentiometric surface - rather than a declining water table - which again is consistent with a confined aquifer setting.

Hantush and Jacob (1955) present a method for analyzing the time-drawdown data obtained from pump tests

conducted in confined, leaky aquifers. Hantush (1960) adapted this method to settings where the confining aquitard releases water from storage during the test and to account for partial penetration of the pumping and/or observation wells or piezometers used (Hantush, 1961; Hantush 1964). Boulton and Streltsova (1975) present a method that accommodates all of these conditions, but it uses equations that are considerably more complex than those presented by Hantush.

The governing equations for drawdown at an observation well that fully penetrates a confined, leaky aquifer are

$$s = \frac{Q}{4\pi T} W(u, r/B) \quad (27)$$

$$W(u, r/B) = \int_u^\infty \frac{1}{y} \exp\left[-y - \frac{r^2}{4B^2 y}\right] dy \quad (28)$$

$$u = \frac{r^2 S}{4Tt} \quad (29)$$

$$B = \sqrt{\frac{T b'}{K}} \quad (30)$$

where

s = drawdown [L]

$W(u, r/B)$ = well function for confined, leaky aquifers

u = dimensionless parameter

B = leakage from the overlying aquitard [dimensionless]

$Q = \text{pump rate [L}^3/\text{T]}$

$T = \text{aquifer transmissivity [L}^2/\text{T]}$

$S = \text{aquifer storativity [unitless]}$

$r = \text{radius from the pumping well to the observation well [L]}$

$b' = \text{aquitard thickness [L]}$

$t = \text{time elapsed from the beginning of the aquifer test [T]}$

$y = \text{variable of integration [dimensionless]}$

Transmissivity is defined as

$$T = Kb \quad (31)$$

where K is the hydraulic conductivity [L/T] and b is the aquifer thickness [L]. Aquifer storativity is the same as the storage coefficient defined by Equation (17) in chapter 2.

The equation governing drawdown at an observation well that fully penetrates a confined, leaky aquifer when the overlying aquitard releases water from storage is

$$s = (Q/4\pi T)H(u, \beta) \quad (32)$$

where the variables s , Q and T are previously defined and $H(u, \beta)$ is the well function that accounts for aquitard storage in leaky aquifers [dimensionless]. The leaky well function, $H(u, \beta)$, is defined as

$$H(u, \beta) = \int_u^\infty \frac{e^{-y}}{y} \operatorname{erfc} \left[\frac{\beta \sqrt{y}}{y(y-u)} \right] dy \quad (33)$$

where the variables u and y were previously defined, β is a dimensionless parameter (defined below), and $erfc(x)$ is the complementary error function (also defined below). The complementary error function, $erfc(x)$, and parameter β are defined by

$$erfc(x) = \frac{2}{\sqrt{\pi}} \int_0^x e^{-y} dy \quad (34)$$

$$\beta = \frac{r}{4} \left[\frac{K' S'}{T S b'} \right]^{1/2} \quad (35)$$

where

$T =$ transmissivity [L^2/T]

$S =$ aquifer storativity [dimensionless]

$S' =$ storativity of the overlying aquitard [dimensionless]

$K' =$ vertical hydraulic conductivity of the overlying aquitard [L/T]

$r =$ radius from the pumping well to the observation well [L]

$b' =$ aquitard thickness [L]

$y =$ variable of integration

Equations (33) through (35) only apply for $t < (b'S')/(10K')$ Hantush (1964). Hantush (1960) presents other equations for analyzing aquifer tests that extend beyond this time window.

The equations governing drawdown around partially screened, partially penetrating wells and piezometers are

$$s_{ave} = \left(\frac{Q}{4\pi K_r b} \right) [W(u_r, r/B_r) + F(u_r, x, r/B_r, l/b, d/b, l_o/b, d_o/b)] \quad (36)$$

$$W(u, r/B_r) = \int_u^\infty \frac{1}{y} \exp \left[-y - \frac{r^2}{4B_r^2 y} \right] dy \quad (37)$$

$$u_r = \frac{r^2 S}{4 K_r b t} \quad (38)$$

$$B_r = \sqrt{\frac{K_r b b'}{K}} \quad (39)$$

$$F(u_r, x, r/B_r, l/b, d/b, l_o/b, d_o/b) = \left[\frac{2b^2}{\pi^2 (l-d)(l_o-d_o)} \right] \sum_{n=1}^{\infty} \left(\frac{1}{n^2} \right) \left[\sin \left(\frac{n\pi l}{b} \right) - \sin \left(\frac{n\pi d}{b} \right) \right] \left[\sin \left(\frac{n\pi l_o}{b} \right) - \sin \left(\frac{n\pi d_o}{b} \right) \right] \quad (40)$$

$$\int_u^\infty \frac{1}{y} \exp \left[-y - \frac{(r/B_r)^2 + (n\pi x)^2}{4y} \right] dy$$

where

s_{ave} = average drawdown over the screened portion of the well [L]

$W(u_r, r/B_r)$ = well function for confined, leaky aquifers [dimensionless]

u_r = dimensionless parameter

B_r = leakage from the overlying aquitard [dimensionless]

$F(u_r, x, r/B_r, l/b, d/b, l_o/b, d_o/b)$ = dimensionless parameter adjusting for partial penetration

Q = pump rate [L³/T]

S = aquifer storativity [unitless]

K_r = aquifer hydraulic conductivity in the radial direction [L/T]

K' = vertical hydraulic conductivity of the overlying aquitard [L/T]

r = radius from the pumping well to the observation well [L]

b = aquifer thickness [L]

b' = aquitard thickness [L]

l = vertical distance from the bottom of the pumping well screen to the bottom of the confining layer [L]

l_o = vertical distance from the bottom of observation well screen to the bottom of the confining layer [L]

d = vertical distance from the top of the pumping well screen to the bottom of the confining layer [L]

d_o = vertical distance from the top of the observation well screen to the bottom of the confining layer [L]

t = time elapsed from the beginning of the aquifer test [T]

y = variable of integration [dimensionless]

n = range variable for the summation operator [dimensionless]

Equations (36) through (40) assume that the amount of water released from storage in the overlying aquitard during the test is negligible (Hantush, 1961). Hantush (1964) points out that for $r > 1.5b\sqrt{K_r/K_z}$ (where r , b , and K_r are previously defined and K_z is the hydraulic conductivity of the aquifer in the vertical direction), the effects of partial penetration are negligible and Equations (27) through (31) may be used in the place of Equations (36) through (40).

To determine hydraulic conductivity using the time-drawdown data collected from a pump test in a confined, leaky aquifer, the following procedure applies.

(1) Prepare a logarithmic graph of type-curves by plotting the applicable well function on the vertical axis and u (or u_r) ranging from 10^{-6} to 10 on the horizontal axis for various values of r/B , β , or r/B_r (depending on the particular method used).

(2) Prepare a logarithmic plot of (observed) drawdown on the vertical axis and time on the horizontal axis using same scale as that used for the type-curves.

(3) Overlay one of the plots against the other keeping the axes aligned until a close match between the observed data points and one of the type-curves is achieved. Annotate a single *match point* on each graph that reflects this best fit, and record the values of the well function, u (or u_r), drawdown, and time for the match-point.

(4) Use the recorded match point values to determine transmissivity from Equation (27), (32), or (36). Use the computed value of transmissivity to determine hydraulic conductivity from Equation (31), and use Equation (29) or (38) to determine storativity if required. With Equations

(30) and (39), estimates of hydraulic conductivity for the overlying aquitard are also possible.

Pump Test Methodology. The pump tests were conducted by draining water from one piezometer (the *pumping well*) while observing the drawdown of water in another piezometer (the *observation well*). The aboveground riser pipes were removed from both piezometers and masking tape was affixed to the clear plastic tubing of the observation piezometer to record the position of the water level over time. To initiate the test, the end of the clear plastic tubing in the pumping piezometer was lowered to a position below that of the hydraulic head in the piezometer; this allowed water to freely drain from the pumping piezometer. The water draining from this piezometer was directed away from the test site and discharged directly into the effluent weir of the wetland by using a garden hose; this prevented the water from mounding over the test site and interfering with the test results. The discharge rate, Q , was determined by measuring the amount of water collected in a plastic container of known volume over time from the end of the garden hose. The tests were run until the water levels in the observation piezometers ceased to decline. The data was then analyzed using was Equations (27) through (40).

For the analysis, the top two soil layers of the wetland comprised the aquitard, while the bottom soil layer and underlying gravel and sand layers served as a composite aquifer layer. Estimates of hydraulic conductivity for the sand and gravel layers were assumed based on the mean of values presented in Charbeneau (2000) for these materials, and Equation (5b) was then used to compute the hydraulic conductivity of the bottom soil layer. The geometric mean of conductivities from the four pump tests conducted provided a baseline conductivity estimate for the bottom soil layer of the wetland.

Porosity. Porosity tests were conducted on two occasions for a total of eight samples tested. Fully saturated soil samples were collected at various locations around the wetland from surface sediments. The samples were collected in metal containers of known weight and volume by depressing the container into the sediments. The saturated samples were covered with plastic wrap and placed in an airtight container to prevent evaporation losses until they could be weighed in the laboratory. The samples were weighed on a model AB204-S Mettler Toledo scale to the nearest 1/1000th of a gram. The first batch of samples was dried in an oven at 105°C until a constant weight was

achieved (approximately 24 hours). Because these samples shrank considerably during the drying process, subsequent samples were dried at 60°C until a constant weight was achieved (approximately 48 hours) as recommended by ASTM D2216-63T (1963) for soils high in organic content. The weight of the dried samples was subtracted from that of the saturated samples and the result was divided by the density of water (at 20°C) to obtain the volume of water - and consequently the volume of voids - in the original sample. Porosity was then computed using Equation (1).

An additional calculation was also performed using

$$n = 1 - \frac{\rho_b}{\rho_m} \quad (41)$$

where ρ_b is dry bulk density [M/L³] and ρ_m is particle density [M/L³]. The equations for dry bulk and particle density are

$$\rho_b = W_S / V_T \quad (42)$$

$$\rho_m = W_S / V_S \quad (43)$$

where W_S is the mass of the solid particles [M], V_T is the original sample volume [L³], and V_S is the volume of the solid particles [L³]. The mass of the solid particles was determined by subtracting the weight of the collection can from the weight of the dried sample. The volume of solid

soil particles was determined by subtracting the computed volume of water from the total sample container volume. According to Fetter (1994), a comparison of Equation (41) with Equation (1) yields an internal check of consistency.

An evaluation of particle density can give an idea of whether organic matter is present in the sampled sediments. For example, while the particle density of mineral soils is often assumed as 2.65 g/cm³, organic matter weighs much less with particle densities ranging from 1.2 to 1.5 g/cm³ (Charbeneau, 2000). Samples with particle densities less than the mineral average imply that organic material may be present in the media.

Specific Yield. The specific yield, S_y , of the soil samples was approximated by gravity draining the porosity test samples prior to oven drying. The saturated samples were drained in an airtight container to prevent evaporation losses, and after 72 hours, the samples were weighed and the specific yield, S_y , was estimated with

$$S_y = \frac{(W_{sample} - W_{gravity\ drained}) / \rho_{water}}{V_{sample}} \quad (44)$$

Although soils have been observed to drain for months in column experiments (Prill, Johnson and Morris, 1965), 72

hours of drainage was assumed adequate for the relatively small sample volumes used in these porosity tests.

Effective Porosity. The effective porosity, n_e , of the soil samples was estimated by comparing the values obtained by gravity draining the samples with advice contained in the literature. Although a soil's specific yield - or *drainable porosity* - is not the same as its effective porosity (it ignores the volume of water retained in the pores due to capillary forces), it provides a closer approximation of effective porosity than total porosity for fine-grained sediments. Effective porosities as low as 0-5% are commonplace for soils with significant amounts of fine particles such as clays and silts (Kresic, 1997).

Numerical Model

A three-dimensional finite-difference, numerical computer model was constructed using Visual MODFLOW[®] by Waterloo Hydrogeologic, Inc. The model was partitioned into 90 columns, 46 rows, and 6 layers. The individual cells were evenly distributed throughout the model with column and row dimensions of 1½' on each side. Inactive cells were assigned to portions of the model that fell outside of the wetland media to define the physical

boundaries of the wetland as depicted in Figure 3-6. The impermeable wetland liner was assigned an elevation of zero for the model to define the bottom layer. The soil layers represented in the model are the same as those shown in Figure 3-2 with the addition of a notional 3" soil layer overlying the top sediments of the wetland to represent the free water surface. All layers were designated as confined in the model except for the top, fictional layer.

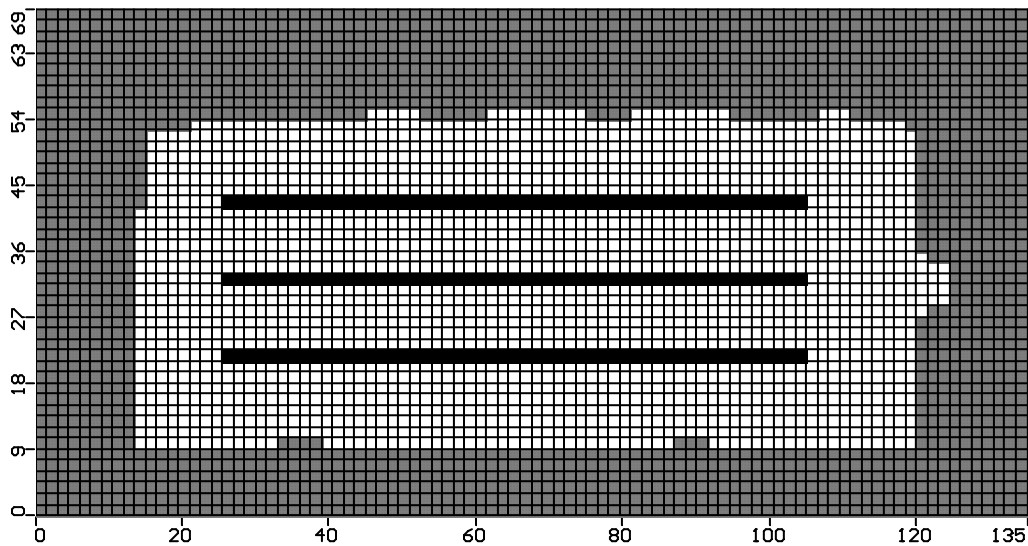


Figure 3-6. Overhead View of the Wetland Model in Visual MODFLOW® (Waterloo Hydrogeologic, Inc.). Dark parallel lines indicate location of constant head pipes in the model.

The piezometers were *installed* as observation wells at relevant points in the model. The weir was simulated as a constant source (i.e. sink) of head with a value equal to

the elevation of the water flowing over it. The water distribution pipes were initially simulated as constant sources of head to facilitate model calibration; the elevation of the aboveground water table surface was also initially simulated as a constant source of head with this aim in mind. The distribution pipes were later simulated as a series of injection wells, and the constant head restriction for the water-surface was removed to allow the model to solve for its elevation.

Hydraulic conductivity values for active cells were kriged for each soil layer of the wetland using the default settings of the (two-dimensional) kriging interpolation option in Surfer®. The hydraulic conductivity values for the sand and gravel layers were assumed to be the arithmetic means of the range of values for these materials presented in the literature (Charbeneau, 2000). Hydraulic conductivity values for the top (fictional soil) layer were obtained by trial and error until the model presented a logical solution. All values of hydraulic conductivity were imported into the model using a Fortran code written by Huang (2001). Values for porosity and effective porosity were entered directly into the model using Visual MODFLOW's window prompts. Estimates for evapotranspiration

(Renwick, 2002) were also entered using the program's default interface.

The model simulations were run using a convergence criterion of 0.01 feet. The deviation between calculated and observed hydraulic heads provided the basis for model calibration. Calibration involved adjusting the baseline hydraulic conductivity estimates at relevant piezometer locations until a good fit between the calculated and observed hydraulic heads was achieved. (Visual MODFLOW® provides a comparative graphing feature that also computes the root mean square error between the calculated and observed hydraulic heads to aid in model calibration.) The two bottom layers of soil were calibrated in this manner to simulate the hydraulic head distribution observed on November 1, 2001. Calibration of these layers took time but was relatively simple as the two demonstrated little relation to each other (i.e. a change of values in one layer had little effect on the values in the other layer). Calibration of the top layer proved much more difficult - a change in the top layer conductivities produced significant changes in the those of the middle layer - and the measured values from hydraulic conductivity tests were kriged and

used without further modification for this layer of the model.

The modeling effort produced essentially two models. The first model used the constant head package to simulate the distribution pipes, effluent weir, and the water table surface. (The values of head in the pipes were determined by trial and error until they produced a good fit with the baseline hydraulic conductivity estimates and the piezometric heads observed on November 1, 2001. The values of head for the water surface were determined by measuring down from the known elevation of the above ground riser coupling to the water surface, and the value at the weir was determined in a similar manner.) These conditions produced a rapid solution and in this respect facilitated model calibration, but they were somewhat restrictive: they essentially forced the water in the model to flow from a position of higher head in the pipes to the lower head at the surface of the wetland and in the weir.

To test the calibrated model under less restrictive conditions, the constant head for the water table surface was removed. This allowed the model to *determine* the proper location of the water table surface based on the water inputs and other boundary conditions. The pipes were

also simulated as a series of injection wells rather than constant sources of head. Sporadic readings from the inflow meter display were averaged to obtain a mean value of flow into the wetland; the output per well was determined by evenly dividing this value by the number of wells used to simulate the distribution pipes. Only one solver - the Preconditioned Conjugate-Gradient Package (PCG2) using the Modified Incomplete Cholesky preconditioning method - produced logical results for these conditions. The model required approximately five minutes to solve using this solver package for the less restrictive boundary conditions.

Validation was attempted by reducing the flow rate into the wetland to test whether the calibrated hydraulic conductivities produced results similar to that for the baseline model conditions. The piezometric data obtained on February 19, 2002 were used for this purpose.

Visual MODFLOW's particle tracking feature was used to estimate the hydraulic residence time of particles placed along the simulated distribution pipes.

IV. Results

Sampling Grid

The sampling grid provided the resolution necessary to reveal spatial trends in the distribution of hydraulic head. The existence of significant soil heterogeneities precluded a rigorous application of flow net construction; however, on-site observations provided valuable insight to confirm what the hydraulic head contours imply. The piezometers in the grid also facilitated measurements of hydraulic conductivity for numerical modeling and calculations of groundwater flow rates in the wetland.

Piezometer Installation

Although the drive point method of installation was found to be more challenging than expected, all of the piezometers - with the exception of number 29C which hit a rock - were successfully hand driven and retracted to the target depth below the surface of the wetland. The results of the total station survey (Appendix A) reveal a standard deviation about the mean piezometer intake elevations of 0.83", 0.71", and 0.74" for the top, middle and bottom soil layers, respectively. The general method of emplacement

(i.e. assuming a level wetland surface, driving the piezometer point down to a set distance, and then pulling back 6" to extract the shield from the screened portion of the piezometer) worked well enough to achieve an acceptable variance of sampling point elevation in the wetland. (The assumption of a level surface was based on the construction history of the wetland as well as a hasty elevation survey conducted prior to installing the piezometer grid.) The small variance in piezometer intake elevations facilitated meaningful interpretation of the potentiometric contours for each soil layer in the wetland.

A few observations concerning the installation of the piezometers may assist with similar groundwater studies in wetlands. The bentonite seal greatly improved the stability of the piezometers in the soft wetland sediments, but its potential impact on the monitoring objectives of researchers studying contaminant degradation is unknown. The presence of a connector coupling located below the surface of the wetland on some of the bottom layer piezometers also seems to have markedly improve stability: the piezometers with these couplings were significantly less prone to vertical movement and settling than those constructed with just a single riser tube. Last, as

already acknowledged, an annular cap of indigenous wetland soil may have provided a more enduring seal than the Quickcrete® caps used given the observation that many of the latter cracked shortly after hydration and did not provide an optimal covering.

Developing the piezometers seems to have altered the hydrogeologic properties surrounding the intake portion of the piezometers. Prior to well development, slug tests performed in the top and middle soil layers yielded mean coefficients of determination (R^2) of 0.995 and 0.973, respectively. Following well development, the mean R^2 values for the top and middle layers were 0.948 and 0.911, respectively. In other words, the data from the slug tests performed prior to piezometer development closely resembled the ideal straight-line appearance of the Bouwer and Rice semi-log plots while deviations from a straight-line fit after piezometer development were commonplace. Such deviations were characterized by a rapid water-level recovery, generally during the first minute of the test; in some cases, a straight-line plot of data points on the semi-logarithmic plot did not appear until towards the very end of the test. Figure 4-1 illustrates these points for a

comparison slug test conducted before and after piezometer development.

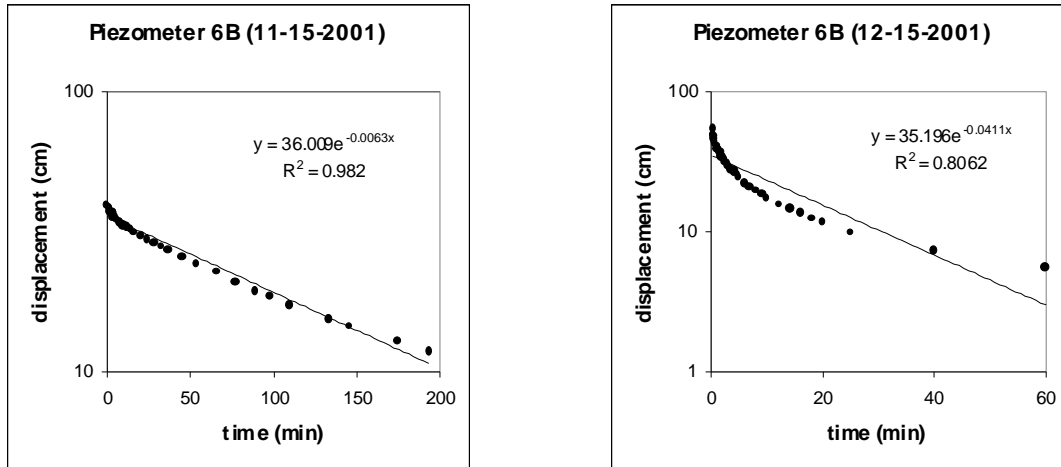


Figure 4-1. General Effect of Developing the Piezometers. Later date is test conducted on developed piezometer; note the deviation from the straight line appearance and more rapid rate of water level recovery relative to the earlier date.

The rapid water level recovery was not due to the presence of a higher permeability sand or gravel pack surrounding the piezometer screen as one does not exist; the possibility that sediments may have been clogging the piezometer screens prior to development is also small owing to the use of the piezometer shields during installation. A more plausible explanation is that developing the piezometers altered the soil properties in close proximity to the piezometer screen; alternatively, development may

also have disturbed the bentonite seal around the riser pipe.

The appearance of data points on the semi-log plot was not the only change observed in slug tests as a result of well development. More significantly, comparisons of slug tests conducted before and after piezometer development on 19 piezometers demonstrated order of magnitude increases in computed conductivities; seven of these differed by more than two orders of magnitude while only three of the 19 increased by less than one order of magnitude.

The possibility that developing the piezometers may have altered the soil properties in the area immediately surrounding the intake screens is based on the elastic properties of soils. Demir and Narasimhan (1994) demonstrate that data points for the Hvorslev test deviate from the theoretical straight line for certain piezometer shape factors as specific storage, S_s , increases, especially where radial flow through the piezometer screen occurs. Although the author's findings pertain to the Hvorslev test, the analytical form of the Bouwer and Rice and Hvorslev equations are similar (Charbeneau, 2001) and the device intake geometries in question both involve radial flow. Demir and Narasimhan (1994) make it clear that deviations

are commonplace in unconsolidated or "soft sediments" where S_S can exceed values of 0.001 m^{-1} . As presented in chapter 2, specific storage, S_S , is

$$S_S = \rho_w g (\alpha + n \beta) \quad (20)$$

where

ρ_w = density of water [M/L^3]

g = gravity [L/T^2]

α = compressibility of the aquifer skeleton [$1/(\text{M/LT}^2)$]

n = porosity [L^3/L^3]

β = compressibility of water [$1/\text{M/LT}^2$]

While the variables ρ_w , g and β are unlikely candidates for change, an increase in either n or α may have occurred as a result of surging too much water into the piezometer during development (assuming the media immediately surrounding the piezometer intake had an opportunity to expand and deform); the resultant increase in specific storage relative to the undeveloped condition could account for the characteristic deviations from straight-line appearance observed on the semi-log plot that were common after developing the piezometers. Likewise, although hydraulic conductivity does not *depend* on either n or α , both parameters are represented in the intrinsic properties and permeability, k , of the soil, so an increase in either n or α could account

for the observed order of magnitude increases in hydraulic conductivity after piezometer development.

It is unlikely that the bentonite seal was completely compromised as the result of developing the piezometers: an ineffective annular seal would manifest itself in static water levels equal to the water table elevation in the presence of vertical groundwater flow gradients (Sigel and Glaser, 1987). Developing may have compromised a portion of the seal close to the piezometer screen however.

Expansive clays such as bentonite can have porosities that range as high as 80% (Kresic, 1997), and as indicated by Equation (20), a high porosity can result in a high value of specific storage (S_s). The data point deviation from a straight-line appearance could indicate that some of the water introduced or extracted during the slug tests was moving into or out of the highly plastic bentonite material but was not fully penetrating the annular seal.

Piezometric Surface

The results of the piezometric measurements indicate areas of preferential flow in the wetland. Potentiometric surfaces for November 1, 2001 and February 19, 2002 are given in appendix B and C, respectively. These contour

plots indicate a fairly uniform distribution of hydraulic head in the bottom soil layer relative to the two upper layers. The potentiometric surfaces for the two upper layers depict regions of higher hydraulic head and preferential flows towards the north side and weir end of the wetland. (Figure 3-1 indicates which direction is north relative to the wetland.) The behavior observed in Appendix B was typical of that observed on seven occasions over a three-week period around the date represented. The magnitude of variation observed in Appendix C appears less than that observed in Appendix B due to a reduced flow rate into the wetland. (Appendix D contains the water level data collected on all days measured.)

The variability depicted in Appendices B and C is quantified in table 4-1. Although the magnitude of variation for all layers might not be significant if it occurred gradually over the full length of the wetland,

Table 4-1. Comparison of Hydraulic Head Distribution for November 1, 2001 and February 19, 2002.

	11/1/2001			2/19/2002		
	Top	Middle	Bottom	Top	Middle	Bottom
Mean (ft)	6.2	6.61	8.04	5.983	6.249	7.616
Standard Deviation (ft)	0.335	0.469	0.093	0.18	0.351	0.068
Maximum Difference in Head (ft)	1.657	2.015	0.581	0.812	1.47	0.319
Maximum Hydraulic Gradient	0.108	0.123	0.055	0.065	0.138	0.019

differences in head as large as 12 to 18 inches are common in piezometers located close to each other in the top two soil layers. Additionally, the large differences are not isolated to single piezometers (which could then be dismissed as mere anomalies or outliers); rather they occur between adjacent regions or groups of piezometers.

The case for preferential flow is further supported by observations on the surface of the wetland near the locations of higher hydraulic head. The sediments around the perimeter of the wetland, particularly along the north, are highly plastic and generally do not support the weight of foot traffic well. The sediments down the center of the wetland, from piezometers 3 and 4 to 33 and 34, are also very soft. (This contrasts with other areas of the wetland where the sediments generally support foot traffic well.) Additionally, moisture above the water table and close to the liner is evident between piezometers 54 and 60. Figure 4-2 displays these areas.

The most convincing observation of preferential flow is not entirely supported by the piezometric data however. The presence of *boiling* or *heave* is evident approximately two feet to the north of nest 29. Generally attributed to cohesionless soils like sand or silt, boiling or heave can

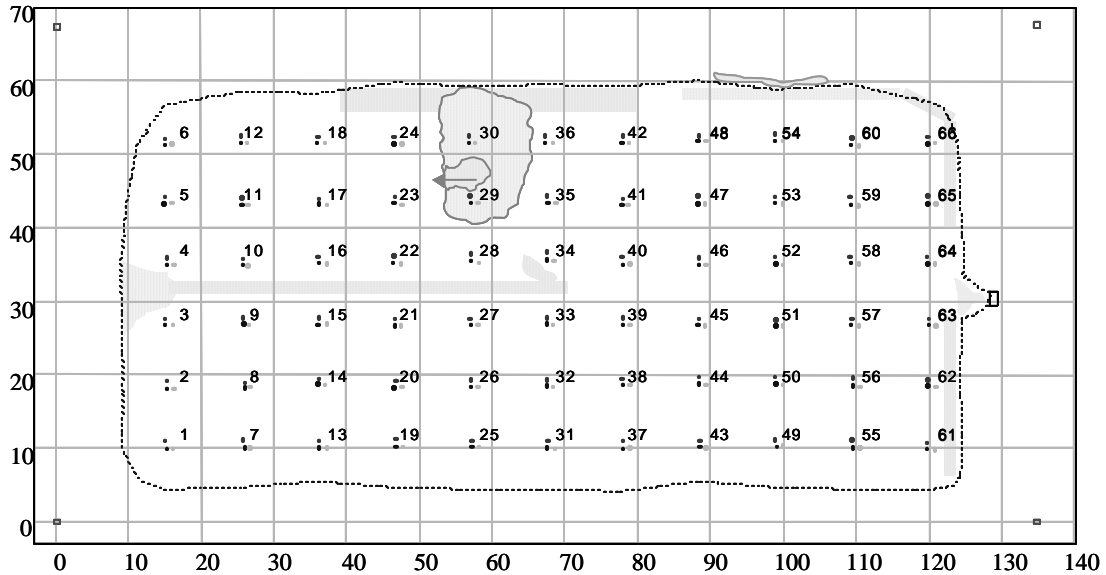


Figure 4-2. Regions of Particularly Poor Trafficability in the Wetland. Shaded regions represent areas of suspected preferential flows. Arrow pointing away from nest 29 indicates observable direction of flow off of the mound.

occur in the presence of vertical gradients that approach a value of unity (Charbeneau, 2000). The generic name applied to this condition is *quicksand*. The phenomenon occurs when the seepage forces acting up on a soil mass balance the weight of the media and water acting down upon it. Although the hydraulic gradient at nest 29 does not approach one, the appearance of the sediments erupting from upward pressures at this point - like a bulge in a tire - is unmistakable. The wetland sediments that are void of roots around this area will not support any foot traffic without the aid of wide boards to distribute the load.

Additionally, water can actually be seen flowing out of the ground and down the mound of eruption at this location. The fact that none of the piezometers register a gradient of one in this particularly wet area of wetland merely indicates that the sampling grid has failed to pinpoint the exact location where the breach has occurred.

Table 4-2 provides a measure of the variability within and between layers for all dates measured. Although the sample sizes (displayed in parentheses next to the column headings) are too small for convincing statistical analysis, they results may imply that a reduced flow rate reduces the variation of hydraulic head within layers.

Table 4-2. Mean Standard Deviation in Hydraulic Head Distribution for All Dates Measured.

	Fall 2001 (7)	Winter 2002 (1)	Mean (8)
Top Soil Layer (ft)	0.376	0.18	0.352
Middle Soil Layer (ft)	0.572	0.351	0.544
Bottom Layer (ft)	0.107	0.068	0.102

Note: sample size displayed in parentheses next to the column heading.

Parameter Analysis

Hydraulic Conductivity. Appendix E displays the results of the slug tests performed. The results range over values indicated by various groundwater texts for

silts, sandy silts, clayey sands, and tills to silty sands and fine sands (Fetter, 1994; Charbeneau, 2000). Overall, the results indicate heterogeneities and variations within and between layers as seen in Table 4-3.

Table 4-3. Hydraulic Conductivity Estimates from In-situ Tests (ft/sec)

	Top Soil Layer		Middle Soil Layer		Bottom Soil Layer	
	Arithmetic Mean	Standard Deviation	Arithmetic Mean	Standard Deviation	Arithmetic Mean	Standard Deviation
Before Developing	6.4×10^{-8}	4.9×10^{-8}	1.5×10^{-6}	3.1×10^{-6}	6.8×10^{-4}	3.4×10^{-4}
After Developing	8.1×10^{-6}	1.1×10^{-5}	5.6×10^{-6}	8.0×10^{-6}	6.8×10^{-4}	3.4×10^{-4}

In Table 4-3, the magnitude of standard deviations relative to the means indicate variation within layers while the means demonstrate variation between layers.

The impact of developing the piezometers can be seen in Table 4-4 by comparing the geometric means of the layers before and after development. (Many hydrologists believe the geometric mean provides a better comparison assessment of mean hydraulic conductivities because an arithmetic mean tends to give more weight to larger values (Fetter, 1994).)

Table 4-4. Geometric Means of Hydraulic Conductivity (ft/sec)

	Top Soil Layer	Middle Soil Layer	Bottom Soil Layer
Before Developing	4.2×10^{-8}	2.5×10^{-7}	5.6×10^{-4}
After Developing	3.4×10^{-6}	2.2×10^{-6}	5.6×10^{-4}

Although hydraulic conductivity appears to increase with depth, the trend is not conclusive. Prior to development, hydraulic conductivity clearly improved with depth, while after development, the (geometric) mean conductivities of the top and middle layers were approximately equal.

The concern over the choice of the appropriate slug test for this study was alleviated somewhat by comparing the results obtained from the Bouwer and Rice (1976) and Hvorslev (1951) methods; results obtained with the Hvorslev method using a shape factor that may approximate that of the piezometers used in this study (Brand and Permichitt, 1980) over-performed the results obtained from the Bouwer and Rice test by only 30% on average. (See Appendix F for an example of the MATHCAD® template used to compute hydraulic conductivity and compare the results of both test methods.) The close results may not be surprising given the similar form of the key equations as well as the similar piezometer intake geometries, although it did provide some degree of reassurance. Also, a 30% disparity is well within the order of magnitude precision that is possible for hydraulic conductivity tests.

The hydraulic conductivity estimates shown in Tables 4-3 and 4-4 for the bottom soil layer reflect the results

of the pump tests conducted on four piezometers in the layer. The fit for the data from two of the tests implied some leakage from the overlying aquitard while the other two did not. The effects of partial penetration were negligible for all four tests. Appendix G contains calculations and plots for one of the four tests.

Porosity. The results of the porosity tests range from 0.46 to 0.63 (sample mean: 0.53). The low end was typical of samples taken from the compacted portion of the wetland, while the higher values were common in samples taken from wet areas in the wetland. The values in this range are typical of silts and clays (Charbeneau, 2000).

Specific Yield and Effective Porosity. The results of the specific yield tests range from 2.2×10^{-4} to 0.069 (sample mean: 0.022.) Because these results do not account for the water retained by capillary forces in the interconnected void spaces, a value of 0.05 - which is higher than the mean for specific yield but representative of soils containing significant amounts of fine particles - was assumed for effective porosity.

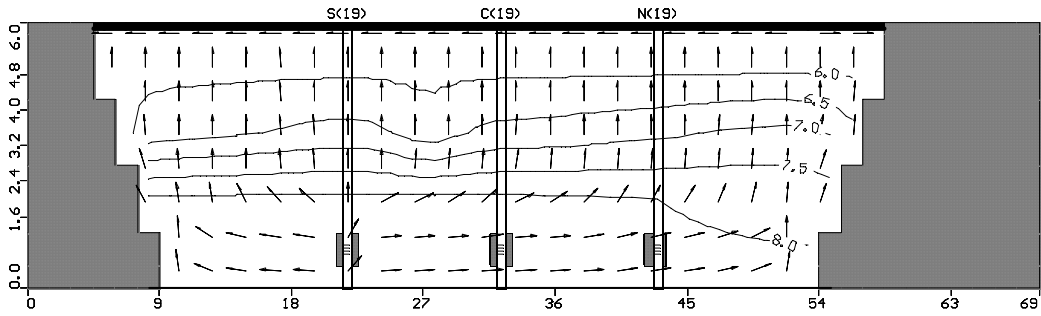
Particle Density. The results of the particle density analysis range from 2.2 to 2.4 g/cm³. These values indicate a presence of organic material in the wetland sediments.

Numerical Model

The output from the model implies a tendency for water to preferentially flow towards the sides of the wetland in the more permeable layers. Flow in the bottom soil and underlying gravel and sand layers is predominately horizontal, while water in the top two soil layers flows predominately straight up. This is illustrated in Figure 4-3. The wider spacing of contour intervals along the sides of the wetland indicates that the sediments have a higher transmissivity and facilitate greater flows relative to the more central portions of the wetland. In general, the output from the model indicates that a greater amount of water moves towards the north side of the wetland.

Visual MODFLOW's particle tracking feature computed an average hydraulic residence time of three days for water particles released from the distribution pipes. The minimum residence time was approximately 16.5 hours. This generally occurred in the vicinity of piezometers 10, 24, 29, 30, and 36 based on observations of the model output. The maximum residence time for particles released was 15 days while approximately 64% of the particles released had a residence time less than the average. The large

(Near Piezometer Nests 25-30)



(Near Piezometer Nests 55-60)

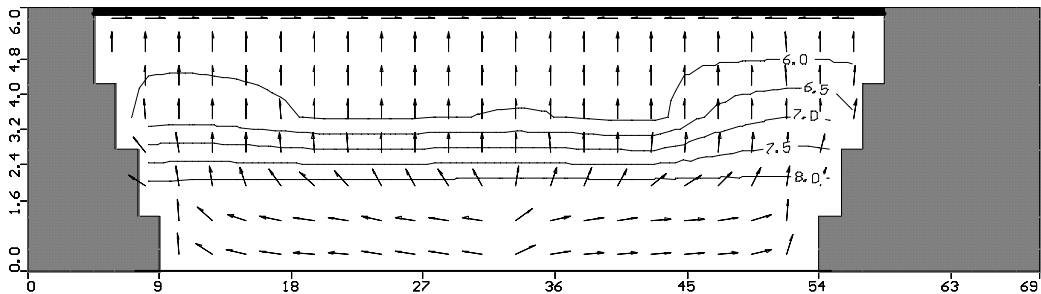


Figure 4-3. Cross Section Views of the Wetland (Displays from Visual MODFLOW®)

variation in computed residence time implies preferential flow in the wetland.

The program's water budget calculation feature indicated that water losses from evapotranspiration were minor, amounting to less than five percent of the wetland's overall water budget for the baseline conditions. This was based on a potential evapotranspiration rate of 10 mm/day for November 1, 2001 (Renwick, 2002). Evapotranspiration

was assumed to be zero for the validation measurements taken during February 2002.

Approximately 50 calibration runs were required to achieve a close fit between computed and observed hydraulic head values for the bottom two layers of soil. (As noted in Chapter 3, hydraulic conductivity was not calibrated for the top layer of soil.) The fit achieved for these layers is displayed in Appendix H. The general method of adjusting hydraulic conductivity for cells at piezometer locations in the model, and then kriging these values to interpolate conductivities for the other cells in the layer, was not 100% successful in bringing all points close to the ideal fit line. Most notably, piezometers 4C, 25C, 1B, 40B, 41B and 61B were particularly problematic and continually overestimated by the model. This helps to illustrate the point that although groundwater models can be helpful in characterizing the general behavior of a subsurface system, they are generally not capable of capturing all geological features hidden within a natural system. Numerical models generate approximate solutions, and the weight placed on such *solutions* must be viewed with this truth in mind.

Figure 4-4 displays the overall fit achieved during model calibration for the conditions and heads observed on

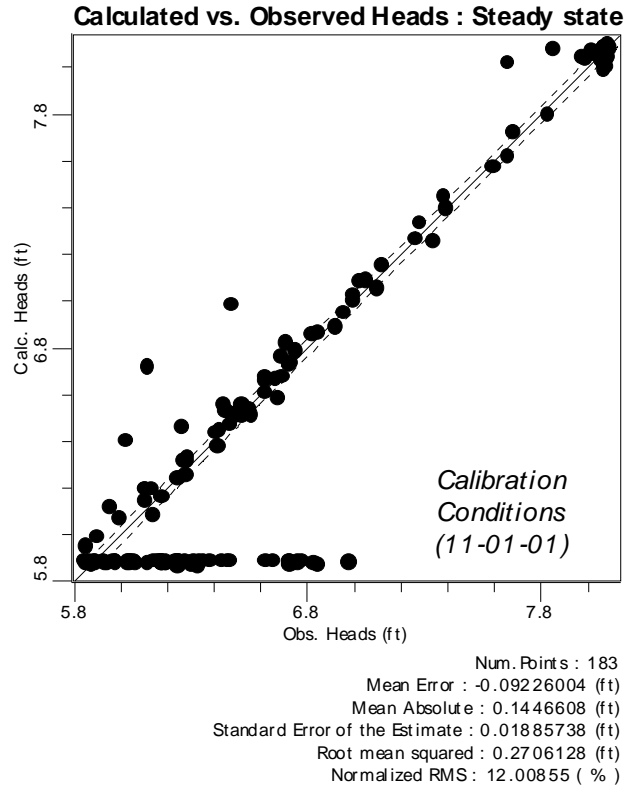


Figure 4-4. Calibrated Model. Grouping of points in the upper right corner represent piezometers in the bottom soil layer. Points forming a horizontal line along the bottom represent piezometers in the top soil layer (not calibrated). Points between these two groups represent piezometers in the middle soil layer.

November 1, 2001. A comparison of Figure 4-4 with Figure 4-5 provides an assessment of how well the calibrated model was able to predict the validation conditions and heads observed on February 19, 2002. The deviation from an exact fit may indicate calibration error, errors in parameter estimation, or transient subsurface conditions. The majority of data points in the center of Figure 4-5 (which

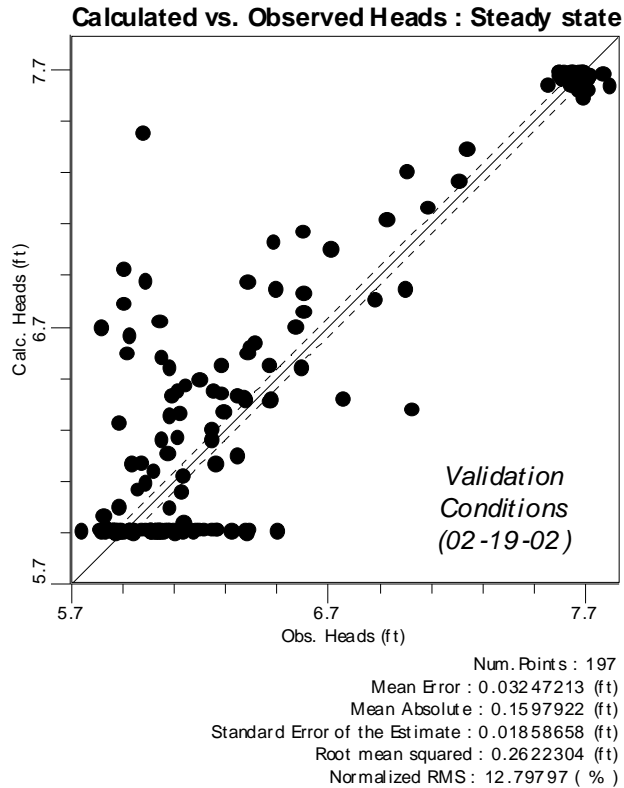


Figure 4-5. Model Validation. The middle soil layer piezometers appear to bracket a line slightly above the best-fit line.

represent the middle soil layer) do appear to bracket a straight line, and this provides for some degree of confidence in the model. The position of these points above the best fit line may indicate that the mean hydraulic conductivity for this layer (or throughout the wetland) has shifted, or it could possibly reflect the influence of the colder temperatures.

V. Conclusions and Recommendations for Further Study

The Wright-Patterson Air Force Base wetland treatment cells are designed to achieve uniform vertical flows by distributing water into a highly permeable layer near the bottom of the wetland and forcing it up through the largely anaerobic subsurface sediments. Conceptually, uniform flows will achieve the most efficient degree of contaminant removal possible by evenly dispersing the groundwater contaminants throughout the full volume of the subsurface media. The existence of uniform, predictable flows would also aid in the development of design criteria for such a treatment technology.

This study shows that the flow of groundwater is not entirely uniform in wetland cell number one. Admittedly, what constitutes *uniform* flows in such a system is a matter of perspective. Aside from being a subjective label, even the seemingly variable distribution of hydraulic heads in the middle soil layer could be scaled in such a manner to appear uniform. Still, the variability in hydraulic heads for the top and middle soil layers was three to five times greater than that for the bottom soil layer. The fact that differences in head of 1-1½ feet are common between groups

of piezometers located in close proximity to one another - rather than being gradually dispersed over the full range of the wetland - supports the case for preferential flow. The high values of hydraulic conductivity measured in these areas are not surprising from an analytical perspective and add weight to this possibility. The output from the numerical model further supports the notion that regions of higher flow are inter-dispersed among regions of nominal flows. The residence time of water particles observed in the model is significantly less in regions of the wetland where the observed heads and hydraulic conductivities are high. Additionally, the flow vectors in the model indicate that groundwater in the more permeable bottom layers prefers to flow horizontally towards the sides of the wetland, and higher hydraulic heads are observed along the north side and weir end of the potentiometric contour maps. Finally, the observations noted on the surface of the wetland also support the case for preferential flows.

The above observations do not imply that only a small portion of the wetland facilitates flow. The existence of water levels above the surface of the water table in virtually all of the functioning piezometers indicates that upward vertical flows occur throughout the subsurface media.

The numerical model supports this evidence by displaying vertical flow vectors and water particle movement through the top and middle soil layers. A large proportion of the wetland media may, therefore, be performing as intended albeit at a somewhat reduced level of efficiency.

Study Strengths

The study used well-established methods to investigate groundwater flow in wetland cell number one. The evidence from these different methods is consistent and supports the finding that some degree of preferential flow is occurring. At the same time, evidence from the piezometers and model simulations confirm that vertical flows also occur through at least 36" of saturated wetland soil.

Study Weaknesses

The effect of the suspected preferential flows on the contaminant degradation processes at work in the wetland was not determined in this study. The eight measurements of hydraulic head taken during this study do not permit meaningful statistical analysis, and the short time span over which the measurements were taken does little to indicate whether the observed flow patterns reflect a

steady state condition or are merely snapshots of a flow system in transition. The question of how varying loading rates affect patterns in groundwater flow was not studied as fully as intended. The method used to develop the piezometers was not well established in the literature, and the reason behind the order-of-magnitude improvements that were typical after development, as well as the deviation from straight-line appearance in the data plots, was never fully resolved. The reliance on specific yield estimates to assume an effective porosity (which provides the basis of hydraulic residence time in the numerical model) lacks precision, although the effective porosity parameter is inherently difficult to measure. Possible strategies to mitigate or discourage preferential flows are not discussed in this study, and the flow behavior in the wetland cell number two was not studied. Last, the measured hydraulic conductivity values required a significant amount of adjustments to calibrate the numerical model, and the fit obtained with the validation conditions, while close, was less than exact.

Recommendations for Further Study

(1) Study the flow in wetland cell number two to determine how it compares to that observed in this study.

(2) Conduct a tracer study in wetland cell number one to substantiate or refute the results obtained in this study.

(3) Continue to monitor the distribution of hydraulic heads in wetland cell number one to determine whether changes are occurring over time.

(4) Vary the flow into the wetland to determine whether preferential flows occur under all practical loading conditions. Attempt to relate soil parameters to the findings to develop design guidelines appropriate for like systems.

(5) Improve on the numerical model by increasing the grid resolution and by conducting additional parameter tests to verify the model's results. Use the model as a predictive tool to investigate the flow behavior of different design approaches.

Appendix A: Piezometer Grid and Construction Data

Piez #	Local Coordinates (ft)		Elevations (ft)			In-ground Riser	
	x	y	coupling	screen	tube	Length	Type
01A	15.902	10.028	6.094	4.646	6.995	1'	S
01B	14.854	10.984	6.610	3.694	8.616	30"	S
01C	14.928	10.039	6.638	2.253	9.550	2'x2'	S
02A	16.072	18.113	6.028	4.627	6.945	1'	S
02B	14.995	19.190	6.020	3.619	7.822	2'	S
02C	14.973	18.195	6.560	2.170	9.425	4'	S
03A	15.863	26.835	5.948	4.532	6.782	1'	S
03B	14.895	27.794	5.982	3.566	7.795	2'	S
03C	14.890	26.873	6.481	2.091	9.403	4'	S
04A	16.053	35.007	6.046	4.650	6.895	1'	S
04B	14.987	36.085	6.029	3.644	7.389	2'	S
04C	14.948	35.041	6.615	2.121	9.344	3'x1'	S
05A	15.722	43.392	5.995	4.594	6.860	1'	S
05B	14.808	44.247	6.065	3.669	7.977	2'	S
05C	14.633	43.319	6.571	2.077	9.358	3'x1'	S
06A	15.786	51.436	6.111	4.695	6.992	1'	S
06B	14.897	52.229	6.091	3.685	7.925	2'	S
06C	14.870	51.358	6.599	2.198	9.584	2'x2'	S
07A	26.509	10.162	6.030	4.634	6.890	1'	S
07B	25.465	11.280	6.070	3.674	7.893	2'	S
07C	25.670	10.153	6.558	2.152	9.454	4'	S
08A	26.559	18.357	6.098	4.702	6.952	1'	S
08B	25.690	19.058	6.171	3.739	7.953	2'	S
08C	25.693	18.228	6.620	2.224	9.454	4'	S
09A	26.412	26.823	6.113	4.702	6.926	1'	S
09B	25.430	27.898	6.130	3.719	8.026	2'	S
09C	25.552	26.901	6.614	2.218	9.541	4'	S
10A	26.291	34.882	6.205	4.789	7.039	1'	S
10B	25.411	35.918	6.167	3.761	8.204	2'	S
10C	25.461	35.019	6.770	2.286	9.583	3'x1'	S
11A	26.225	43.166	6.118	4.702	6.957	1'	S
11B	25.295	44.224	6.117	3.716	8.076	2'	S
11C	25.375	43.207	6.678	2.215	9.480	3'x1'	S
12A	26.168	51.604	6.064	4.663	6.918	1'	S
12B	25.230	52.563	6.090	3.689	7.991	2'	S
12C	25.211	51.681	6.564	2.174	9.465	4'	S

Piez #	Local Coordinates (ft)		Elevations (ft)			In-ground Riser	
	x	y	coupling	screen	tube	Length	Type
13A	37.019	10.086	6.113	4.712	7.020	1'	S
13B	35.924	11.092	6.572	3.682	8.593	30"	S
13C	35.904	10.083	6.671	2.171	9.661	2'x2'	S
14A	36.869	18.623	6.125	4.703	6.969	1'	S
14B	35.949	19.545	6.531	3.646	8.552	30"	S
14C	35.853	18.766	6.672	2.178	9.646	2'x2'	S
15A	36.942	26.953	6.135	4.719	6.948	1'	S
15B	35.953	27.851	6.704	3.793	8.715	30"	S
15C	35.857	26.876	6.730	2.246	9.694	2'x2'	S
16A	36.929	35.092	6.126	4.715	6.991	1'	S
16B	35.833	36.183	6.047	3.651	7.886	2'	S
16C	35.941	35.228	6.666	2.172	9.375	3'x1'	S
17A	36.905	43.101	6.062	4.666	6.979	1'	S
17B	35.890	44.100	6.152	3.730	8.038	2'	S
17C	35.895	43.225	6.692	2.208	9.458	3'x1'	S
18A	36.701	51.522	6.128	4.717	6.998	1'	S
18B	35.833	52.417	6.130	3.714	8.047	2'	S
18C	35.707	51.500	6.642	2.158	9.371	3'x1'	S
19A	47.412	10.328	6.092	4.691	6.952	1'	S
19B	46.562	11.378	6.104	3.698	8.078	2'	S
19C	46.569	10.241	6.521	2.125	9.495	4'	S
20A	47.297	18.387	6.201	4.800	7.087	1'	S
20B	46.471	19.379	6.203	3.792	8.047	2'	S
20C	46.314	18.344	6.622	2.221	9.523	4'	S
21A	47.197	26.743	6.011	4.584	6.886	1'	S
21B	46.331	27.752	6.080	3.669	7.955	2'	S
21C	46.368	26.757	6.424	2.034	9.325	4'	S
22A	47.111	35.156	6.176	4.770	7.020	1'	S
22B	46.214	36.240	6.132	3.721	7.950	2'	S
22C	46.182	35.193	6.676	2.202	9.473	3'x1'	S
23A	47.311	43.143	6.224	4.802	7.078	1'	S
23B	46.407	44.362	6.102	3.686	7.930	2'	S
23C	46.323	43.347	6.728	2.228	9.510	3'x1'	S
24A	47.258	51.362	6.048	4.652	6.913	1'	S
24B	46.315	52.453	5.978	3.572	7.780	2'	S
24C	46.268	51.443	6.584	2.090	9.303	3'x1'	S
25A	57.867	10.239	6.084	4.673	6.928	1'	S
25B	56.944	11.205	6.591	3.690	8.628	30"	S
25C	56.951	10.284	6.622	2.226	9.565	2'x2'	S

Piez #	Local Coordinates (ft)		Elevations (ft)			In-ground Riser	
	x	y	coupling	screen	tube	Length	Type
26A	57.817	18.458	6.169	4.758	7.013	1'	S
26B	56.791	19.418	6.652	3.772	8.668	30"	S
26C	56.832	18.388	6.704	2.230	9.631	2'x2'	S
27A	57.829	26.856	6.117	4.701	6.909	1'	S
27B	56.730	27.684	6.094	3.693	7.922	2'	S
27C	56.816	26.827	6.546	2.150	9.515	4'	S
28A	57.932	35.430	6.024	4.618	6.868	1'	S
28B	56.876	36.484	5.976	3.560	7.768	2'	S
28C	56.863	35.553	6.584	2.110	9.366	3'x1'	S
29A	57.796	43.487	6.322	4.900	7.176	1'	S
29B	56.660	44.382	6.145	3.744	8.020	2'	S
29C	56.827	43.576	7.704	3.225	9.460	3'x1'	S
30A	57.428	51.677	6.169	4.737	6.966	1'	S
30B	56.580	52.530	6.128	3.722	7.946	2'	S
30C	56.574	51.683	6.700	2.195	9.466	3'x1'	S
31A	68.427	9.960	6.016	4.610	6.865	1'	S
31B	67.506	11.055	6.504	3.614	8.530	30"	S
31C	67.354	10.115	6.510	2.052	9.500	2'x2'	S
32A	68.161	18.386	6.149	4.722	6.993	1'	S
32B	67.280	19.499	6.582	3.697	8.619	30"	S
32C	67.270	18.503	6.677	2.203	9.615	2'x2'	S
33A	68.166	26.824	6.152	4.762	7.048	1'	S
33B	67.346	27.865	6.684	3.788	8.549	30"	S
33C	67.242	26.981	6.745	2.277	9.745	2'x2'	S
34A	68.214	35.694	6.004	4.598	6.838	1'	S
34B	67.257	36.813	5.982	3.566	7.889	2'	S
34C	67.159	35.799	6.446	1.988	9.280	3'x1'	S
35A	68.456	43.356	6.071	4.634	6.931	1'	S
35B	67.307	44.434	6.050	3.639	7.821	2'	S
35C	67.403	43.409	6.616	2.142	9.356	3'x1'	S
36A	68.058	51.702	6.141	4.709	6.954	1'	S
36B	66.995	52.534	6.107	3.691	7.956	2'	S
36C	67.051	51.689	6.669	2.206	9.497	3'x1'	S
37A	78.677	10.092	6.103	4.676	6.921	1'	S
37B	77.622	11.099	6.634	3.744	8.718	30"	S
37C	77.669	10.015	6.683	2.189	9.569	2'x2'	S
38A	78.715	18.647	6.145	4.734	6.963	1'	S
38B	77.497	19.554	6.702	3.780	8.702	30"	S
38C	77.612	18.739	6.716	2.258	9.706	2'x2'	S

Piez #	Local Coordinates (ft)		Elevations (ft)			In-ground Riser	
	x	y	coupling	screen	tube	Length	Type
39A	78.744	26.805	6.145	4.749	6.968	1'	S
39B	77.792	27.828	6.702	3.801	8.739	30"	S
39C	77.840	26.789	6.700	2.216	9.622	2'x2'	S
40A	78.678	35.129	6.074	4.663	6.892	1'	S
40B	77.561	36.118	6.054	3.669	7.455	2'	S
40C	77.702	35.039	6.599	2.115	9.365	3'x1'	S
41A	78.500	43.090	6.105	4.678	6.933	1'	S
41B	77.727	44.080	6.085	3.663	7.867	2'	S
41C	77.542	43.141	6.717	2.233	9.446	3'x1'	S
42A	78.590	51.624	6.064	4.658	6.653	1'	S
42B	77.647	52.600	6.054	3.643	7.955	2'	S
42C	77.578	51.695	6.667	2.199	9.407	3'x1'	S
43A	89.175	10.163	6.048	4.632	6.840	1'	S
43B	88.211	11.134	6.550	3.649	8.582	30"	S
43C	88.278	10.318	6.590	2.106	9.559	2'x2'	S
44A	89.181	18.737	6.162	4.740	6.824	1'	S
44B	88.155	19.840	6.651	3.740	8.667	30"	S
44C	88.132	18.827	6.719	2.230	9.652	2'x2'	S
45A	89.029	26.666	6.055	4.649	6.873	1'	S
45B	88.076	27.717	6.624	3.702	8.635	30"	S
45C	88.024	26.834	6.662	2.183	9.574	2'x2'	S
46A	89.107	34.983	6.136	4.720	6.918	1'	S
46B	88.148	35.984	6.104	3.688	7.990	2'	S
46C	88.173	35.044	6.698	2.230	9.448	3'x1'	S
47A	89.057	43.251	6.154	4.732	7.055	1'	S
47B	87.964	44.413	6.049	3.648	7.924	2'	S
47C	87.978	43.319	6.736	2.226	9.596	3'X1'	S
48A	89.176	51.800	6.112	4.701	6.784	1'	S
48B	88.089	52.645	6.125	3.724	7.985	2'	S
48C	88.033	51.760	6.630	2.156	9.417	3'X1'	S
49A	99.776	10.359	5.942	4.526	6.755	1'	S
49B	98.652	11.331	6.580	3.664	8.601	30"	S
49C	98.891	10.317	6.636	2.152	9.647	2'x2'	S
50A	99.672	18.657	6.152	4.741	6.928	1'	S
50B	98.650	19.803	6.106	3.690	7.950	2'	S
50C	98.660	18.791	6.679	2.205	9.695	2'x2'	S
51A	99.634	26.672	6.156	4.750	6.984	1'	S
51B	98.739	27.612	6.192	3.791	8.088	2'	S
51C	98.711	26.733	6.731	2.252	9.658	2'x2'	S

Piez #	Local Coordinates (ft)		Elevations (ft)			In-ground Riser	
	x	y	coupling	screen	tube	Length	Type
52A	99.613	35.029	6.228	4.796	6.890	1'	S
52B	98.578	36.144	6.210	3.778	8.096	2'	S
52C	98.663	35.119	6.717	2.259	9.551	3'X1'	S
53A	99.657	43.225	6.172	4.776	6.933	1'	S
53B	98.543	44.323	6.043	3.642	7.929	2'	S
53C	98.575	43.354	6.763	2.248	9.451	3'X1'	S
54A	99.596	51.771	6.043	4.642	6.689	1'	G
54B	98.550	52.821	6.148	3.732	7.966	2'	S
54C	98.572	51.815	6.671	2.192	9.499	3'X1'	S
55A	110.178	10.128	6.030	4.624	6.671	1'	G
55B	109.229	11.250	6.153	3.726	8.122	2'	S
55C	109.268	10.101	6.630	2.146	9.568	2'x2'	S
56A	110.236	18.435	6.069	4.673	6.710	1'	G
56B	109.282	19.667	6.117	3.721	8.018	2'	S
56C	109.326	18.566	6.673	2.210	9.621	2'x2'	S
57A	110.057	26.716	6.109	4.708	6.760	1'	G
57B	109.154	27.804	6.192	3.770	7.989	2'	S
57C	109.052	26.823	6.725	2.241	9.757	2'x2'	S
58A	110.163	35.170	6.108	4.707	6.733	1'	G
58B	108.920	36.192	6.168	3.757	8.012	2'	S
58C	109.060	35.214	6.709	2.220	9.449	3'X1'	S
59A	109.990	42.997	6.136	4.730	6.782	1'	G
59B	108.991	44.258	6.175	3.748	8.035	2'	S
59C	109.000	43.153	6.735	2.251	9.569	3'X1'	S
60A	110.135	51.133	6.172	4.771	6.860	1'	G
60B	109.137	52.304	6.149	3.727	7.972	2'	S
60C	109.093	51.249	6.672	2.198	9.459	3'X1'	S
61A	120.532	9.941	5.922	4.521	6.579	1'	G
61B	119.570	10.946	6.065	3.643	7.951	2'	S
61C	119.506	9.959	6.597	2.212	9.576	2'x2'	S
62A	120.696	18.438	6.061	4.665	6.994	1'	G
62B	119.707	19.402	6.080	3.638	7.997	2'	S
62C	119.669	18.490	6.610	2.126	9.548	2'x2'	S
63A	120.714	26.716	6.055	4.649	6.878	1'	G
63B	119.790	27.749	6.089	3.678	7.975	2'	S
63C	119.792	26.793	6.713	2.208	9.713	2'x2'	S
64A	120.617	35.092	6.166	4.765	7.047	1'	G
64B	119.475	36.183	6.226	3.794	8.060	2'	S
64C	119.679	35.152	6.699	2.215	9.496	3'X1'	S

Piez #	Local Coordinates (ft)		Elevations (ft)			In-ground Riser	
	x	y	coupling	screen	tube	Length	Type
65A	120.688	43.250	6.127	4.726	6.992	1'	G
65B	119.620	44.427	6.104	3.708	7.990	2'	S
65C	119.632	43.212	6.779	2.279	9.581	3'x1'	S
66A	120.530	51.529	6.049	4.659	6.867	1'	G
66B	119.612	52.427	6.113	3.717	8.046	2'	S
66C	119.656	51.456	6.682	2.286	9.641	2'x2'	S
S1	0.000	0.000	6.572				
S2	134.648	0.000	7.589				
S3	0.003	67.409	8.357				
S4	134.616	67.551	9.256				
WEIR	127.682	29.790	7.190				

Notes:

(1) The conversion to local coordinates is based on a survey conducted 12-05-2001 using Total Station Survey equipment. Construction stake S1 forms the origin for the coordinate system. Elevations are relative to the approximate elevation of the impermeable wetland liner, assumed to be at 817.6097' mean sea level.

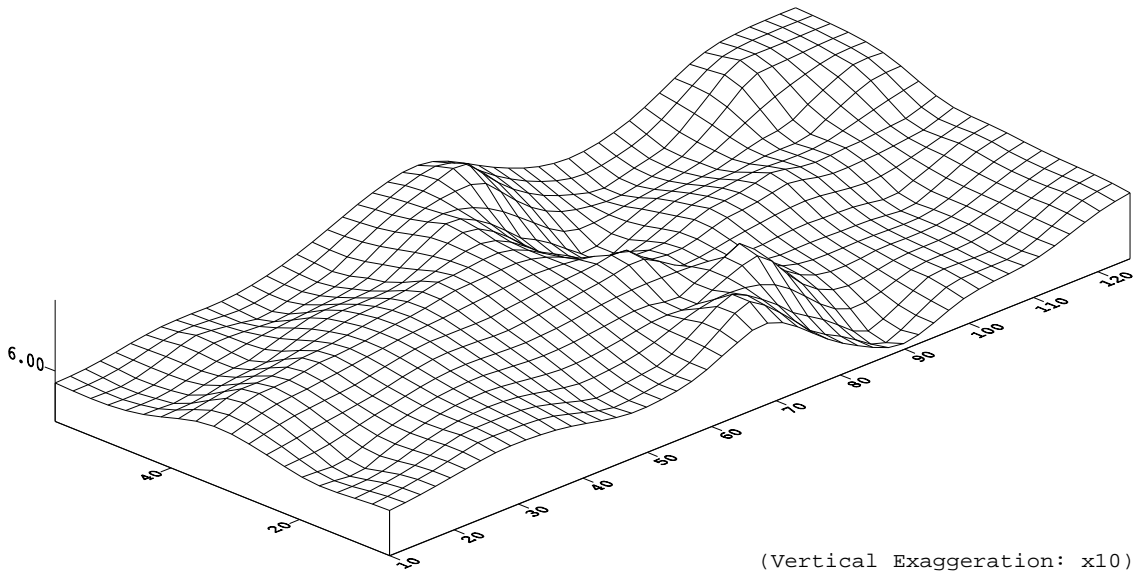
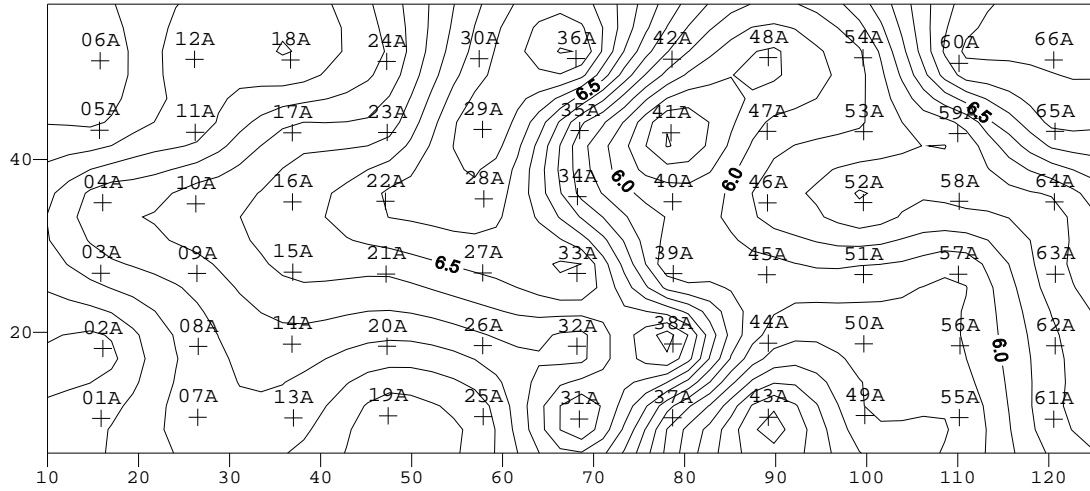
(2) "Coupling" elevation is the elevation of the above ground coupling; "screen elevation" is the elevation at the midpoint of the piezometer screen; "tube elevation" is the elevation at the top of the exposed 1/2" Teflon tube.

(3) "S" indicates stainless steel is used for the riser; "G" indicates galvanized steel is used for the riser.

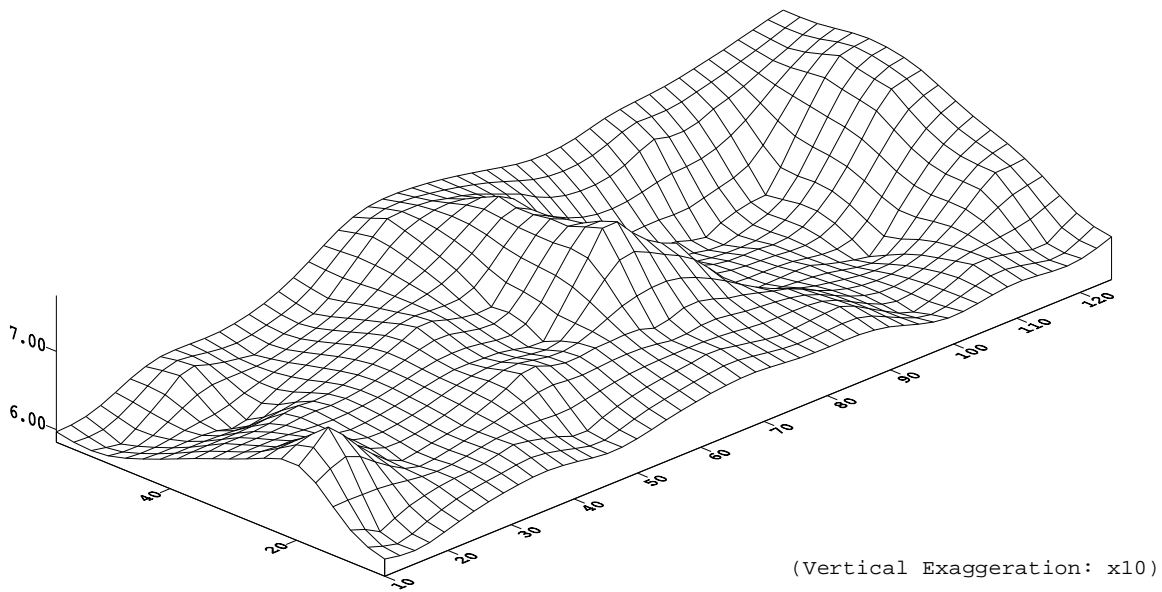
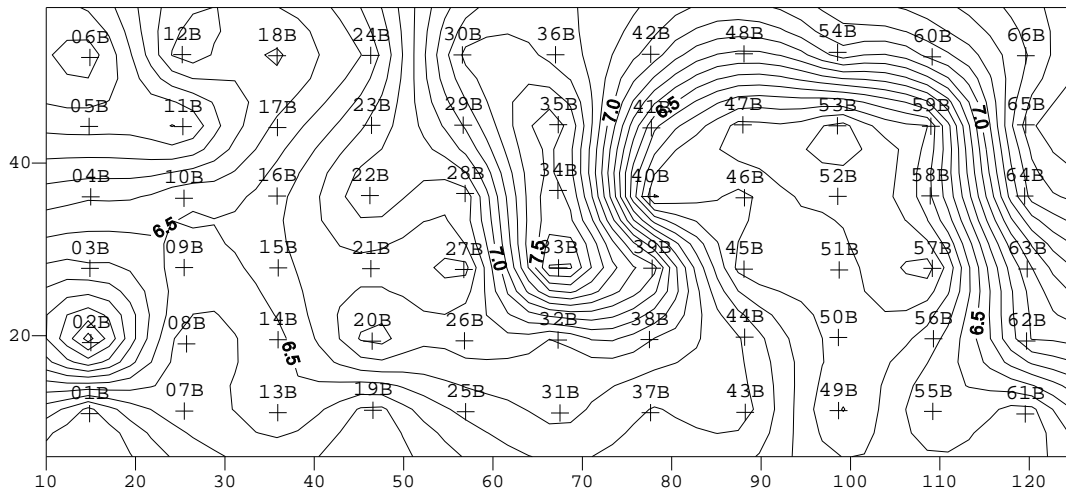
(4) Piezometer 61B is severely canted. Piezometer 6C has never registered a water level. Piezometer 29C hit a rock during installation and is positioned in the middle soil layer.

Appendix B: Contours of Hydraulic Head (11-01-2001)

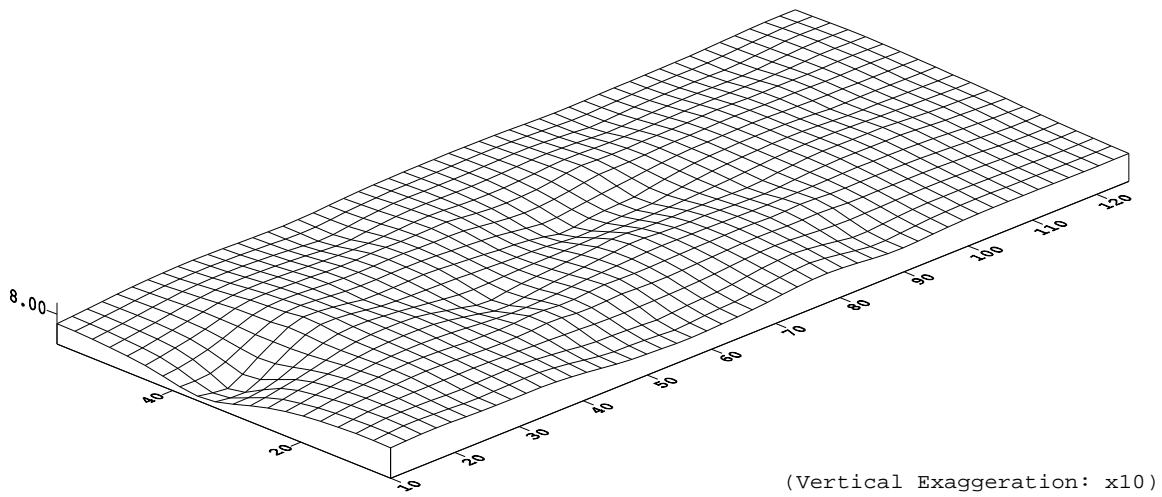
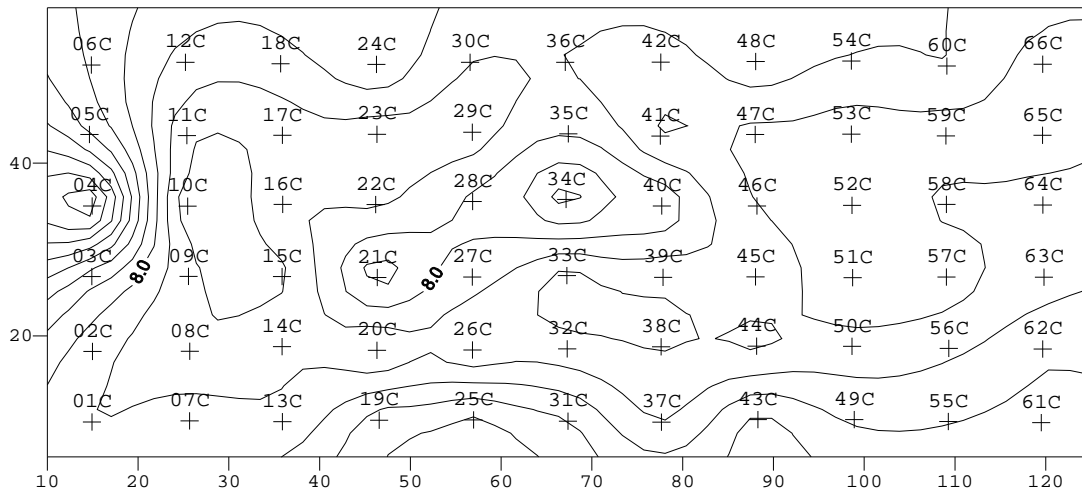
Hydraulic Head: Top Soil Layer (11-01-2001)



Hydraulic Head: Middle Soil Layer (11-01-2001)



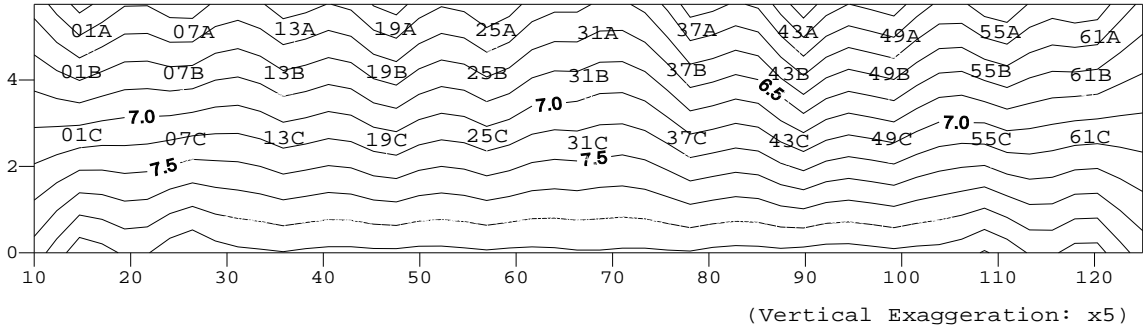
Hydraulic Head: Bottom Soil Layer (11-01-2001)



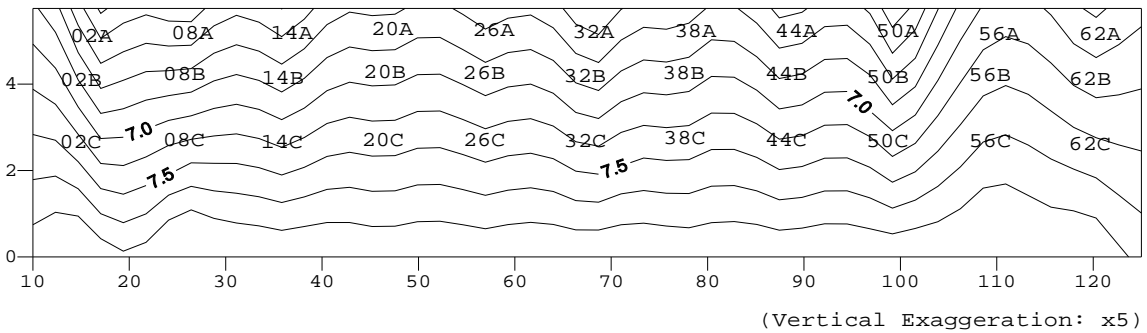
(Vertical Exaggeration: x10)

Profile View of Equipotentials: 11-01-2001

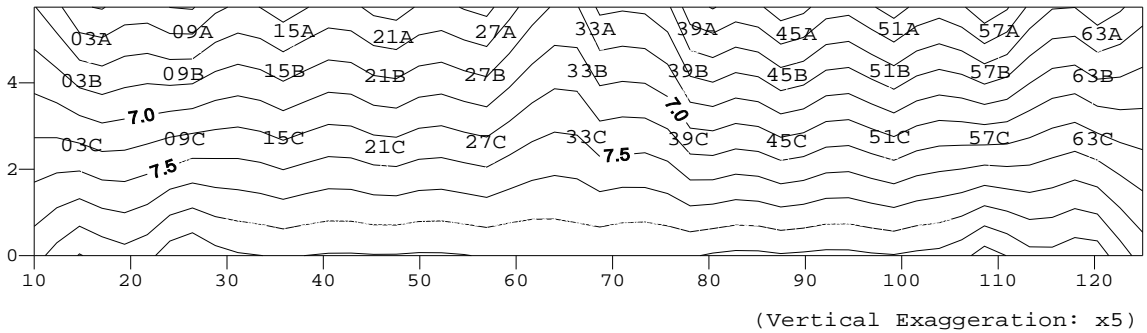
Piezometers: 1, 7, 13, 19, 25, 31, 37, 43, 49, 55, 61



Piezometers: 2, 8, 14, 20, 26, 32, 38, 44, 50, 56, 62

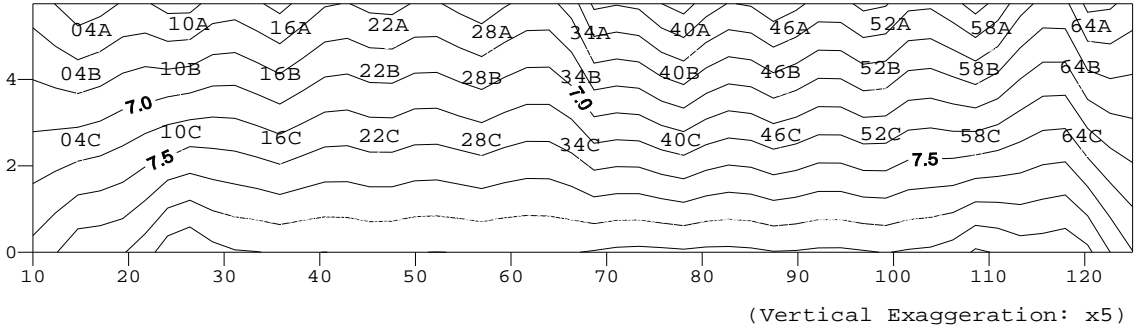


Piezometers: 3, 9, 15, 21, 27, 33, 39, 45, 51, 57, 63

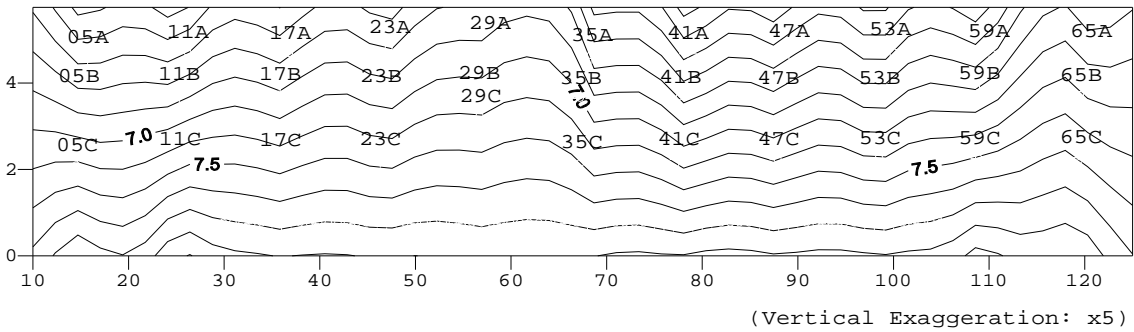


Profile View of Equipotentials: 11-01-2001

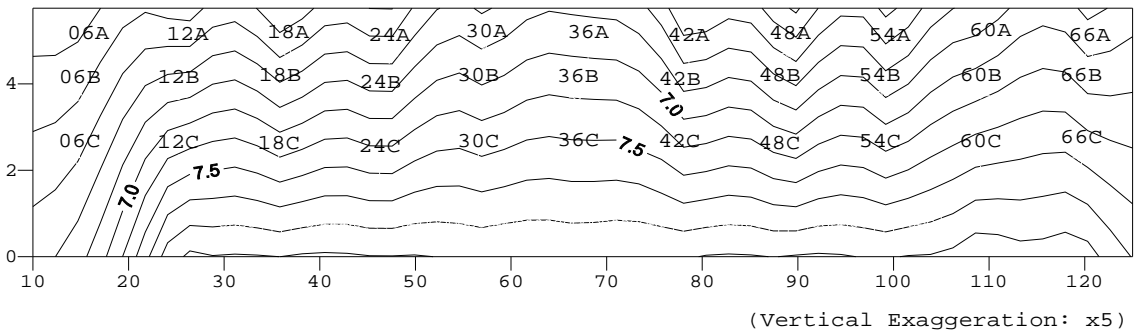
Piezometers: 4, 10, 16, 22, 28, 34, 40, 46, 52, 58, 64



Piezometers: 5, 11, 17, 23, 29, 35, 41, 47, 53, 59, 65

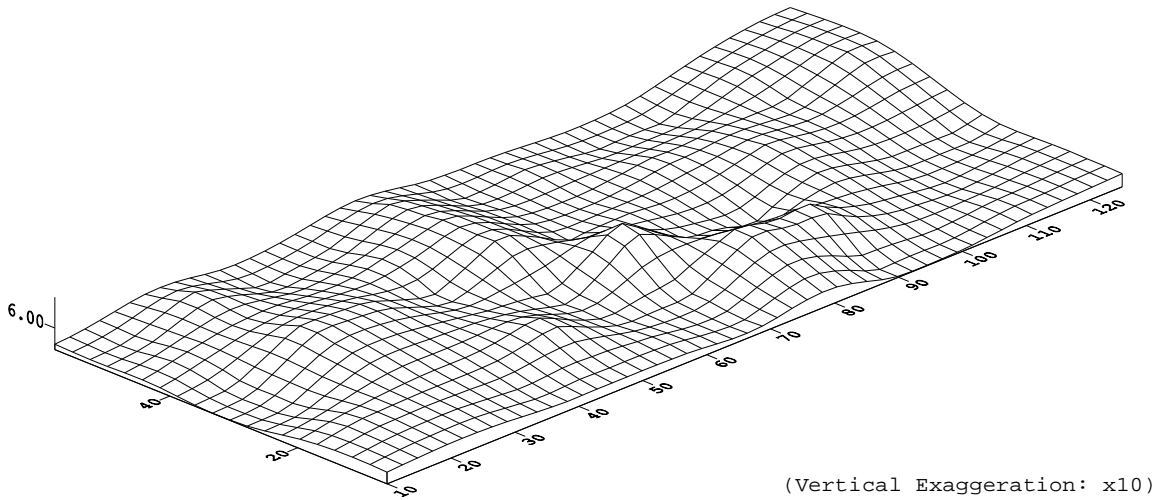
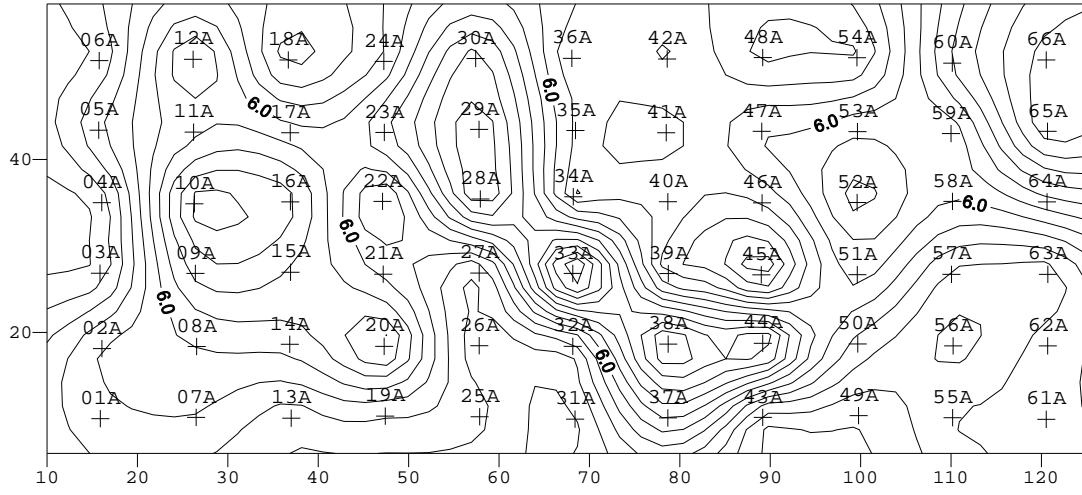


Piezometers: 6, 12, 18, 24, 30, 36, 42, 48, 54, 60, 66

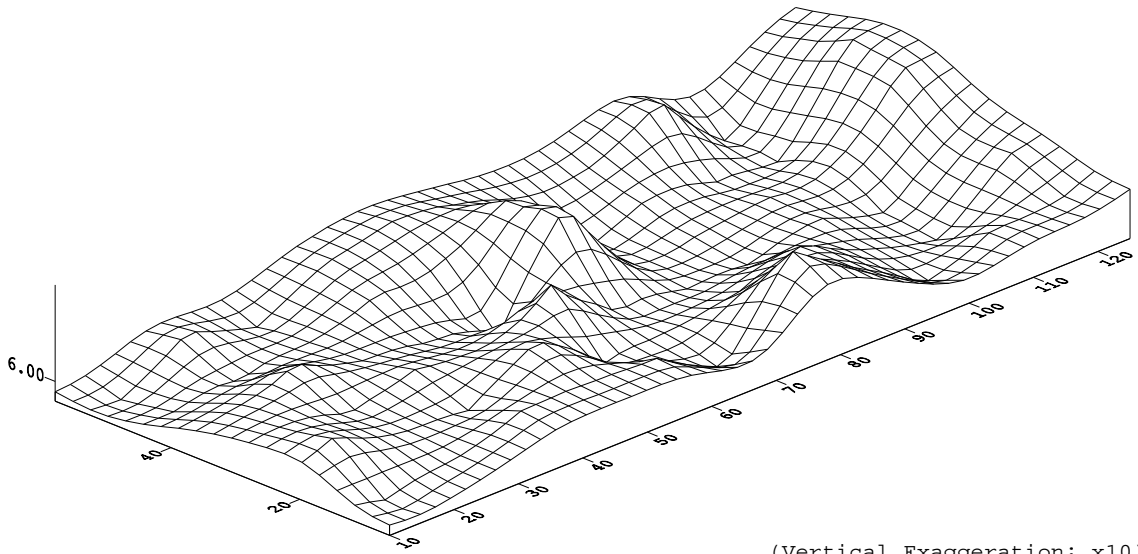
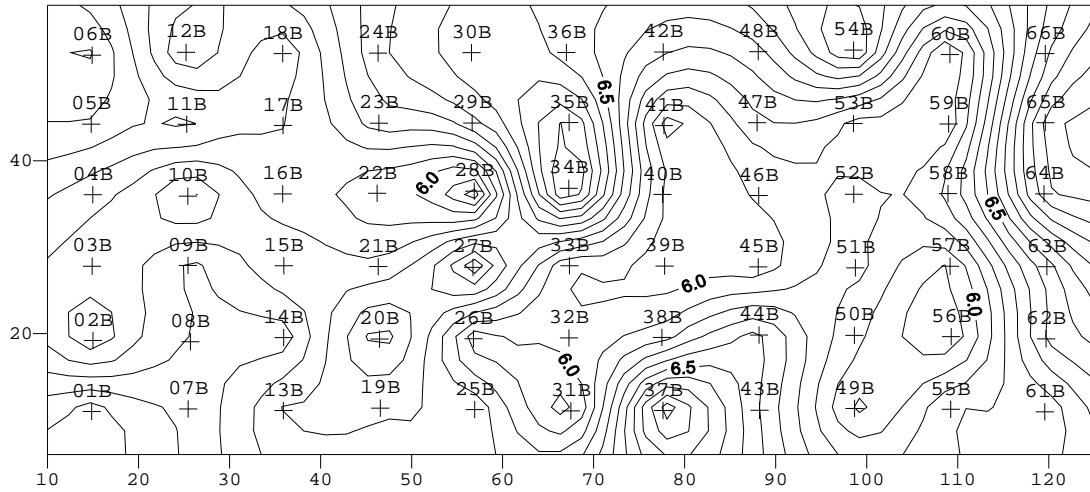


Appendix C: Contours of Hydraulic Head (02-19-2002)

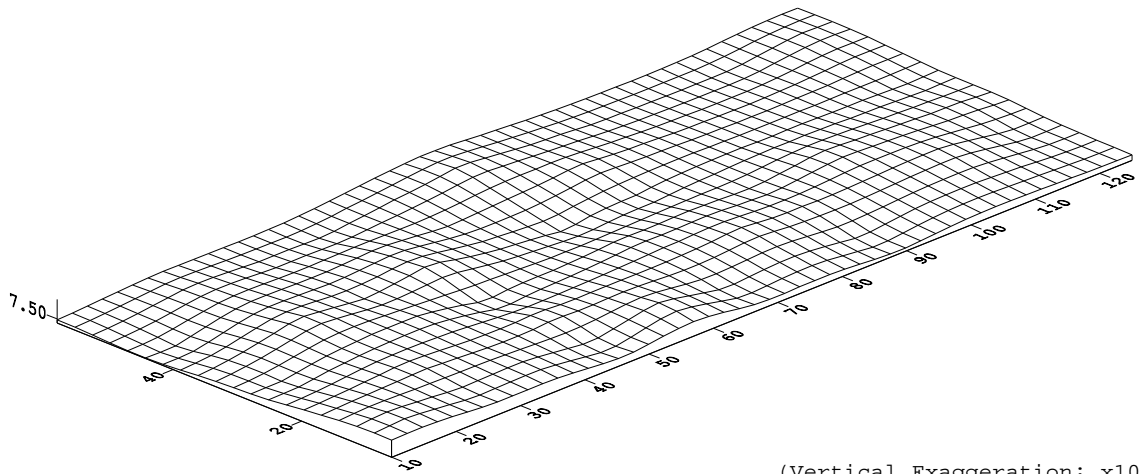
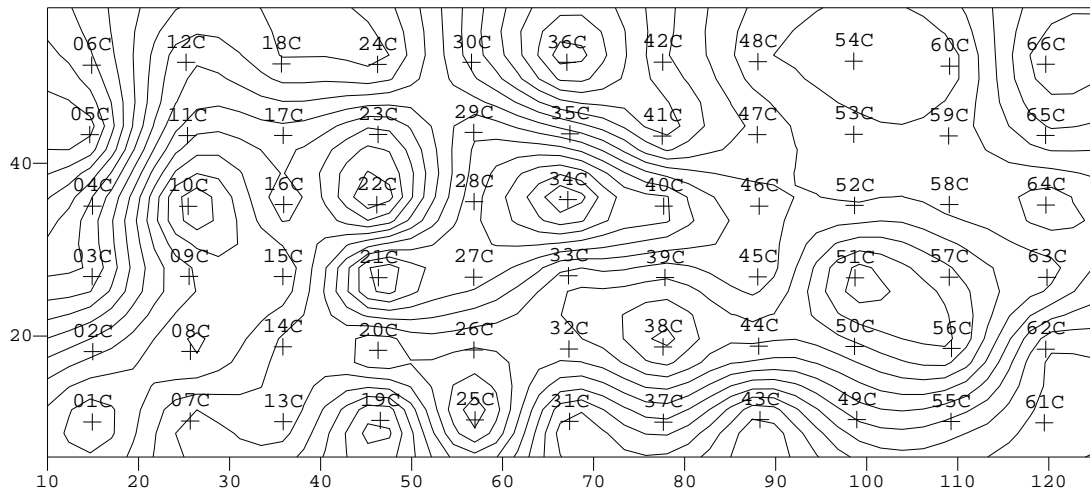
Hydraulic Head: Top Soil Layer (02-19-2002)



Hydraulic Head: Middle Soil Layer (02-19-2002)



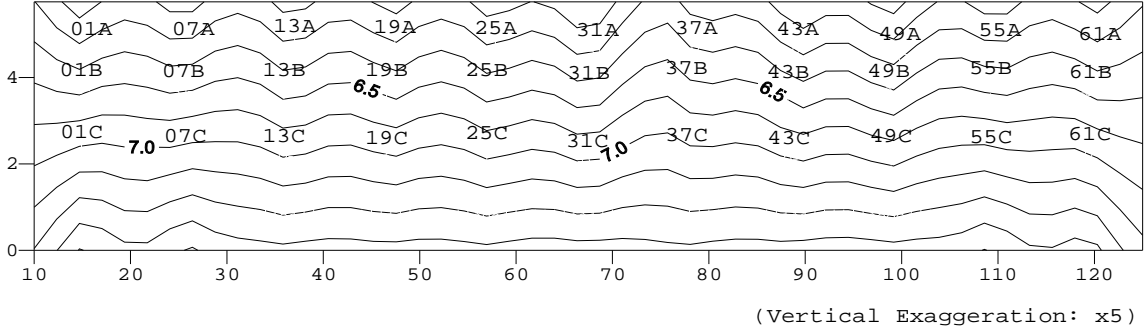
Hydraulic Head: Bottom Soil Layer (02-19-2002)



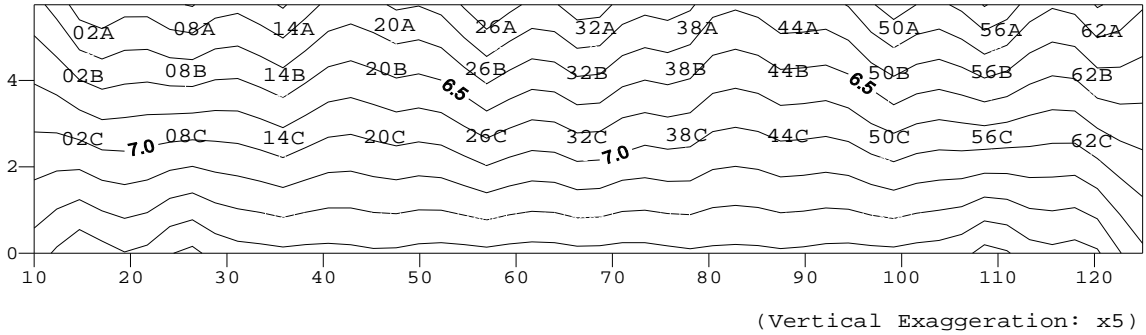
(Vertical Exaggeration: x10)

Profile View of Equipotentials: 02-19-2002

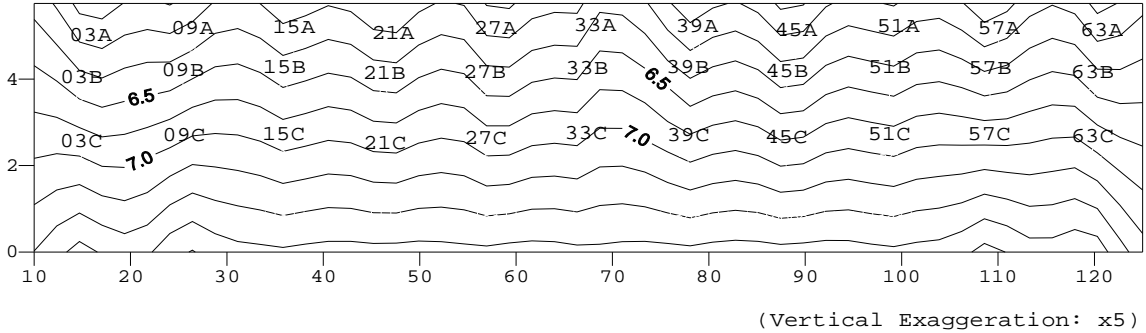
Piezometers: 1, 7, 13, 19, 25, 31, 37, 43, 49, 55, 61



Piezometers: 2, 8, 14, 20, 26, 32, 38, 44, 50, 56, 62

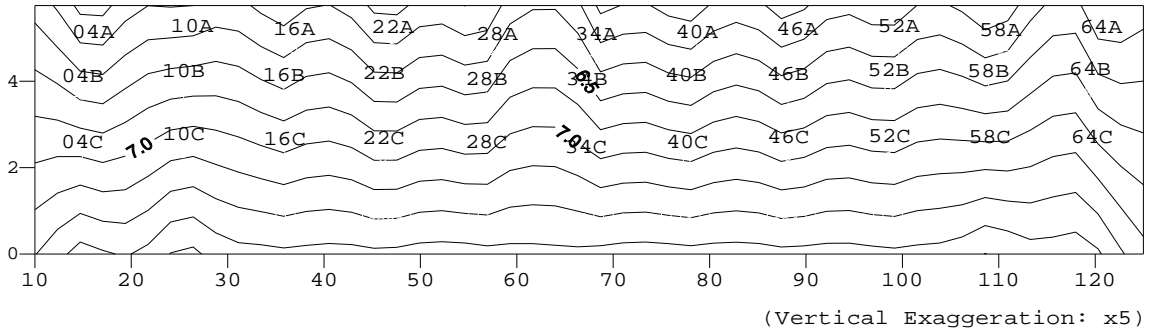


Piezometers: 3, 9, 15, 21, 27, 33, 39, 45, 51, 57, 63

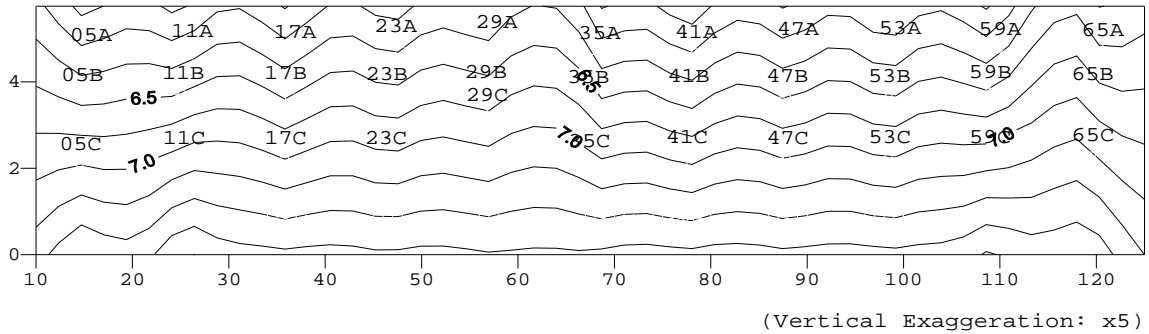


Profile View of Equipotentials: 02-19-2002

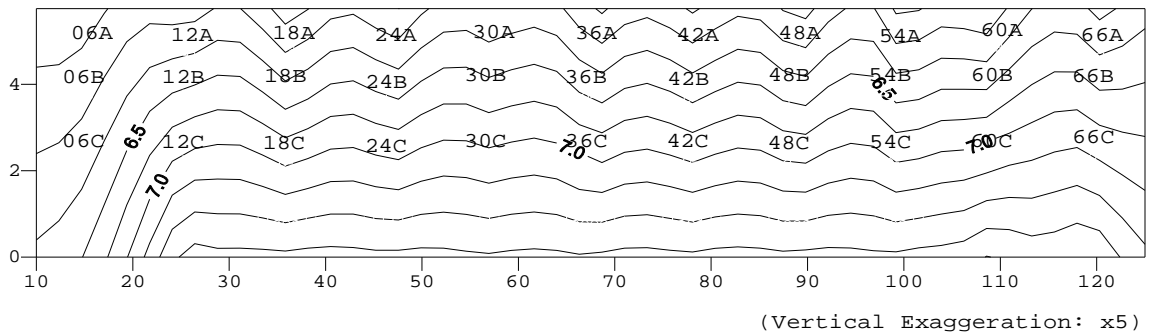
Piezometers: 4, 10, 16, 22, 28, 34, 40, 46, 52, 58, 64



Piezometers: 5, 11, 17, 23, 29, 35, 41, 47, 53, 59, 65



Piezometers: 6, 12, 18, 24, 30, 36, 42, 48, 54, 60, 66



Appendix D: Water Level Measurements

Piez #	10/17/01	10/18/01	10/19/01	10/22/01	10/29/01	11/1/01	11/8/01	2/19/02
01A	0.850	0.125	0.219	0.292	0.810	0.980	1.050	1.040
01B	2.490	2.200	2.270	2.380	2.590	2.610	2.700	2.780
01C	1.520	1.530	1.500	1.510	1.600	1.580	1.515	1.920
02A	1.410	1.300	1.190	0.990	1.170	1.080	1.620	0.950
02B	0.580	0.640	0.610	0.530	0.855	0.580	1.235	1.380
02C	1.370	1.360	1.330	1.294	1.390	1.370	1.320	1.770
03A	0.510	0.520	0.500	0.443	0.645	0.550	1.278	0.945
03B	1.307	1.220	1.075	0.980	1.360	1.090	1.150	1.455
03C	1.350	1.350	1.310	1.273	1.370	1.360	1.298	1.755
04A	0.600	0.570	0.530	0.469	0.680	0.575	0.570	1.120
04B	0.960	0.880	0.860	0.820	1.010	0.970	0.930	1.185
04C	1.720	1.680	1.630	1.620	1.770	1.710	1.640	1.720
05A	0.990	0.960	0.890	0.820	1.050	0.910	0.920	0.915
05B	1.930	1.580	1.800	1.770	1.985	1.890	1.960	2.050
05C	1.370	1.350	1.315	1.268	1.370	1.360	1.304	1.800
06A	1.260	1.240	1.170	1.060	1.320	1.170	1.304	1.190
06B	2.200	2.150	2.070	2.020	2.210	2.095	2.075	2.140
06C								
07A	0.700	0.590	0.500	0.440	0.745	0.670	0.770	0.910
07B	1.580	1.510	1.440	1.380	1.635	1.510	1.590	1.855
07C	1.400	1.380	1.370	1.350	1.420	1.400	1.360	1.813
08A	1.025	0.940	0.795	0.700	1.010	0.810	0.875	0.960
08B	1.910	1.780	1.650	1.565	1.885	1.680	1.735	1.885
08C	1.390	1.370	1.360	1.350	1.415	1.400	1.350	1.800
09A	0.430	0.370	0.360	0.470	0.710	0.690	0.635	0.810
09B	1.460	1.410	1.385	1.465	1.705	1.595	2.145	1.980
09C	1.490	1.480	1.450	1.435	1.510	1.490	1.445	1.920
10A	0.525	0.490	0.480	0.500	0.710	0.700	0.725	0.840
10B	1.570	1.520	1.520	1.510	1.720	1.730	1.820	1.780
10C	1.525	1.500	1.490	1.470	1.540	1.530	1.480	1.940
11A	1.030	1.020	0.975	0.855	1.130	0.930	1.615	0.935
11B	2.220	2.220	2.185	2.080	2.330	2.140		2.130

Piez #	10/17/01	10/18/01	10/19/01	10/22/01	10/29/01	11/1/01	11/8/01	2/19/02
11C	1.420	1.400	1.385	1.370	1.430	1.420	1.370	1.870
12A	0.795	0.910	0.910	0.770	1.180	0.790	1.170	0.780
12B	1.700	1.790	1.700	1.520	2.030	1.490	1.580	1.670
12C	1.410	1.400	1.380	1.365	1.440	1.430	1.380	1.850
13A	1.110	1.030	0.900	0.755	1.135	0.870	1.000	1.170
13B	1.400	3.210	2.150	2.030	2.490	2.090	2.220	2.265
13C	1.610	1.570	1.560	1.550	1.620	1.600	1.560	2.005
14A	0.840	0.900	0.840	0.670	1.120	0.715	0.820	0.960
14B	2.290	2.350	2.200	2.020	2.580	2.050	2.140	2.485
14C	1.580	1.550	1.550	1.530	1.600	1.580	1.535	2.005
15A	0.600	0.450	0.380	0.370	0.710	0.535	0.479	0.870
15B	2.290	2.190	2.090	2.080	2.440	2.210	2.180	2.475
15C	1.630	1.600	1.600	1.590	1.650	1.640	1.600	2.068
16A	0.445	0.385	0.375	0.417	0.620	0.540	0.417	0.820
16B	1.310	1.290	1.325	1.190	1.495	1.289	1.220	1.730
16C	1.318	1.310	1.283	1.236	1.340	1.312	1.268	1.740
17A	0.980	0.980	0.810	0.565	1.215	0.610	0.730	0.945
17B	2.210	2.130	1.840	1.595	2.240	1.630	1.745	1.960
17C	1.390	1.350	1.360	1.350	1.420	1.400	1.350	1.849
18A	1.770	1.560	1.340	0.995	1.180	1.035		1.200
18B	2.980	1.910	1.710	1.660	2.050	1.780	1.855	2.040
18C	1.318	1.270	1.273	1.242	1.320	1.315	1.256	1.780
19A	0.990	0.930	0.920	0.900	1.080	1.045	1.060	1.060
19B	1.930	1.840	1.725	1.680	2.000	1.850	1.875	1.780
19C	1.500	1.470	1.490	1.460	1.540	1.500	1.470	1.920
20A								0.935
20B	1.580	1.580	1.420	1.160	1.845	1.225	1.345	1.520
20C	1.460	1.410	1.430	1.410	1.480	1.450	1.410	1.875
21A	0.420	0.430	0.400	0.203	0.620	0.443	1.400	0.850
21B	1.470	1.435	1.290	1.185	1.650	1.278	1.120	1.720
21C	1.245	1.220	1.225	1.210	1.772	1.269	1.210	1.680
22A	0.188	0.172	0.177	0.198	0.420	0.417	0.182	1.200
22B	0.770	0.760	0.750	0.795	1.040	1.050	0.510	1.950
22C	1.420	1.370	1.380	1.360	1.430	1.420	1.370	1.755
23A	0.560	0.520	0.530	0.545	0.820	0.780	0.720	1.030

Piez #	10/17/01	10/18/01	10/19/01	10/22/01	10/29/01	11/1/01	11/8/01	2/19/02
23B	1.276	1.240	1.170	1.130	1.435	1.200	1.220	1.560
23C	1.450	1.410	1.420	1.410	1.480	1.470	1.410	1.870
24A	1.050	0.960	0.810	0.650	1.000	0.700	0.875	0.950
24B	1.150	1.140	1.150	1.145	1.729	1.180	2.445	1.230
24C	1.250	1.210	1.220	1.200	1.623	1.250	1.200	1.660
25A	0.520	0.490	0.430	0.375	0.750	0.890	0.840	1.045
25B	2.330	2.320	2.240	2.020	2.555	2.100	2.345	2.330
25C	1.800	1.760	1.700	1.695	1.810	1.730	1.730	1.900
26A								1.250
26B	2.060	2.190	2.080	1.810	2.470	1.960	2.020	2.800
26C	1.570	1.530	1.545	1.520	1.590	1.580	1.585	2.036
27A								1.100
27B	3.470	3.220	2.960	2.290	1.500	1.380		1.210
27C	1.440	1.410	1.415	1.400	1.460	1.440	1.400	1.910
28A	0.266	0.271	0.203	0.047	0.390	0.167	0.375	0.520
28B	1.281	1.210	1.020	0.950	1.835	0.970	0.052	2.000
28C	1.297	1.260	1.268	1.216	1.320	1.309	1.256	1.730
29A	0.208	0.193	0.255	0.240	0.375	0.417	0.156	0.950
29B	0.830	0.850	0.860	0.840	0.975	0.940	0.930	1.570
29C	2.135	2.090	2.000	1.970	2.110	2.000	1.890	2.510
30A	0.182	0.151	0.115	0.130	0.328	0.333	0.313	0.745
30B	0.610	0.570	0.550	0.545	0.700	0.630	0.650	1.283
30C	1.410	1.380	1.380	1.370	1.450	1.420	1.390	1.823
31A	0.560	0.420	0.156	0.042	0.510	0.156	0.229	1.040
31B	2.210	2.140	1.930	1.770	2.230	1.840	1.910	2.650
31C	1.440	1.400	1.400	1.385	1.460	1.445	1.410	1.830
32A	0.890	0.850	0.800	0.905	0.980	0.830	0.820	1.170
32B	2.150	2.125	2.020	1.875	2.290	1.975	2.040	2.580
32C	1.540	1.510	1.515	1.500	1.570	1.550	1.520	2.000
33A					0.750	0.385	0.198	0.594
33B	0.830	0.840	0.835	0.980	1.000	0.745	1.200	2.620
33C	1.670	1.630	1.650	1.640	1.700	1.680	1.645	2.177
34A	0.670	0.550	0.490	0.453	0.680	0.610	0.555	0.910
34B	0.318	0.292	0.240	0.188	0.339	0.229	0.161	0.698
34C	1.210	1.185	1.195	1.570	1.245	1.230	1.195	1.640

Piez #	10/17/01	10/18/01	10/19/01	10/22/01	10/29/01	11/1/01	11/8/01	2/19/02
35A	0.610	0.560	0.580	0.560	0.770	0.760	0.730	0.970
35B	0.370	0.348	0.292	0.281	0.318	0.188	0.057	0.860
35C	1.271	1.260	1.252	1.250	1.320	1.304	1.266	1.700
36A	0.151	0.073	0.026	0.000	0.188	0.000	-0.135	1.070
36B	0.835	0.810	0.755	0.705	0.790	0.700	0.665	1.400
36C	1.445	1.410	1.420	1.405	1.480	1.460	1.420	1.755
37A	0.980	0.900	0.905	0.880	1.070	1.050	1.040	0.850
37B	2.370	2.300	2.170	2.120	2.565	2.270	2.370	1.740
37C	1.500	1.475	1.480	1.465	1.535	1.510	1.480	1.990
38A	0.385	0.346	0.276	0.109	0.302	0.219	0.980	0.635
38B	1.960	1.940	1.870	1.785	2.200	2.050	2.500	2.600
38C	1.640	1.610	1.630	1.620	1.680	1.660	1.630	2.075
39A					1.330	1.140		1.150
39B	1.580	2.040	2.070	1.750	2.105	1.640	1.200	2.880
39C	1.550	1.520	1.530	1.560	1.585	1.565	1.530	2.010
40A	0.980	1.055	0.980	0.720	1.135	0.880	0.890	0.930
40B	1.770	1.560	1.520	1.250	1.600	1.360	1.390	1.450
40C	1.305	1.290	1.290	1.320	1.350	1.320	1.283	1.750
41A					1.785	1.320	1.915	1.050
41B	1.550	1.530	1.520	1.420	1.590	1.410	1.595	2.010
41C	1.380	1.355	1.365	1.380	1.420	1.400	1.365	1.802
42A	0.760	0.620	0.470	0.286	0.710	0.490	0.515	0.670
42B	1.120	1.110	1.010	0.895	1.220	0.950	1.010	1.610
42C	1.330	1.315	1.304	1.320	1.380	1.350	1.320	1.755
43A						1.495		1.070
43B	1.940	2.080	2.080	1.830	2.360	1.985	2.775	2.160
43C	1.490	1.460	1.480	1.480	1.530	1.510	1.470	1.995
44A								0.542
44B	2.135	2.180	2.200	2.165	2.160	2.205		2.240
44C	1.570	1.540	1.550	1.555	1.610	1.590	1.555	2.040
45A	1.000	0.950	0.890	0.780	1.110	0.910	1.100	1.180
45B	2.810	2.700	2.570	2.420	2.810	2.515	2.630	2.720
45C	1.500	1.460	1.475	1.470	1.530	1.520	1.480	1.970
46A	1.275	1.263	1.065	0.810	1.370	0.755	1.215	1.025
46B	2.500	2.440	2.150	1.615	2.450	1.730	2.080	1.960

Piez #	10/17/01	10/18/01	10/19/01	10/22/01	10/29/01	11/1/01	11/8/01	2/19/02
46C	1.390	1.350	1.370	1.360	1.430	1.395	1.365	1.880
47A	1.400	1.450	1.370	0.900	1.590	1.030		1.060
47B	2.260	2.370	2.265	1.780	2.550	1.840	2.390	1.705
47C	1.520	1.480	1.490	1.490	1.550	1.530	1.490	1.995
48A	1.330	1.220	1.100	0.910	1.080	0.940	1.294	0.960
48B	3.170	3.070	2.780	2.030	1.430	1.320		1.635
48C	1.360	1.320	1.330	1.283	1.380	1.370	1.325	1.781
49A	0.895	0.920	0.820	0.690	1.085	0.825	1.180	0.910
49B	2.370	2.520	2.540	2.410	2.875	2.490	3.050	2.710
49C	1.580	1.550	1.550	1.540	1.610	1.590	1.560	2.021
50A	0.970	0.960	0.955	0.950	1.100	1.100	1.100	1.075
50B							3.910	1.910
50C	1.630	1.600	1.605	1.590	1.665	1.635	1.610	2.060
51A	1.430	1.294	1.170		1.560	1.070		0.980
51B	2.210	2.040	1.945	1.820	2.140	2.000	2.030	2.000
51C	1.580	1.555	1.570	1.540	1.625	1.610	1.570	2.005
52A	0.810	0.770	0.680	1.273	0.800	0.600	1.340	0.800
52B				2.710	2.190	2.050		2.000
52C	1.490	1.470	1.470	1.450	1.530	1.500	1.470	2.000
53A	0.870	0.800	0.770	0.690	0.950	0.890	0.880	0.920
53B	1.940	1.875	1.840	1.750	2.030	1.955	1.955	1.850
53C	1.380	1.350	1.360	1.335	1.420	1.395	1.360	1.900
54A	0.860	0.670	0.520	0.286	0.765	0.590	0.640	0.830
54B	1.010	1.080	1.050	0.870	1.708	0.990	2.200	1.130
54C	1.435	1.410	1.415	1.400	1.470	1.450	1.415	1.917
55A	0.710	0.660	0.680	0.660	0.830	0.835	0.810	0.780
55B	1.470	1.590	1.640	1.600	1.920	1.725	3.570	1.920
55C	1.490	1.460	1.480	1.465	1.520	1.510	1.470	1.950
56A								0.920
56B								2.230
56C	1.540	1.500	1.530	1.500	1.580	1.560	1.520	1.960
57A	0.990	0.890	0.830	0.760	0.930	0.905		0.940
57B	2.110	2.020	1.985	1.930	2.180	2.110	2.105	2.150
57C	1.690	1.660	1.670	1.650	1.720	1.700	1.665	2.150
58A	0.605	0.515	0.440	0.344	0.560	0.500	0.500	0.740

Piez #	10/17/01	10/18/01	10/19/01	10/22/01	10/29/01	11/1/01	11/8/01	2/19/02
58B	1.880	1.780	1.720	1.650	1.830	1.765	1.760	1.815
58C	1.390	1.360	1.370	1.350	1.420	1.400	1.360	1.870
59A	1.000	0.910	0.730	0.469	0.870	0.610	1.410	0.800
59B	2.050	2.000	1.900	1.740	2.080	1.875	2.385	2.060
59C	1.500	1.470	1.490	1.465	1.530	1.520	1.480	2.020
60A	0.302	1.570	0.400	0.000	0.286	0.052	0.115	0.730
60B	1.170	1.100	1.380	1.330	1.400	0.945	1.210	2.030
60C	1.400	1.390	1.380	1.370	1.440	1.420	1.385	1.885
61A	0.417	0.400	0.335	0.094	0.570	0.292		0.610
61B	1.790	1.700	1.830	1.785	2.005	1.710	2.870	1.700
61C	1.570	1.550	1.570	1.560	1.640	1.620	1.590	2.070
62A								1.100
62B	1.080	1.200	1.190	0.920	1.580	1.060	1.560	1.435
62C	1.470	1.430	1.445	1.435	1.500	1.480	1.445	1.953
63A	0.670	0.670	0.595	0.450	0.830	0.570	0.830	1.050
63B	0.970	1.050	1.015	0.870	1.335	1.000	1.500	1.415
63C	1.640	1.615	1.630	1.610	1.680	1.660	1.615	2.099
64A	0.920	0.865	0.800	0.670	0.990	0.820	0.880	0.990
64B	0.830	0.780	0.680	0.595	0.930	0.700	0.735	1.020
64C	1.440	1.405	1.415	1.400	1.460	1.440	1.415	1.938
65A	0.167	0.162	0.104	0.135	0.328	0.281	0.339	0.656
65B	0.354	0.345	0.297	0.286	0.427	0.417	0.380	0.830
65C	1.520	1.485	1.500	1.480	1.550	1.530	1.510	1.990
66A	0.078	0.078	0.021	0.016	0.120	0.042	0.365	0.531
66B	0.605	0.890	0.595	0.610	0.705	0.670	0.720	1.170
66C	1.580	1.530	1.550	1.540	1.610	1.595	1.560	2.020
water table	1.208	1.214	1.214	1.214	1.370	1.375	1.370	1.391

Notes:

(1) All measurements in feet.

(2) Distance to the water level in the piezometers is measured from the top of the ½" plastic piezometer tube.

(3) Distance to the water table is measured from the south edge of the horizontal metal bar on the weir.

Appendix E: Bouwer and Rice Slug Test Results

Top Soil Layer

Piez	Test Date	Early K	Middle K	Overall K	R ²	Dev	Type	Recov
01A	12/07/01	1.54E-05	7.96E-06	7.22E-06	0.92	2	+	95.5%
01A	12/07/01	1.65E-05	1.16E-05	1.04E-05	0.97	2	+	98.0%
02A	12/07/01			1.31E-05	1.00	1	+	96.6%
03A	12/07/01			too fast		1	+	
04A	12/07/01			3.66E-05	0.99	2	+	97.4%
05A	12/07/01	8.37E-06	1.50E-06	1.11E-06	0.94	2	+	95.0%
06A	12/07/01			1.53E-05	1.00	1	+	98.9%
07A	12/07/01			1.47E-06	0.98	2	+	93.1%
08A								
09A	11/08/01			1.68E-08	1.00	-	+	74.4%
09A	12/04/01			3.45E-07	1.00	2	+	68.9%
10A								
11A	11/16/01			2.28E-06	0.99	1	+	97.9%
12A								
13A	12/07/01	1.22E-05	1.90E-06	1.57E-06	0.82	2	+	88.6%
14A	12/11/01			3.32E-06	0.99	2	+	89.3%
15A	11/08/01			1.59E-07	0.99	-	-	60.4%
15A	11/16/01			1.22E-07	0.99	-	+	81.6%
15A	12/15/01	2.43E-06	1.09E-06	7.72E-07	0.90	2	+	87.9%
16A	12/07/01	3.22E-05	1.06E-05	1.27E-05	0.90	2	+	96.4%
17A								
18A	12/07/01	1.20E-05	6.92E-06	4.77E-06	0.97	1	+	89.9%
19A	12/07/01	4.60E-05	1.77E-05	1.91E-05	0.94	2	+	97.9%
20A								
21A	12/07/01	1.16E-05	1.60E-06	1.58E-06	0.94	1	+	96.4%
22A								
23A	11/14/01			1.27E-07	1.00	-	+	87.8%
23A	12/11/01			1.41E-05	0.99	2	+	67.9%
23A	12/11/01			3.06E-05	1.00	2	+	77.1%
24A								
25A	12/04/01	6.03E-06	3.59E-06	2.96E-06	0.97	2	+	91.0%
26A	12/07/01	1.84E-06	7.28E-07	2.61E-07	0.72	1	+	38.9%
27A	12/04/01	5.13E-06	8.56E-07	6.16E-07	0.82	1	+	75.9%
28A	12/04/01	4.98E-06		1.15E-06	0.97	1	-	61.5%
29A	12/04/01			too fast				

Piez	Test Date	Early K	Middle K	Overall K	R ²	Dev	Type	Recov
30A	12/11/01	6.71E-05		3.27E-05	0.80	2	-	94.1%
31A	11/02/01			8.56E-08	1.00	-	-	63.4%
31A	12/11/01			1.33E-06	0.98	2	+	88.5%
32A	12/11/01			1.59E-05	1.00	2	+	98.8%
32A	12/11/01			1.50E-05	1.00	2	+	98.1%
33A	11/02/01			3.92E-09	1.00	-	+	2.5%
33A	11/21/01			1.02E-08	1.00	-	-	57.6%
33A	12/15/01			2.30E-06	0.99	2	+	89.9%
34A	11/02/01			5.82E-08	0.98	-	+	50.5%
34A	11/16/01			9.15E-08	1.00	-	+	77.8%
34A	12/07/01	9.91E-06		2.74E-06	0.90	2	+	70.3%
35A	12/11/01	1.72E-05		1.00E-05	0.97	2	+	92.1%
36A	11/02/01			1.04E-07	1.00	-	-	73.8%
36A	12/11/01	1.28E-05	7.08E-06	8.04E-06	0.96	2	+	90.7%
37A	10/19/01			5.56E-08	1.00	-	+	26.8%
37A	11/16/01			5.14E-08	1.00	-	+	55.8%
37A	12/15/01			too fast		2	+	
38A	11/02/01			9.92E-09	0.99	-	-	7.9%
38A	11/21/01			3.87E-06	0.99	1	+	93.7%
38A	12/04/01			2.07E-06	0.99	1	+	75.7%
39A	12/04/01	6.68E-06	4.07E-06	2.97E-06	0.93	1	+	90.5%
40A								
41A	11/21/01	4.77E-06	2.62E-06	1.85E-06	0.96	1	+	96.1%
42A								
43A	12/05/01	6.50E-06	2.28E-06	1.51E-06	0.90	1	+	89.1%
44A	12/05/01			5.68E-08	0.98	1	+	43.5%
45A	12/05/01			4.92E-05	1.00	1	+	99.2%
46A	12/05/01	5.23E-06	1.24E-06	9.42E-07	0.98	2	+	99.3%
47A	12/05/01	4.52E-06	1.16E-06	3.21E-07	0.60	1	+	79.7%
48A	12/05/01	1.05E-05	2.03E-07	5.25E-07	0.88	2	+	96.6%
49A								
50A	12/11/01			2.49E-05	1.00	2	+	28.1%
51A								
52A	11/16/01			2.42E-06	0.98	1	+	97.8%
53A								
54A	12/11/01	1.15E-05	5.58E-06	1.96E-06	0.79	2	+	90.4%
55A	12/11/01	4.63E-05		2.84E-05	0.97	2	+	76.9%
56A								
57A	12/11/01	3.70E-05		1.18E-05	0.89	2	+	96.5%

Piez	Test Date	Early K	Middle K	Overall K	R ²	Dev	Type	Recov
58A								
59A	12/11/01	7.94E-06	2.63E-06	2.06E-06	0.93	2	+	82.6%
60A	11/20/01			2.66E-08	0.99	-	-	22.7%
61A	11/16/01	3.75E-07	1.88E-07	1.71E-07	0.94	1	+	76.4%
62A	12/11/01	6.34E-06	3.14E-06	2.06E-06	0.86	1	+	58.7%
63A								
64A	12/11/01	3.34E-06		1.80E-06	0.98	2	+	87.6%
65A								
66A	12/11/01	2.43E-05	4.90E-06	6.71E-06	0.87	2	+	92.1%

Notes:

(1) Units for hydraulic conductivity are feet/second.

(2) Hydraulic conductivity for early and late data computed for tests with R² < 0.98.

(3) "Dev" indicates whether the test was conducted on an undeveloped piezometer (-) or on a piezometer developed on 11/08/2001 (1) or 11/28/2001 (2).

(4) "Type" indicates whether water was added (+), extracted (-) or displaced (d).

(5) "%Recov" indicates percent recovery relative to the pre-test equilibrium water levels.

Middle Soil Layer

Piez	Test Date	Early K	Middle K	Overall K	R ²	Dev	Type	Recov
01B	12/15/01			too fast		2	+	
02B	11/15/01			1.25E-08	1.000	-	d	65.2%
02B	12/03/01	6.23E-06	1.48E-06	8.70E-07	0.934	2	+	95.1%
03B	11/02/01			1.33E-07	0.994	-	-	38.3%
03B	12/07/01	6.39E-06	1.08E-06	1.10E-06	0.788	2	+	91.2%
04B	12/07/01	1.15E-05	7.89E-06	5.71E-06	0.960	2	+	93.4%
05B	12/15/01	9.56E-07	4.83E-07	4.63E-07	0.973	2	+	92.8%
06B	11/15/01			1.26E-07	0.982	-	+	69.8%
06B	12/15/01	3.76E-06	1.51E-06	8.24E-07	0.806	2	+	89.4%
07B								
08B	12/15/01	4.22E-05	1.39E-05	4.64E-06	0.807	2	+	84.2%
09B								
10B	11/15/01			5.67E-07	0.993	-	+	96.7%
10B	12/15/01			4.40E-05	0.985	2	+	97.9%
10B	12/15/01	5.14E-05		3.44E-05	0.941	2	+	98.5%
11B								
12B	12/15/01	1.76E-06	5.83E-07	4.96E-07	0.916	2	+	90.6%
13B	12/15/01	1.85E-06	4.30E-07	1.93E-07	0.714	2	+	55.8%
14B	11/15/01			7.19E-08	0.978	-	+	55.5%
15B	12/15/01	3.85E-06	1.31E-06	7.66E-07	0.804	2	+	82.8%
16B								
17B	12/15/01	1.99E-05	7.64E-06	4.57E-06	0.784	2	+	84.3%
18B	11/15/01			4.50E-07	0.995	-	+	93.7%
19B								
20B	12/16/01	8.15E-06	4.75E-06	3.58E-06	0.931	2	+	91.8%
21B								
22B	10/18/01			3.83E-06	0.999	-	d	76.6%
22B	10/31/01			1.38E-06	0.993	-	d	81.3%
22B	11/05/01			1.52E-06	0.987	-	-	98.0%
22B	12/15/01	3.80E-05	2.12E-05	1.91E-05	0.945	2	+	97.0%
23B								
24B	12/16/01	2.66E-06		1.16E-07	0.357	2	+	36.5%
24B	12/16/01	1.31E-06	2.63E-07	1.43E-07	0.938	2	-	32.8%
25B	12/16/01	9.78E-06	5.02E-06	3.17E-06	0.891	2	+	95.4%
26B	11/15/01			1.44E-06	0.918	-	+	97.3%
27B	12/16/01			1.28E-06	0.981	1	+	77.7%
28B	11/05/01			7.79E-06	0.991	-	-	99.1%

Piez	Test Date	Early K	Middle K	Overall K	R ²	Dev	Type	Recov
29B	12/04/01			2.37E-05	0.981	2	+	98.5%
29C	12/04/01	1.16E-06	5.47E-07	6.36E-07	0.977	-	+	52.5%
30B	11/15/01			2.03E-08	0.999	-	-	77.3%
30B	12/04/01	7.87E-07	5.73E-07	4.23E-07	0.885	2	-	82.0%
31B								
32B	12/16/01	1.66E-05	5.94E-06	5.54E-06	0.959	2	+	96.3%
33B	11/01/01			3.53E-07	0.997	-	d	75.9%
34B	12/16/01	7.54E-07	1.70E-07	1.93E-07	0.978	2	-	72.8%
35B	11/05/01	2.49E-05	1.13E-05	1.23E-05	0.853	-	-	97.7%
36B	12/16/01	7.38E-06	2.04E-06	1.96E-06	0.890	2	+	85.8%
37B	12/05/01	1.39E-05	3.71E-06	2.82E-06	0.893	2	+	95.3%
38B								
39B	12/16/01	2.44E-06	6.15E-07	5.72E-07	0.898	2	+	80.4%
40B								
41B	12/16/01	1.63E-05	8.02E-06	3.93E-06	0.847	2	+	95.5%
42B								
43B	12/05/01	2.59E-06	8.13E-07	3.85E-07	0.858	2	+	71.9%
44B	11/13/01	4.50E-06	3.57E-07	1.03E-07	0.824	1	+	40.7%
45B	12/05/01	6.01E-06	2.16E-06	1.54E-06	0.807	2	+	92.3%
46B	11/13/01	3.15E-08		1.45E-08	0.965	-	+	68.2%
47B								
48B								
49B	12/11/01	1.42E-05	7.07E-06	3.85E-06	0.922	2	+	91.9%
50B								
51B	11/13/01			6.73E-08	0.991	-	+	49.0%
51B	12/11/01	1.13E-05	4.57E-06	3.44E-06	0.845	2	+	91.1%
52B								
53B	11/13/01	8.37E-07	5.23E-07	6.14E-07	0.964	-	+	74.9%
53B	12/11/01	2.44E-05	1.22E-05	1.39E-05	0.895	2	+	97.9%
54B								
55B								
56B	11/13/01	9.17E-08	3.92E-08	3.99E-08	0.890	1	+	24.3%
56B	12/05/01	2.20E-07		3.09E-08	0.826	1	+	33.7%
57B								
58B	11/13/01			1.48E-08	0.980	-	+	61.1%
58B	12/05/01	1.96E-05	1.00E-05	6.85E-06	0.901	2	+	99.2%
58B	12/05/01	2.21E-05	1.10E-05	8.31E-06	0.893	2	+	97.7%
59B	12/05/01	9.12E-06	4.18E-06	1.87E-06	0.847	1	+	97.1%
60B								

Piez	Test Date	Early K	Middle K	Overall K	R ²	Dev	Type	Recov
61B	12/11/01	3.30E-06	2.10E-06	1.20E-06	0.952	2	+	96.3%
62B								
63B	12/11/01	1.16E-06	4.55E-07	2.94E-07	0.912	2	+	72.6%
66B	10/18/01			6.02E-07	0.984	-	d	31.9%
66B	11/05/01	3.74E-06	2.16E-06	1.83E-06	0.902	-	d	82.6%
66B	12/11/01	1.45E-05	5.42E-06	3.99E-06	0.958	2	+	85.3%

Notes:

(1) Units for hydraulic conductivity are feet/second.

(2) Hydraulic conductivity for early and late data computed for tests with $R^2 < 0.98$.

(3) "Dev" indicates whether the test was conducted on an undeveloped piezometer (-) or on a piezometer developed on 11/08/2001 (1) or 11/28/2001 (2).

(4) "Type" indicates whether water was added (+), extracted (-) or displaced (d).

(5) "%Recov" indicates percent recovery relative to the pre-test equilibrium water levels.

Appendix F: Mathcad® Template for Slug Tests

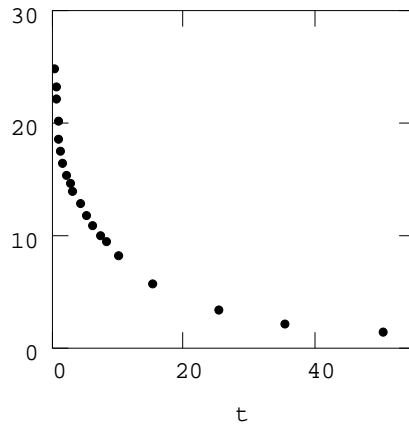
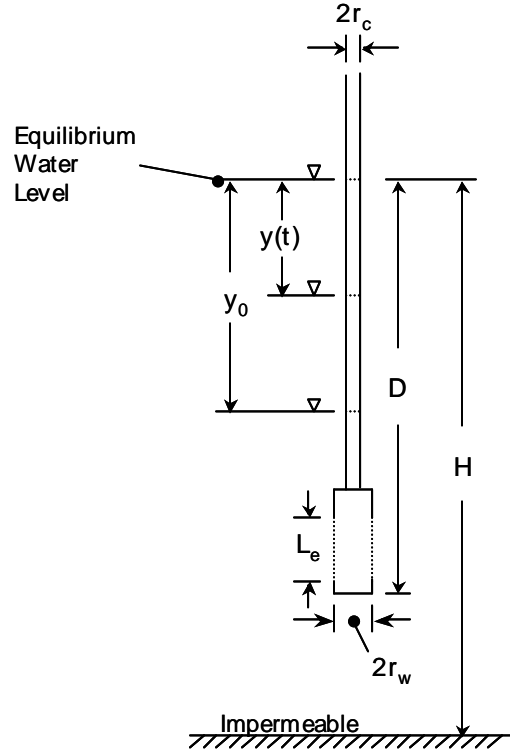
Piezometer: 05A

Date: 12-07-2001

Type: Add Water

1. Display and plot the test data:

$t :=$	$\left(\begin{array}{c} 0.17 \\ 0.33 \\ 0.50 \\ 0.67 \\ 0.83 \\ 1 \\ 1.5 \\ 2 \\ 2.5 \\ 3 \\ 4 \\ 5 \\ 6 \\ 7 \\ 8 \\ 10 \\ 15 \\ 25 \\ 35 \\ 50 \end{array} \right)$	$y :=$	$\left(\begin{array}{c} 24.79 \\ 23.19 \\ 22.09 \\ 20.08 \\ 18.50 \\ 17.37 \\ 16.28 \\ 15.29 \\ 14.56 \\ 13.90 \\ 12.72 \\ 11.68 \\ 10.77 \\ 9.92 \\ 9.29 \\ 8.18 \\ 5.55 \\ 3.35 \\ 2.13 \\ 1.37 \end{array} \right)$
--------	--	--------	---



2. Define relevant piezometer data:

Casing radius: $r_c := .25 \cdot \text{in}$

Intake radius: $r_w := .5 \cdot \text{in}$

Effective screen length: $L_e := 2.625 \cdot \text{in}$

Distance from piezometer tip to center of screen: $\text{tip} := 2.1875 \cdot \text{in}$

Piezometer length (tip to above-ground coupling): $\text{PL} := 30.625 \cdot \text{in}$

Midpoint elevation of piezometer screen: $P_{\text{elev}} := 4.5943 \cdot \text{ft}$

Water level in piezometer down from top of tube: $w_l := .915 \cdot \text{ft}$

Distance from equilibrium water level to bottom of screen intake (D) and distance of equilibrium water level above the impermeable wetland liner (H):

$$D := \text{PL} - \text{tip} - w_l \quad h := P_{\text{elev}} - \frac{L_e}{2}$$

$$H := D + h$$

3. Determine best fit line and compute R^2 for semi-log plot of $y(t)$ versus time. This is done by using built-in Mathcad functions and adapting the *principle of least squares* as presented by Devore for an intrinsically linear (in this case exponential) function (see pages 497-506 & 552 of Devore (2000) for a theoretical explanation).

ORIGIN \equiv 1 $n := \text{rows}(t)$ $i := 1.. n$

Define the best-fit line:

$$\beta_0 := \exp(\text{intercept}(t, \ln(y)))$$

$$\beta_1 := \text{slope}(t, \ln(y))$$

$$\text{line}(t) := \beta_0 \cdot e^{\beta_1 \cdot t}$$

Compute the error sum of squares:

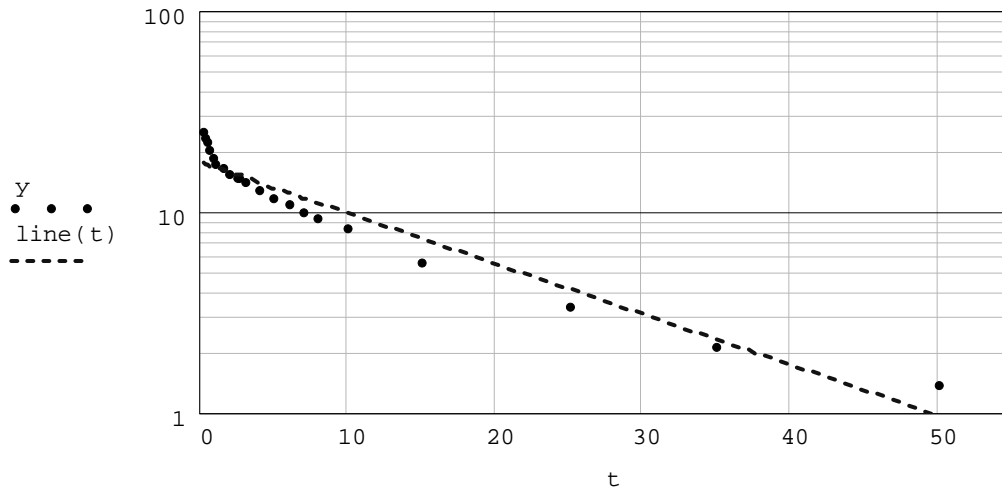
$$\varepsilon := \ln(y) - \ln(\text{line}(t)) \quad \text{SSE} := \sum_{i=1}^n (\varepsilon_i)^2$$

Compute the total sum of squares:

$$\ln_{-}y_{\text{bar}} := \sum_{i=1}^n \ln(y_i) \cdot \frac{1}{n} \quad \text{SST} := \sum_{i=1}^n (\ln(y_i) - \ln_{-}y_{\text{bar}})^2$$

Compute the *coefficient of determination* and plot the best fit line against the observed data:

$$R_{\text{squared}} := 1 - \frac{\text{SSE}}{\text{SST}} \quad R_{\text{squared}} = 0.9405$$



4. Use the Bouwer and Rice Method to Compute K:

$$y_0 := \beta_0 \quad y_n := \text{line}(t_n) \quad t_{\text{scale}} := \min$$

Define constants "A" and "B":, for $\frac{L_e}{r_w} = 5.25$

$$A := 1.75 \quad B := .25 \quad (\text{Source: figure 3.3.6, Charbeneau, 2000})$$

Determine the value for $\ln[(H-D)/r_w]$:

$$\ln\left(\frac{H-D}{r_w}\right) = 4.679 \quad (\text{Note: if } \ln[(H-D)/r_w] > 6, \text{ use } 6.)$$

Determine $\ln(R_e/r_w)$ and define as "X":

$$X := \left[\frac{1.1}{\ln\left(\frac{D}{r_w}\right)} + \frac{\left(A + B \cdot \ln\left(\frac{H-D}{r_w}\right) \right)}{\frac{L_e}{r_w}} \right]^{-1} \quad \text{(Equation 3.6.14, p.148, Charbeneau, 2000)}$$

Compute hydraulic conductivity K:

$$K_{br} := \frac{r_c^2 \cdot X}{2 \cdot L_e} \cdot \frac{1}{t_n \cdot t_{scale}} \cdot \ln\left(\frac{Y_0}{Y_n}\right) \quad \text{(Equation 3.6.13, p.147, Charbeneau, 2000)}$$

$$K_{br} = 1.113 \times 10^{-6} \frac{\text{ft}}{\text{sec}}$$

5. Use Hvorslev's Method (Source: Charbeneau):

Define the Shape Factor F:

$$F := \frac{2.4 \cdot \pi \cdot L_e}{\ln\left[\frac{1.2L_e}{2 \cdot r_w} + \sqrt{1 + \left(\frac{1.2L_e}{2 \cdot r_w}\right)^2} \right]} \quad \text{(Equation 9, Brand and Permchitt, 1980)}$$

Compute K:

$$K_{hv} := \frac{\pi \cdot (r_c)^2}{F} \cdot \frac{1}{t_n \cdot t_{scale}} \cdot \ln\left(\frac{Y_0}{Y_n}\right) \quad \text{(Equation 3.6.5, p.143, Charbeneau, 2000)}$$

$$K_{hv} = 1.497 \times 10^{-6} \frac{\text{ft}}{\text{sec}}$$

Compare Methods: $\frac{K_{hv}}{K_{br}} = 1.345$

6. Determine K for Early Data:

$$t := \begin{pmatrix} 0.17 \\ 0.33 \\ 0.50 \\ 0.67 \\ 0.83 \\ 1.00 \end{pmatrix} \quad y := \begin{pmatrix} 24.7892 \\ 23.1892 \\ 22.0892 \\ 20.0792 \\ 18.4992 \\ 17.3692 \end{pmatrix}$$

Compute coefficient of determination (R^2):

$$\text{ORIGIN} \equiv 1 \quad n := \text{rows}(t) \quad i := 1..n$$

$$\beta_0 := \exp(\text{intercept}(t, \ln(y)))$$

$$\beta_1 := \text{slope}(t, \ln(y)) \quad \text{line}(t) := \beta_0 \cdot e^{\beta_1 \cdot t}$$

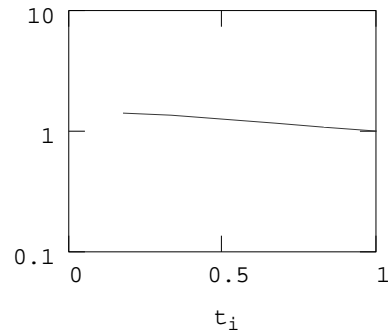
$$\varepsilon := \ln(y) - \ln(\text{line}(t)) \quad \text{SSE} := \sum_{i=1}^n (\varepsilon_i)^2$$

$$\ln_y\text{bar} := \sum_{i=1}^n \ln(y_i) \cdot \frac{1}{n} \quad \text{SST} := \sum_{i=1}^n (\ln(y_i) - \ln_y\text{bar})^2$$

$$R_{\text{squared}} := 1 - \frac{\text{SSE}}{\text{SST}}$$

$$R_{\text{squared}} = 0.99286$$

$$\frac{Y_i}{Y_0}$$



Compute and Compare K Values:

$$Y_0 := \beta_0 \quad Y_n := \text{line}(t_n)$$

$$K_{\text{br}} := \frac{r_c^2 \cdot X}{2 \cdot L_e} \cdot \frac{1}{t_n \cdot t_{\text{scale}}} \cdot \ln\left(\frac{Y_0}{Y_n}\right)$$

$$K_{\text{br}} = 8.373 \times 10^{-6} \frac{\text{ft}}{\text{sec}}$$

$$K_{\text{hv}} := \frac{\pi \cdot (r_c)^2}{F} \cdot \frac{1}{t_n \cdot t_{\text{scale}}} \cdot \ln\left(\frac{Y_0}{Y_n}\right)$$

$$K_{\text{hv}} = 1.126 \times 10^{-5} \frac{\text{ft}}{\text{sec}}$$

$$\frac{K_{\text{hv}}}{K_{\text{br}}} = 1.345$$

7. Determine K for Middle Data:

$t :=$	1.50	$y :=$	16.2792
	2.00		15.2892
	2.50		14.5592
	3.00		13.8992
	4.00		12.7192
	5.00		11.6792
	6.00		10.7692
	7.00		9.9192
	8.00		9.2892
	10.00		8.1792
	15.00		5.5492

Compute coefficient of determination (R^2):

ORIGIN \equiv 1 $n :=$ rows(t) $i :=$ 1.. n

$\beta_0 :=$ exp(intercept(t , ln(y)))

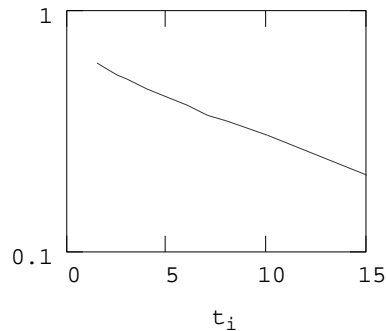
$\beta_1 :=$ slope(t , ln(y)) line(t) $:=$ $\beta_0 \cdot e^{\beta_1 \cdot t}$

$\epsilon :=$ ln(y) - ln(line(t)) $SSE := \sum_{i=1}^n (\epsilon_i)^2$

$\ln_ybar := \sum_{i=1}^n \ln(y_i) \cdot \frac{1}{n}$ $SST := \sum_{i=1}^n (\ln(y_i) - \ln_ybar)^2$

$R_{squared} := 1 - \frac{SSE}{SST}$

$R_{squared} = 0.99579$



Compute and Compare K Values:

$y_0 := \beta_0$ $y_n :=$ line(t_n)

$K_{br} := \frac{r_c^2 \cdot X}{2 \cdot L_e} \cdot \frac{1}{t_n \cdot t_{scale}} \cdot \ln\left(\frac{y_0}{y_n}\right)$

$K_{br} = 1.497 \times 10^{-6} \frac{ft}{sec}$

$K_{hv} := \frac{\pi \cdot (r_c)^2}{F} \cdot \frac{1}{t_n \cdot t_{scale}} \cdot \ln\left(\frac{y_0}{y_n}\right)$

$K_{hv} = 2.015 \times 10^{-6} \frac{ft}{sec}$

$\frac{K_{hv}}{K_{br}} = 1.345$

8. Determine K for Late Data:

$$t := \begin{pmatrix} 25 \\ 35 \\ 50 \end{pmatrix} \quad y := \begin{pmatrix} 3.3528 \\ 2.1336 \\ 1.3716 \end{pmatrix}$$

Compute coefficient of determination (R^2):

$$\text{ORIGIN} \equiv 1 \quad n := \text{rows}(t) \quad i := 1..n$$

$$\beta_0 := \exp(\text{intercept}(t, \ln(y)))$$

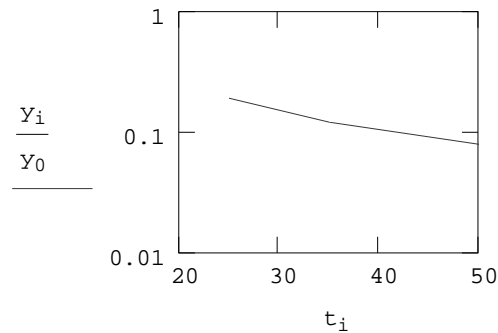
$$\beta_1 := \text{slope}(t, \ln(y)) \quad \text{line}(t) := \beta_0 \cdot e^{\beta_1 \cdot t}$$

$$\varepsilon := \ln(y) - \ln(\text{line}(t)) \quad \text{SSE} := \sum_{i=1}^n (\varepsilon_i)^2$$

$$\ln_y\text{bar} := \sum_{i=1}^n \ln(y_i) \cdot \frac{1}{n} \quad \text{SST} := \sum_{i=1}^n (\ln(y_i) - \ln_y\text{bar})^2$$

$$R_{\text{squared}} := 1 - \frac{\text{SSE}}{\text{SST}}$$

$$R_{\text{squared}} = 0.98531$$



Compute and Compare K Values:

$$y_0 := \beta_0 \quad y_n := \text{line}(t_n)$$

$$K_{\text{br}} := \frac{r_c^2 \cdot X}{2 \cdot L_e} \cdot \frac{1}{t_n \cdot t_{\text{scale}}} \cdot \ln\left(\frac{y_0}{y_n}\right)$$

$$K_{\text{br}} = 6.733 \times 10^{-7} \frac{\text{ft}}{\text{sec}}$$

$$K_{\text{hv}} := \frac{\pi \cdot (r_c)^2}{F} \cdot \frac{1}{t_n \cdot t_{\text{scale}}} \cdot \ln\left(\frac{y_0}{y_n}\right)$$

$$K_{\text{hv}} = 9.059 \times 10^{-7} \frac{\text{ft}}{\text{sec}} \quad \frac{K_{\text{hv}}}{K_{\text{br}}} = 1.345$$

Appendix G: Mathcad® Template for Pump Tests

Pump Test: 11-20-2001

Pumping Well: 21C

Observation Piezometer: 15C

Hantush Match-point Method for a Leaky Confined Aquifer with Partially Screened, Partially Penetrating Wells:

1. Define the distance between the pumping and observation wells (r), the aquifer thickness (b), the aquitard thickness (b'), and the pump rate (Q).

$$r := 10.51139026 \cdot \text{ft}$$

ORIGIN \equiv 1

$$b := (1.5 + 1.25) \cdot \text{ft}$$

$$b_{\text{prime}} := 3 \cdot \text{ft}$$

$$Q := \frac{1 \cdot \text{gal}}{71 \cdot \text{sec}}$$

2. Define elevation of layer surface and the approximate piezometer screen length (ASL):

$$\text{Layer_C_elev}_{\text{top}} := 2.75 \cdot \text{ft}$$

$$\text{ASL} := 2.625 \cdot \text{in}$$

3. Define screen midpoint elevations (SME) for the pumping and observation well and compute l_p , d_p , l_o , d_o :

$$\text{SME}_{\text{pump_well}} := 2.0337 \cdot \text{ft}$$

$$l_p := \text{Layer_C_elev}_{\text{top}} - \text{SME}_{\text{pump_well}} + \frac{\text{ASL}}{2} \quad l_p = 0.826 \text{ ft}$$

$$d_p := \text{Layer_C_elev}_{\text{top}} - \text{SME}_{\text{pump_well}} - \frac{\text{ASL}}{2} \quad d_p = 0.607 \text{ ft}$$

$$SME_{obs_well} := 2.2459 \cdot ft$$

$$l_o := Layer_C_elev_{top} - SME_{obs_well} + \frac{ASL}{2} \quad l_o = 0.613 \text{ ft}$$

$$d_o := Layer_C_elev_{top} - SME_{obs_well} - \frac{ASL}{2} \quad d_o = 0.395 \text{ ft}$$

4. Estimate K_z/K_r and compute x :

$$Kz_over_Kr := 1$$

$$x := \frac{r}{b} \cdot \sqrt{Kz_over_Kr}$$

5. Define the range of values for " u_r ", " $1/u_r$ ", and " r/B_r ":

$r_over_B :=$	$\left(\begin{array}{c} .001 \\ .15 \\ .3 \\ .45 \\ .6 \\ .75 \\ 1 \\ 1.3 \\ 1.6 \\ 2 \end{array} \right)$	(Note: " u_r " spans values from .00001 to 10 but is not defined in the margins.)
		$i := 1, 2 .. rows(u_r)$
		$one_over_u_{r_i} := \frac{1}{u_{r_i}}$
		$j := 1, 2 .. 10$

6. Define the Well Function, $W(u_r, r/B_r)$, for partial penetration:

Note: The summation of the partial penetration correction factor, n , ranges from 1 to 100 (instead of 1 to infinity as directed in the reference) to allow solution with this software application.

$$F_{i,j} := \left[\frac{2 \cdot b^2}{\pi^2 \cdot (l_p - d_p)(l_o - d_o)} \right] \sum_{n=1}^{100} \left(\frac{1}{n^2} \right) \left(\sin\left(\frac{n \cdot \pi \cdot l_p}{b}\right) - \sin\left(\frac{n \cdot \pi \cdot d_p}{b}\right) \right) \cdot \left(\sin\left(\frac{n \cdot \pi \cdot l_o}{b}\right) - \sin\left(\frac{n \cdot \pi \cdot d_o}{b}\right) \right) \int_{u_i}^{\infty} \frac{1}{y} \cdot e^{-y \frac{(r_{\text{over_Bj}})^2 + (n \cdot \pi \cdot x)^2}{4y}} dy \quad (\text{equation 12.14, Dawson and Istok, 1991})$$

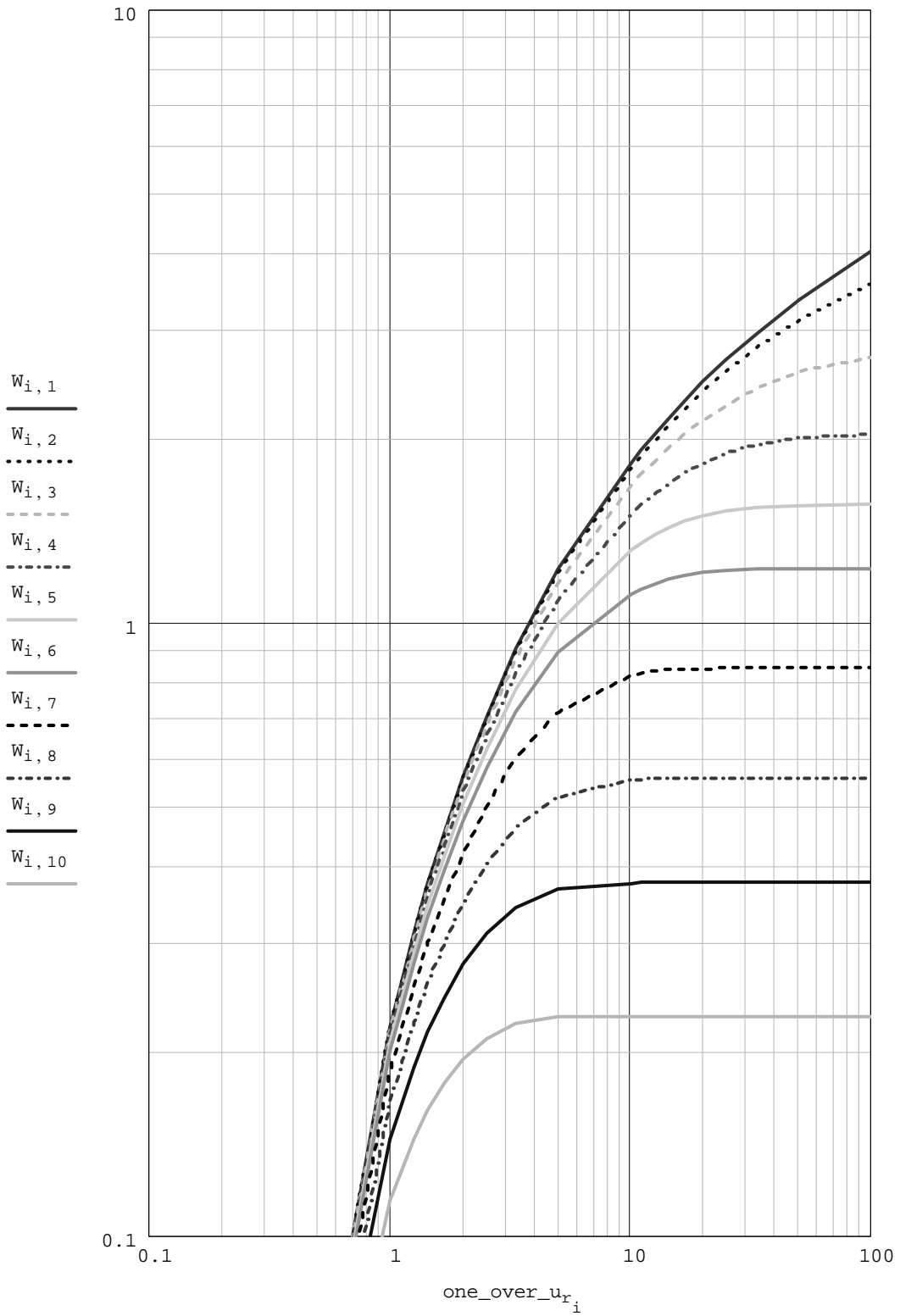
7. Define the Well Function, $W(u_r, r/B_r)$, for partial penetration:

$$W_{i,j} := \int_{u_{r_i}}^{\infty} \frac{1}{y} \cdot e^{-y \frac{(r_{\text{over_Bj}})^2}{4y}} dy + F_{i,j} \quad (\text{equation 12.12, Dawson and Istok, 1991})$$

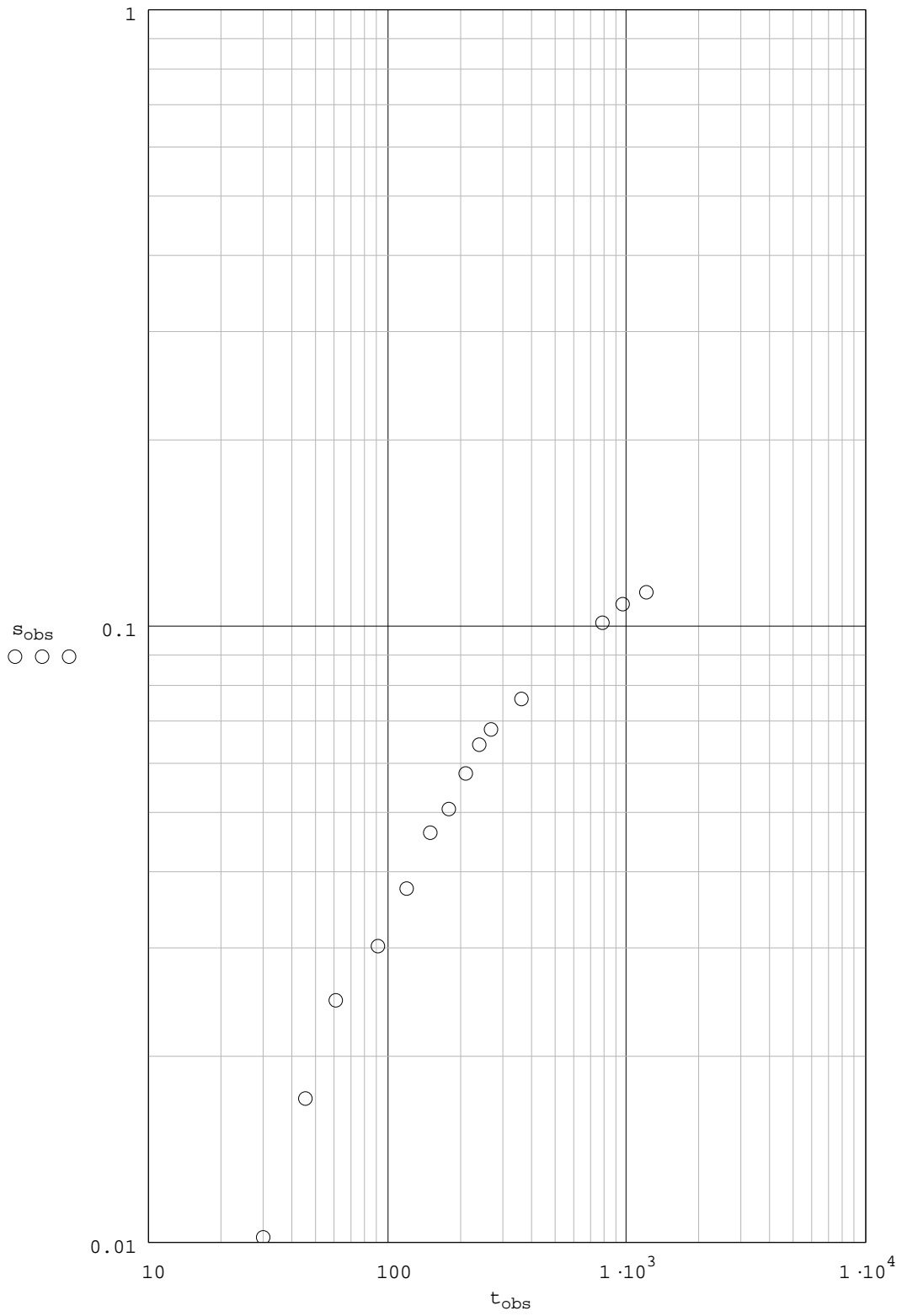
8. Display the time/drawdown data from the aquifer test:

$$t_{\text{obs}} := \begin{pmatrix} 0.5 \\ 0.75 \\ 1 \\ 1.5 \\ 2 \\ 2.5 \\ 3 \\ 3.5 \\ 4 \\ 4.5 \\ 6 \\ 13 \\ 16 \\ 20 \end{pmatrix} \cdot \text{min} \quad s_{\text{obs}} := \begin{pmatrix} 0.31 \\ 0.52 \\ 0.75 \\ 0.92 \\ 1.14 \\ 1.4 \\ 1.53 \\ 1.75 \\ 1.95 \\ 2.07 \\ 2.31 \\ 3.08 \\ 3.29 \\ 3.45 \end{pmatrix} \cdot \text{cm}$$

9. Plot the type-curves for the well function $W(u_r, r/B_r)$:



10. Plot the observed time drawdown curve:



11. Calculate aquifer hydraulic conductivity:

a. List match-points for $W(u,r/B)$ and drawdown, s :

$$W_{\text{star}} := 1.75 \quad s_{\text{star}} := .108 \cdot \text{ft}$$

b. Compute transmissivity, T , and hydraulic conductivity, K :

$$T := \frac{Q \cdot W_{\text{star}}}{4 \cdot \pi \cdot s_{\text{star}}} \quad T = 2.428 \times 10^{-3} \frac{\text{ft}^2}{\text{sec}} \quad (\text{equation 9.8, Dawson and Istok, 1991})$$

$$K := \frac{T}{b} \quad K = 8.828 \times 10^{-4} \frac{\text{ft}}{\text{sec}}$$

12. Calculate aquifer storativity, S :

a. List match-point for $1/u$ and define u^* :

$$\text{one_over_u}_{\text{star}} := 19 \quad u_{\text{star}} := \frac{1}{\text{one_over_u}_{\text{star}}}$$

b. List the match-point for time, t :

$$t_{\text{star}} := 960 \cdot \text{sec}$$

c. Compute storativity, S : (equation 9.10, Dawson and Istok, 1991)

$$S := \frac{4 \cdot T \cdot t_{\text{star}} \cdot u_{\text{star}}}{r^2} \quad S = 4.441 \times 10^{-3}$$

13. Calculate hydraulic conductivity, K' , for the overlying aquitard:

- a. List the match-point value for r/B and determine the leakage factor, B :

$$r_{\text{over}_B\text{star}} := .15 \quad B := \frac{r}{r_{\text{over}_B\text{star}}}$$

- b. Compute K' : *(equation 9.2, Dawson and Istok, 1991)*

$$K_{\text{prime}} := \frac{T \cdot b_{\text{prime}}}{B^2} \quad K_{\text{prime}} = 1.483 \times 10^{-6} \frac{\text{ft}}{\text{sec}}$$

14. Determine hydraulic conductivity for the bottom soil layer of the wetland:

- a. Estimate gravel and sand layer conductivities and define layer thicknesses (source of estimates: Charbeneau, 2000):

$$b_{\text{gravel}} := .75 \cdot \text{ft} \quad K_{\text{gravel}} := 1 \times 10^0 \frac{\text{cm}}{\text{sec}}$$

$$b_{\text{sand}} := .5 \cdot \text{ft} \quad K_{\text{sand}} := 1 \times 10^{-2} \frac{\text{cm}}{\text{sec}}$$

- b. Define soil layer thickness and compute K_{soil} :

$$b_{\text{soil}} := 1.5 \cdot \text{ft}$$

$$K_{\text{soil}} := \frac{b_{\text{soil}}}{\frac{b}{K} - \frac{b_{\text{sand}}}{K_{\text{sand}}} - \frac{b_{\text{gravel}}}{K_{\text{gravel}}}} \quad \text{(Equation 2.2.10, Charbeneau, 2000.)}$$

$$K_{\text{soil}} = 9.566 \times 10^{-4} \frac{\text{ft}}{\text{sec}}$$

Hantush Match-point Method for Leaky Confined Aquifers
with Aquitard Storage:

Note: this method assumes the effects of partial penetration introduce little error when $r > 1.5m(K_r/K_z)^{1/2}$ (p. 199, Dawson and Istok, 1991) and can be ignored.

1. Test Range of K_r versus K_z that assumption is valid over:

$$b := (1.5 + 1.25) \cdot \text{ft} \quad r := 10.51139026 \cdot \text{ft}$$

$$\text{assume: } K_r := 6 \quad K_z := 1$$

$$r_{\text{test}} := 1.5 \cdot b \cdot \sqrt{\frac{K_r}{K_z}} \quad r_{\text{test}} = 10.104 \text{ ft}$$

2. Define values for "u" and "β":

$$\beta := \begin{pmatrix} 0.01 \\ 0.05 \\ 0.1 \\ 0.2 \\ 0.5 \\ 1 \\ 2 \\ 5 \\ 10 \\ 20 \end{pmatrix}$$

Note: "u" spans values from .000001 to 3 but is not defined in the margins.

3. Define the range of variables for the Well Function, $H(u, \beta)$, for Leaky Aquifers with Aquitard Storage:

$$j := 1, 2.. 10 \quad i := 1, 2.. \text{rows}(u)$$

4. Define $1/u$:

$$\text{one_over_}u_i := \frac{1}{u_i}$$

5. Define the Well Function, $H(u, \beta)$:

$$H_{i,j} := \int_{u_i}^{\infty} \frac{e^{-y}}{y} \cdot \text{erfc} \left[\frac{\beta_j \cdot \sqrt{u_i}}{\sqrt{y \cdot (y - u_i)}} \right] dy \quad (\text{equation 10.18, Dawson and Istok, 1991})$$

6. Define relevant test and aquifer parameters to support below calculations:

a. Distance between pumping well and observation well:

$$r := 10.51139026 \cdot \text{ft}$$

b. Aquifer thickness:

$$b := (1.5 + 1.25) \cdot \text{ft}$$

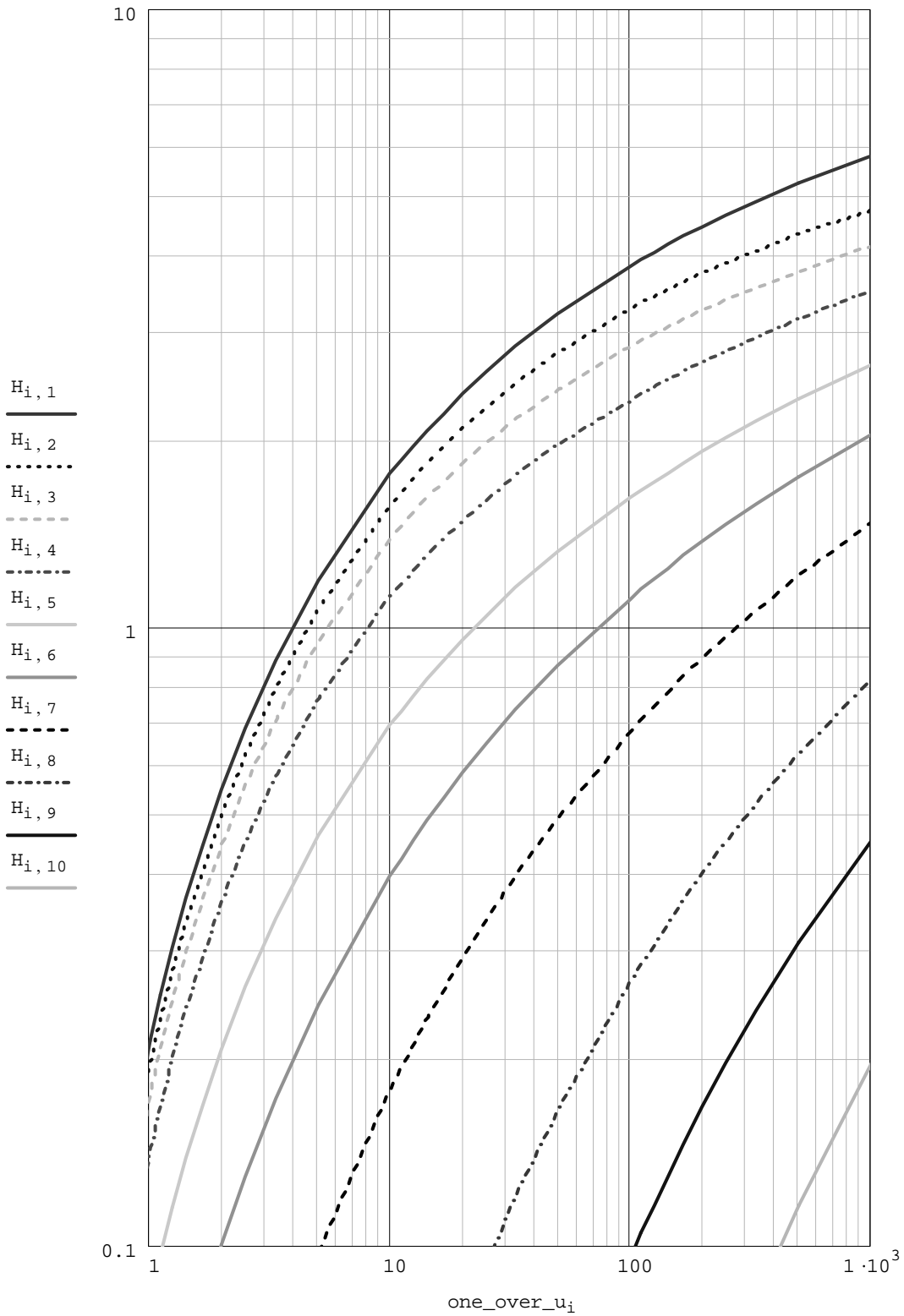
c. Aquitard thickness:

$$b_{\text{prime}} := 3 \cdot \text{ft}$$

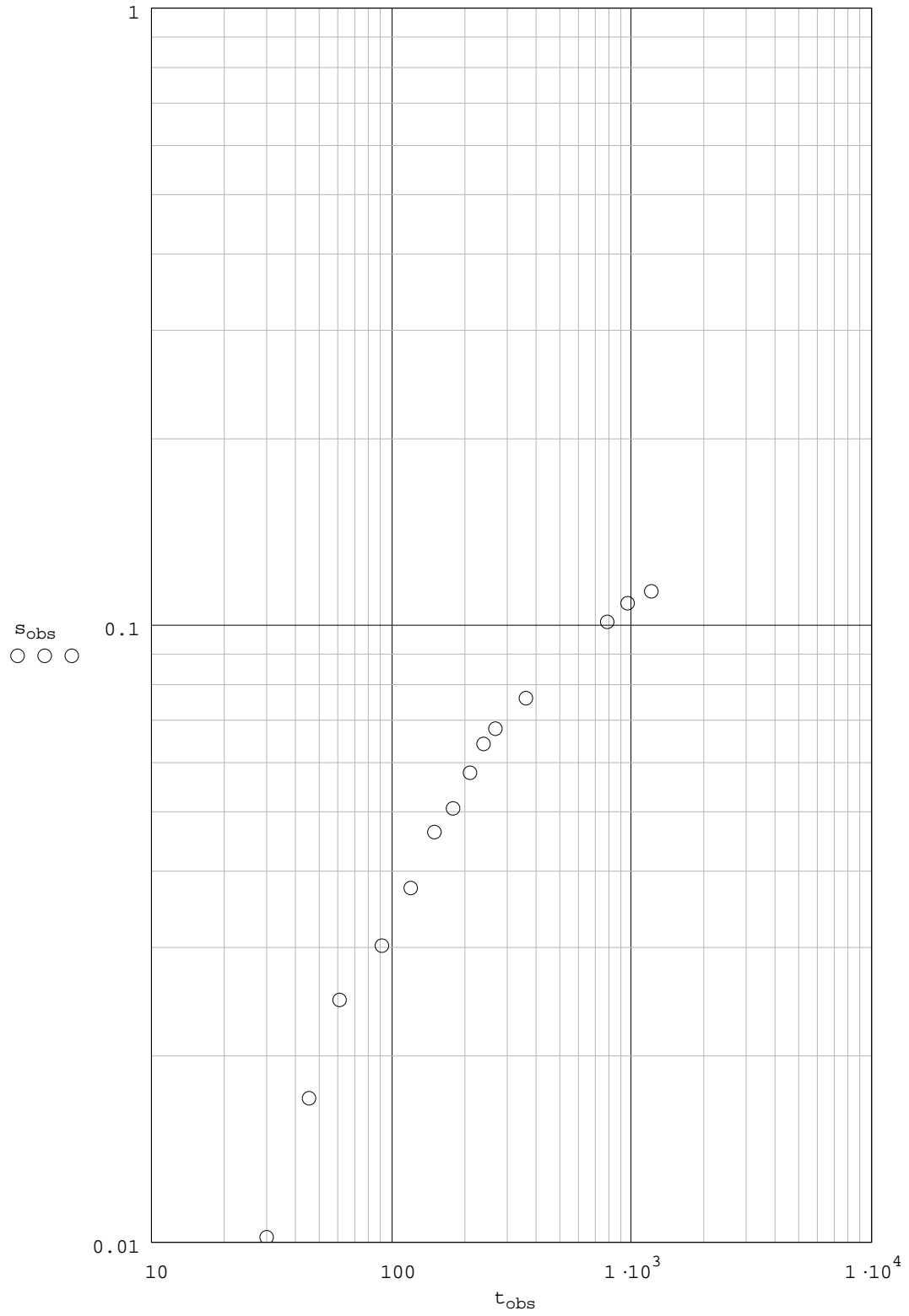
d. Pump Rate:

$$Q := \frac{1 \cdot \text{gal}}{71 \cdot \text{sec}}$$

7. Plot the $H(u,\beta)$ vs. $1/u$ and Observed Time/Drawdown Curves:



8. Plot the observed time drawdown curve:



9. Calculate hydraulic conductivity for the bottom soil layer:

a. List the match-points $H(u, \beta)^*$, $1/u^*$, s^* , and t^* and define u^* :

$$H_{\text{star}} := 1.6 \quad \text{one_over_u_star} := 29 \quad u_{\text{star}} := \frac{1}{\text{one_over_u_star}}$$

$$s_{\text{star}} := 3.08 \cdot \text{cm} \quad t_{\text{star}} := 13 \cdot \text{min}$$

b. Compute transmissivity (T), hydraulic conductivity (K), and storativity (S):

$$T := \frac{Q \cdot H_{\text{star}}}{4 \cdot \pi \cdot s_{\text{star}}} \quad T = 2.372 \times 10^{-3} \frac{\text{ft}^2}{\text{sec}} \quad (\text{equation 10.15, Dawson and Istok, 1991})$$

$$K := \frac{T}{b} \quad K = 8.627 \times 10^{-4} \frac{\text{ft}}{\text{sec}}$$

$$S := \frac{4 \cdot T \cdot t_{\text{star}} \cdot u_{\text{star}}}{r^2} \quad S = 2.31 \times 10^{-3} \quad (\text{equation 10.16, Dawson and Istok, 1991})$$

c. Estimate gravel and sand layer conductivities and define layer thicknesses (source of estimates: Charbeneau, 2000):

$$b_{\text{gravel}} := .75 \cdot \text{ft} \quad K_{\text{gravel}} := 1 \times 10^0 \frac{\text{cm}}{\text{sec}}$$

$$b_{\text{sand}} := .5 \cdot \text{ft} \quad K_{\text{sand}} := 1 \times 10^{-2} \frac{\text{cm}}{\text{sec}}$$

$$b_{\text{soil}} := 1.5 \cdot \text{ft}$$

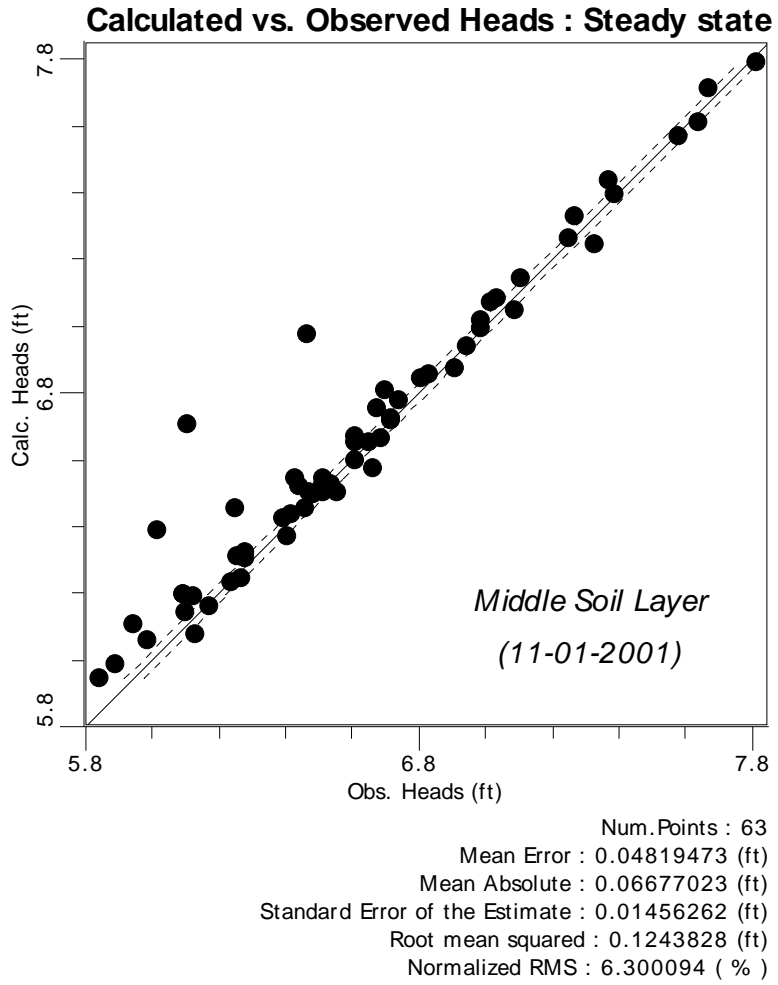
d. Determine the hydraulic conductivity of the bottom soil layer of the wetland (K_{soil}):

$$K_{\text{soil}} := \frac{b_{\text{soil}}}{\frac{b}{K} - \frac{b_{\text{sand}}}{K_{\text{sand}}} - \frac{b_{\text{gravel}}}{K_{\text{gravel}}}}$$

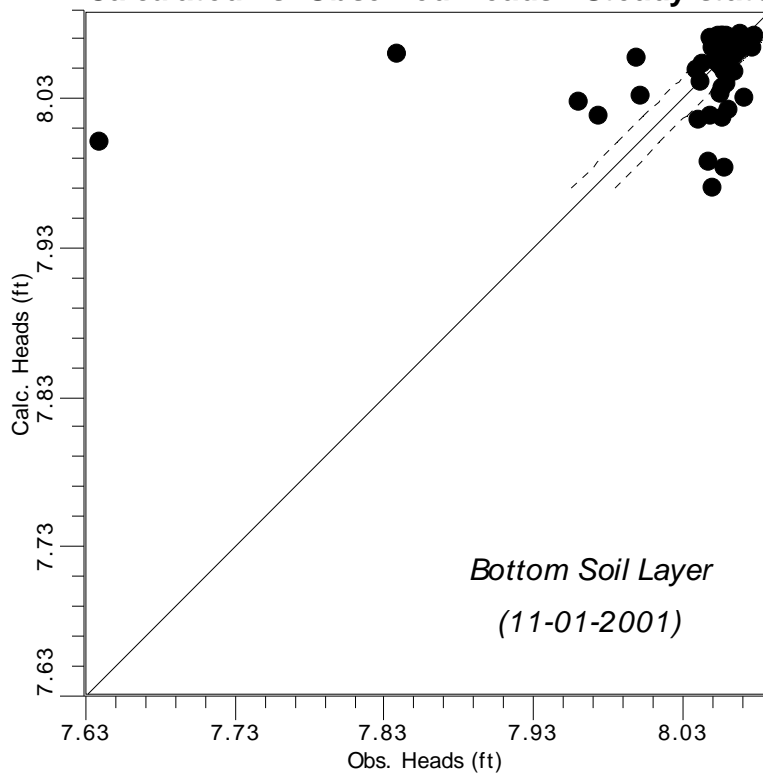
$$K_{\text{soil}} = 9.142 \times 10^{-4} \frac{\text{ft}}{\text{sec}}$$

(Equation 2.2.10, Charbeneau, 2000.)

Appendix H: Calibration Plots



Calculated vs. Observed Heads : Steady state



Num.Points : 64
Mean Error : 0.007224859 (ft)
Mean Absolute : 0.02538688 (ft)
Standard Error of the Estimate : 0.007304927 (ft)
Root mean squared : 0.05842946 (ft)
Normalized RMS : 13.26435 (%)

Bibliography

- ASTM D2216-63T. "Tentative Method for Laboratory Determination of Moisture Content of Soil," in *Procedures for Testing Soils* (4th Edition). Philadelphia, PA: American Society for Testing and Materials, 1964.
- Boulton, N.S. and T.D. Streltsova. "New Equations for Determining the Formation Constants of an Aquifer From Pumping Test Data," *Water Resources Research*, 11(1): 148-153 (1975).
- Bouwer, H. and R.C. Rice. "A Slug Test for Determining Hydraulic Conductivity of Unconfined Aquifers With Completely or Partially Penetrating Wells," *Ground Water*, 12(3): 423-428 (1976).
- Bouwer, H. *McGraw Hill Series in Water Resources and Environmental Engineering: Groundwater Hydrology*. New York, NY: McGraw-Hill, Inc., 1978.
- Bouwer, H. "The Bouwer and Rice Slug Test - An Update," *Ground Water*, 27(3): 304-309 (1989).
- Bowmer, K.H. "Nutrient Removal from Effluents by an Artificial Wetland: Influence of Rhizosphere Aeration and Preferential Flow Studied Using Bromide and Dye Tracers," *Water Research*, 21(5): 591-599 (1987).
- Bradley, P.M. and F.H. Chappelle. "Kinetics of DCE and VC Mineralization Under Methanogenic and Fe(III)-Reducing Conditions," *Environmental Science & Technology*, 31(9): 2692-2696 (1997).
- Brand, E.W. and J. Permichitt. "Shape Factors of Cylindrical Piezometers," *Geotechnique*, 30(5): 369-384 (1980).
- Brix, H. "Functions of Macrophytes in Constructed Wetlands," *Water Science & Technology*, 29(4): 71-78 (1994).
- Cedergren, H.R. *Seepage, Drainage and Flow Nets* (3rd Edition). New York, NY: John Wiley and Sons, 1989.

- Charbeneau, R.J. *Groundwater Hydraulics and Pollutant Transport*. Upper Saddle River, NJ: Prentice Hall, 2000.
- Dawson, K.J. and J.D. Istok. *Aquifer Testing*. Chelsea, MI: Lewis Publishers, Inc., 1991.
- Demir, Z. and T.N. Narasimhan. "Improved Interpretation of Hvorslev Tests," *Journal of Hydraulic Engineering*, 120(4): 477-494 (1994).
- Devore, J.L. *Probability and Statistics for Engineering and the Sciences*. Pacific Grove, CA: Duxbury Thomson Learning, 2000.
- Fetter, C.W. *Applied Hydrogeology* (3rd Edition). Englewood Cliffs, NJ: Prentice-Hall, Inc., 1994.
- Fisher, P.J. "Hydraulic Characteristics of Constructed Wetlands at Richmond, NSW, Australia," in *Constructed Wetlands in Water Pollution Control*. Eds. P.F. Cooper and B.C. Findlanter. Oxford, UK: Pergamon Press, 1990.
- Fogel, S., R. Lewis, D. Groher, and M. Findley. "PCE Treatment in Saturated Soil Columns with Methanogens," in *Bioremediation of Chlorinated Solvents*. Eds. R.E. Hinchee, A. Leeson, and L. Semprini. Columbus, OH: Battelle Press, 1995.
- Freeze, R.A. and J.A. Cherry. *Groundwater*. Englewood Cliffs, NJ: Prentice-Hall, 1979.
- Gallagher, L.M. "Clean Water Act," in *Environmental Law Handbook* (15th Edition). Ed. T.F.P. Sullivan. Rockville, MD: Government Institutes, 1999.
- Gilbert, R.O. *Statistical Methods for Environmental Pollution Monitoring*. New York, NY: Van Nostrand Reinhold, 1987.
- Hantush, M.S. and C.E. Jacob. "Non-steady Radial Flow in an Infinite Leaky Aquifer," *Transactions, American Geophysical Union*, 36: 95-100 (1955).
- Hantush, M.S. "Modification of the Theory of Leaky Aquifers," *Journal of Geophysical Research*, 65(11): 3713-3725 (1960).

- Hantush, M.S. "Aquifer Tests on Partially Penetrating Wells," *Proceedings, ASCE*, 87(HY-4): 171-195 (1961).
- Hantush, M.S. "Hydraulic of Wells," in *Advances in Hydroscience, Vol. 1*. Ed. V.T. Chow. New York, NY: Academic Press, 1964.
- Hantush, M.S. "Analysis of Data from Pumping Tests in Anisotropic Aquifers," *Journal of Geophysical Research*, 71(2): 421-426 (1966).
- Haynos, Thomas L. *Characterization of the Aquifer System Underlying the Beaver Creek Wetlands Area, Greene County, Ohio*. M.S. Thesis, Department of Geological Sciences, Wright State University, Dayton, OH, 1991.
- Herzog, B.L. and W.J. Morse. "Comparison of Slug Test Methodologies for Determination of Hydraulic Conductivity in Fine Grained Sediments," in *Ground Water and Vadose Zone Monitoring, ASTM STP 1053*. Eds. D.M. Nielsen and A.I. Johnson. Philadelphia, PA: American Society for Testing and Materials, 1990.
- Hilton, B.L. "Performance Evaluation of a Closed Ecological Life Support System (CELSS) Employing Constructed Wetlands," in *Constructed Wetlands for Water Quality Improvement*. Ed. G.A. Moshiri. Boca Raton, FL: Lewis Publishers, 1993.
- Hoefar, C.D. *Modeling Chlorinated Ethene Removal in Constructed Wetlands: A System Dynamics Approach*. M.S. Thesis, AFIT/GEE/ENV/00M-09. School of Engineering and Management, Air Force Institute of Technology (AU), Wright-Patterson AFB, OH, 2000.
- Huang, J. Research Assistant, School of Engineering and Management, Air Force Institute of Technology, Wright-Patterson AFB, OH. Programming Assistance, 2001.
- Hvorslev, M.J. "Time-lag and Soil Permeability in Ground-water Observations," *Waterways Experiment Station Bulletin 36*. Vicksburg, MS: U.S. Army Corps of Engineers, 1951.
- Kadlec, R.H. and R.L. Knight. *Treatment Wetlands*. Boca Raton, FL: CRC Lewis Publishers, 1996.

- Kraemer, C.A., J.B. Hawkins, and C.J. Mohrbacher. "Selection of Single-Well Hydraulic Test Methods for Monitoring Wells," in *Ground Water and Vadose Zone Monitoring, ASTM STP 1053*. Eds. D.M. Nielsen and A.I. Johnson. Philadelphia, PA: American Society for Testing and Materials, 1990.
- Kresic, N. *Quantitative Solutions in Hydrogeology and Groundwater Monitoring*. Boca Raton, FL: CRC Lewis Publishers, 1997.
- Lee, M.D., J.M. Odom and R.J. Buchanan Jr. "New Perspectives on Microbial Dehalogenation of Chlorinated Solvents: Insights from the Field," *Annual Reviews*, 52: 423-452 (1998).
- Lorah, M.M. and L.D. Olsen. "Natural Attenuation of Chlorinated Volatile Organic Compounds in a Freshwater Tidal Wetland: Field Evidence of Anaerobic Biodegradation," *Water Resources Research*, 35(12): 3811-3827 (1999).
- Marsteiner, E.L., *Subsurface Flow Constructed Wetland Hydraulics*. M.S. Thesis, Clarkson University, Potsdam, NY, 1997.
- Masters, G.M. *Introduction to Environmental Engineering and Science* (2nd Edition). Upper Saddle River, NJ: Prentice Hall, 1998
- Mathcad. Version 2000 Professional. Computer software. MathSoft, Inc., Cambridge, MA, 1999.
- McDonald M.G. and A.W. Harbaugh. "A Modular Three-dimensional Finite-difference Groundwater Flow Model," *U.S. Geological Survey Techniques of Water-Resources Investigations, Book 6*. Denver, CO: U.S. Geological Survey, 1988.
- McIntyre, B.D. and S. Riha. "Hydraulic Conductivity and Nitrogen Removal in an Artificial Wetland System," *Journal of Environmental Quality*, 20: 259-263 (1991).
- Millard, S.P. and N.K. Neerchal. *Environmental Statistics with S-PLUS*. Boca Raton, FL: CRC Press LLC, 2001.

- Mitsch, W.J. and J.G. Gooselink. *Wetlands* (2nd Edition).
New York: Van Nostrand Reinhold, 1993.
- Moshiri, G.A. (Ed.). *Constructed Wetlands for Water
Quality Improvement*. Boca Raton, FL: Lewis Publishers,
1993.
- National Research Council. *Alternatives for Ground Water
Cleanup*. Washington, DC: National Academy Press, 1994.
- Newman, L.A., S.E. Strand, N. Choe, J. Duffy, G. Ekuan,
M. Ruszaj, B. Brook Shurtleff, J. Wilmoth, P. Heilman,
and M.P. Gordon. "Uptake and Biotransformation of
Trichloroethylene by Hybrid Poplars," *Environmental
Science & Technology*, 31 (4): 1062-1067 (1997).
- Nielsen, D.M. and R. Schalla. "Design and Installation of
Ground-water Monitoring Wells," in *Practical Handbook of
Ground-water Monitoring*. Ed. D.M. Nielsen. Chelsea,
MI: Lewis Publishers, Inc., 1991.
- Nietch, C.T., J.T. Morris and D.A. Vroblesky.
"Biophysical Mechanisms of Trichloroethene Uptake and
Loss in Baldcypress Growing in Shallow Contaminated
Groundwater," *Environmental Science & Technology*, 33
(17): 2899-2904 (1999).
- Pohll, G.M. *Modeling Regional Flow and Flow to Drains*.
M.S. Thesis, University of Nevada, Reno, NV, 1993.
- Prill, R.C., A.I. Johnson and D.A. Morris. *Specific Yield
- Laboratory Experiments Showing the Effect of Time on
Column Drainage* (W 1662-B). Reston, VA: U.S. Geological
Survey, 1965.
- Reed, S.C., R.W. Crites, and E.J. Middlebrooks. *Natural
Systems for Waste Management and Treatment* (2nd Edition).
New York: McGraw-Hill, Inc., 1995.
- Renwick, T.G. Chief, DOC3, Air Force Combat Climatology
Center (AFCCC). Electronic-mail response to support
assistance request. 6 February 2002.
- Sawyer, C.N., P.L. McCarty and G.F. Parkin. *Chemistry for
Environmental Engineering* (4th Edition). New York, NY:
McGraw-Hill, Inc., 1994.

- Shelley, M.L. Associate Professor, School of Engineering and Management, Air Force Institute of Technology, Wright-Patterson AFB, OH. Routine personal communications, 2001.
- Siegal, D.I. and P.H. Glaser. "Groundwater Flow in a Bog-fen Complex, Lost River Peatland, Northern Minnesota," *Journal of Ecology*, 75: 743-754 (1987).
- Sprecher, S.W. "Installing Monitoring Wells/piezometers in Wetlands", *WRAP Technical Notes Collection* (ERDC TN-WRAP-00-02). Vicksburg, MS: U.S. Army Research and Development Center, 2000.
- Surfer. Version 5.03. Computer software. Golden Software, Inc., Golden, CO, 1995.
- Thompson, C. *Hydrogeology of Iowa Fens (Peatlands, Water Quality)*. The University of Iowa, Iowa City, IA, 1993.
- U.S. Environmental Protection Agency (U.S. EPA), Office of Research and Development. *Ground Water Handbook*. Rockville, MD: Government Institutes, Inc., 1992.
- Visual MODFLOW. Version 2.8.2.22. Waterloo Hydrogeologic, Inc., Waterloo, Ontario Canada, 1999.
- Ward, A.D. and J. Dorsey. "Infiltration and Soil Water Processes," in *Environmental Hydrology*. Eds. Ward, A.D. and W.J. Elliot. Boca Raton, FL: Lewis Publishers, 1995.
- Wetlands Research Program. *Hydrology and Hydraulic Design Criteria for the Creation and Restoration of Wetlands* (Technical Note HY-RS-3.1). Vicksburg, MS: U.S. Army Corps of Engineers, 1993.
- Wu, W., J. Nye, R.F. Hickey, M.K. Jain, and J.G. Zeikus. "Dechlorination of PCE and TCE to Ethane Using an Anaerobic Microbial Consortium," in *Bioremediation of Chlorinated Solvents*. Eds. R.E. Hinchee, A. Leeson, and L. Semprini. Columbus, OH: Battelle Press, 1995.

Vita

Major Andrew C. Entingh graduated from Wayne Central High School in June 1982. He entered undergraduate studies at Geneva College in Beaver Falls, Pennsylvania where he graduated with a Bachelor of Science degree in Civil Engineering in May 1986. He enlisted in the United States Marine Corps Reserve in 1983, and he received a commission in the United States Marine Corps upon graduation from his undergraduate studies in 1986.

As a commissioned officer, Major Entingh has served as a platoon commander with the 2nd Combat Engineer Battalion, 2nd Marine Division, Camp Lejeune, North Carolina; series officer, executive officer, and commanding officer with the 3rd Recruit Training Battalion, Recruit Training Regiment, Parris Island, South Carolina; student at the U.S. Army Engineer Officer Advanced Course, Fort Leonard Wood, Missouri; detachment officer-in-charge of the 3rd Force Service Support Group Marine Liaison Team, Taegu, Korea; detachment officer-in-charge of the III Marine Expeditionary Force (III MEF) Marine Expeditionary Camp, Pohang, Korea; Inspector-Instructor for Bridge Company Alpha, 6th Engineer Support Battalion, 4th Force Service Support Group, Battle Creek, Michigan; assistant operations

officer for Marine Wing Support Group 37 (MWSG-37), 3rd Marine Aircraft Wing (3rd MAW), Marine Corps Air Station El Toro, California; and operations officer, Marine Wing Support Squadron 373, MWSG-37, 3rd MAW, Marine Corps Air Station Miramar, California. Major Entingh entered the Graduate School of Engineering and Management, Air Force Institute of Technology during August 2000. Following graduation, he will be assigned to the Marine Corps Base, Camp Pendleton, California.

REPORT DOCUMENTATION PAGE

Form Approved
OMB No. 074-0188

The public reporting burden for this collection of information is estimated to average 1 hour per response, including the time for reviewing instructions, searching existing data sources, gathering and maintaining the data needed, and completing and reviewing the collection of information. Send comments regarding this burden estimate or any other aspect of the collection of information, including suggestions for reducing this burden to Department of Defense, Washington Headquarters Services, Directorate for Information Operations and Reports (0704-0188), 1215 Jefferson Davis Highway, Suite 1204, Arlington, VA 22202-4302. Respondents should be aware that notwithstanding any other provision of law, no person shall be subject to a penalty for failing to comply with a collection of information if it does not display a currently valid OMB control number.

PLEASE DO NOT RETURN YOUR FORM TO THE ABOVE ADDRESS.

1. REPORT DATE (DD-MM-YYYY) 26-03-2002		2. REPORT TYPE Master's Thesis		3. DATES COVERED (From - To) Aug 2000 - Mar 2002	
4. TITLE AND SUBTITLE GROUNDWATER FLOW THROUGH A CONSTRUCTED TREATMENT WETLAND			5a. CONTRACT NUMBER		
			5b. GRANT NUMBER		
			5c. PROGRAM ELEMENT NUMBER		
6. AUTHOR(S) Entingh, Andrew, C., Major, USMC			5d. PROJECT NUMBER		
			5e. TASK NUMBER		
			5f. WORK UNIT NUMBER		
7. PERFORMING ORGANIZATION NAMES(S) AND ADDRESS(S) Air Force Institute of Technology Graduate School of Engineering and Management (AFIT/EN) 2950 P Street, Building 640 WPAFB OH 45433-7765			8. PERFORMING ORGANIZATION REPORT NUMBER AFIT/GEE/ENV/02M-03		
9. SPONSORING/MONITORING AGENCY NAME(S) AND ADDRESS(ES) AFRL/MLQ Dr. Tom Stauffer Barnes Avenue Tyndall AFB, FL 32403 (850)283-6859			10. SPONSOR/MONITOR'S ACRONYM(S) AFRL/MLQ		
			11. SPONSOR/MONITOR'S REPORT NUMBER(S)		
12. DISTRIBUTION/AVAILABILITY STATEMENT APPROVED FOR PUBLIC RELEASE; DISTRIBUTION UNLIMITED.					
13. SUPPLEMENTARY NOTES					
14. ABSTRACT <p>This study examines the flow of groundwater through a constructed treatment wetland. The wetland was built to explore the viability of constructed wetlands as a treatment technology for groundwater contaminated with perchloroethylene, and it employs an upward vertical flow design. A major goal of the study is to determine whether the system design facilitates uniform vertical flows through the subsurface soil sediments or if preferential flows occur. Conceptually, uniform flows will achieve the most efficient degree of contaminant removal possible by evenly dispersing the groundwater contaminants throughout the full volume of the subsurface media.</p> <p>A three-dimensional grid of piezometers is used to generate potentiometric contour maps, and in-situ tests of hydraulic conductivity facilitate construction of a numerical computer model. The contours of hydraulic head, measured conductivities, and numerical model simulations imply preferential flows and a wetland operating at less than an optimal level of efficiency. Hydraulic residence times for representative water particles released in the model range from 16.5 hours to 15 days with a mean residence time of three days. The divergence from the uniform flow ideal suggests an alternative construction approach may be appropriate.</p>					
15. SUBJECT TERMS Groundwater Flow, Constructed Treatment Wetland, Upward Vertical Flow, Nested Piezometers					
16. SECURITY CLASSIFICATION OF:			17. LIMITATION OF ABSTRACT	18. NUMBER OF PAGES	19a. NAME OF RESPONSIBLE PERSON
a. REPORT	b. ABSTRACT	c. THIS PAGE			19b. TELEPHONE NUMBER (Include area code)
U	U	U	UU	182	Michael L. Shelley, PhD, Associate Professor, AFIT (937) 255-3636, ext 4594; e-mail: Michael.Shelley@afit.edu